SUPPLEMENTAL INFORMATION

Human lung tumor FOXP+ Tregs upregulate four "Treg-locking" transcription factors

Tatiana Akimova,[1] Tianyi Zhang,[1] Dmitri Negorev,[1] Sunil Singhal,[2] Jason Stadanlick,[2] Abhishek Rao,[2] Michael Annunziata,[2] Matthew H. Levine,[3] Ulf H. Beier,[4] Joshua M. Diamond,[5] Jason D. Christie,[5,6] Steven M. Albelda,[5] Evgeniy B. Eruslanov,[2] and Wayne W. Hancock[1]*

[1]Division of Transplant Immunology, Department of Pathology and Laboratory Medicine, and Biesecker Center for Pediatric Liver Diseases, Children's Hospital of Philadelphia and Perelman School of Medicine at the University of Pennsylvania, Philadelphia, PA, USA.

[2]Division of Thoracic Surgery, Department of Surgery, University of Pennsylvania, Philadelphia, PA, USA.

[3]Department of Surgery, Penn Transplant Institute, Hospital of the University of Pennsylvania and University of Pennsylvania, and Department of Surgery, Children's Hospital of Philadelphia, Philadelphia, PA, USA.

[4]Division of Nephrology, Department of Pediatrics, Children's Hospital of Philadelphia and University of Pennsylvania, Philadelphia, PA, USA.

[5]Division of Pulmonary, Allergy and Critical Care Medicine, Department of Medicine, University of Pennsylvania, Philadelphia, PA, USA.

[6]Department of Biostatistics and Epidemiology, University of Pennsylvania, Philadelphia, PA, USA

Authorship note: Current affiliation of Dmitri Negorev is now the Pathology Bioresource, Department of Pathology and Laboratory Medicine, University of Pennsylvania, Philadelphia, PA, USA.

*Correspondence: Wayne W. Hancock, Division of Transplant Immunology, Department of Pathology and Laboratory Medicine, Children's Hospital of Philadelphia, 3615 Civic Ctr. Blvd., Philadelphia PA 19104; Telephone: (215) 590-8709, E-mail: whancock@mail.med.upenn.edu

SUPPLEMENTAL MATERIALS AND METHODS

Patients and tissue samples

Lung cancer and non-cancer controls

Eligibility criteria included the following: i) no prior chemotherapy or radiation therapy within 2 yr, ii) no other malignancy, and iii) an absence of small cell carcinoma, histologically confirmed. All patients had undergone surgery. Median tumor size was 2.6 cm, ranged 0.5-12.0 cm, with 25%-75% percentiles were 1.65-4.3 cm. Clinical data reported in Supplemental Table 7. When clinical data were analyzed, we have found that males and females differed significantly in their smoking status (Suppl. Table 10), but no other significant differences in clinical variables were found. 17 patients who donated the second blood samples at 3 months post-operatively, were representative to the main group for their age, gender, tumor stages, tumor types and other clinical data. For TSDR demethylation assay, we studied 8 tumors, 5 lungs, 14 LN and 4 PBMC samples. Those patients also did not differ from leftovers for their clinical variables, but, as FOXP3 is located at X chromosome, all TSDR FOXP3 evaluated patients were males.

Lung transplant, pre-transplant

As expression of T cell maturation markers (1-5), CD8+ T cells numbers(5), Treg-associated markers and Treg numbers (5-9) alter with age and may be affected in smokers and in COPD (10, 11), we used lung disease patients as an additional reference group. Those patients were listed for lung transplant (LT). Most of them had COPD (Figure S43), and they were gender- and age-matched to LC group. Importantly, co-morbidity profiles of LC and LT patients were shown to have the best match with each other to serve as reference groups (12-14). To compare blood Treg suppressive function with lung cancer and healthy donors, we evaluated 57 LT patients, mean age 57.3±1.5 years old, 59.6% males, and those patients were younger than LC group, so for flow cytometry studies presented in Figures 1 A-D and Supplemental Figure 2A and B, we picked up the older subgroup, 64.0 ± 2.0 yr old, 62.5% males. For TSDR FOXP3 demethylation assay, we collected an additional group of the 6 youngest male LT patients, aged 30-44, mean ± SEM 38.5 ± 2.4 yr (Figure 3E).

Liver transplant

We evaluated TSDR FOXP3 demethylation in 8 patients (53.3 ± 2.9 years old, 75% males) who received liver allografts. Post-transplant, patients had a standard triple therapy of calcineurin inhibitor (Prograf ,2-5 mg BID at 3 months post-Tx), corticosteroids (in 50% of patients at 3 months post-Tx, 5-10 mg QD) and an antimetabolite (Azathioprine, in 5 patients at 3 months post-Tx, 100 mg QD). We collected 50 mL of blood pre-Tx, plus in the first 1-2 weeks post-Tx, at 3 months and 1 year post-Tx. Adult liver allograft studies were approved by the Institutional Review Board of the Hospital of the University of Pennsylvania (#810878).

Cell culture and cell preparation reagents

The enzymatic cocktail for tumor digestion consisted of serum-free Hyclone Leibovitz L-15 medium supplemented with 1% penicillin-streptomycin, collagenase type I and IV (170 mg/L = 45-60 U/mL), collagenase type II (56 mg/L = 15-20 U/mL), DNase I (25 mg/L) and elastase (25 mg/L), all from Worthington Biochemical. T cell media consisted with RPMI 1640 (Invitrogen), supplemented with 10% heat-inactivated FBS, penicillin and streptomycin, and 2-mercaptoethanol (100 μM).

Preparation of a single-cell suspension and lymphocytes isolation

Surgically-removed fresh lung tumors were freed from visible necrotic areas, and sliced into 1-2 mm^3 pieces by scissors. Distant lung tissue was at least 5 cm apart from tumors and was well preserved macroscopically. Fine-cut tissues were placed to 50 mL tubes with enzymatic cocktail and incubated at 37°C for 45 minutes, then evaluated, and, if needed, vigorously pipetted to enhance disaggregation and incubated for 30-50 minutes more. Cells were disaggregated by pipetting, filtered through a 70 μM nylon cell strainer (BD Falcon) and erythrocytes lysed with RBC Lysis Buffer (Santa Cruz Biotechnology). Cells were washed twice in T cell media, evaluated and counted, and rested overnight in the flasks in concentration $1x10^6$/ml. Next day, cell culture media was collected, filtered, aliquoted and cryopreserved to use as tumor conditioned media (TCM)

and normal lung conditioned media (NCM) in corresponding experiments (Figure 12A-F). Cells were washed, evaluated and counted, and used for Treg isolation, co-culture, qPCR or flow cytometry experiments. We mechanically dissected lung lymph nodes (LNs), using tissue grinder homogenizer kit (Sigma) and a 70μM nylon cell strainer (BD Falcon), filtered, washed, evaluated and counted cells, and then rested them overnight. In preliminary experiments, we tested effects of enzymatic cocktail digestion on Treg and T cells markers, and found that CD25 expression was significantly sheared, but recovered after an overnight incubation in T cell media. As CD25 is required for Treg isolation, we performed all experiments with overnight rested cells. Because of that, we were free of additional artifacts caused by the presence or absence of enzymatic digestions of some samples vs. others, and we compared tumors, distant lungs, LN and PBMC cells with fully recovered phenotype.

Cryopreservation

We used the modified, improved method of cryopreservation with CryoStor® CS5 cell cryopreservation media (Sigma) (15). Post-thawed viability of cryopreserved healthy donors PBMC was ≥95-97% with an absence of any differences in phenotype between fresh and cryopreserved cells. Expression of CD62L, known to be sensitive to cryopreservation with standard methods (16, 17), was used as a quality control to ensure no loss of CD62L+ phenotype on cryopreserved vs. previously characterized freshly isolated samples.

Flow cytometry

We randomly picked samples to evaluate different set of markers in 1-4 flow cytometry panels at one experiment, each time we also included 1-3 healthy donors PBMC (HD PBMC). When marker was run at least 3 times for any type of samples (tumor, lungs, LN, PBMC or HD PBMC), we evaluated whether its expression similar in data from different experiments, and performed additional staining with more samples if they were, in some cases using same vs. different fluorochromes and combinations of antibodies. In many cases, we included aliquots of the same HD PBMC into various independent experiments to ensure low technical variabilities and, when needed, for troubleshooting. If expression of tested marker was low, we tried other antibodies clones, but in most cases we started with the same clones that were described in published reports. However, some antibody clones indeed affected results of flow cytometry: CXCR3, CD62, Tim3, GARP and LAP. In the Supplemental table 11, we listed only clones with the best performance. The additional controls included use of fresh vs. cryopreserved cells for every newly evaluated marker to ensure an absence of negative effects of cryopreservation, and staining of non-fixed vs. fixed cells with every new marker, to ensure an absence of artifacts due to Fixation/Permeabilization, the steps that were required to identify FOXP3+ Tregs.

When we ensured an absence of inter-experimental differences and sufficient antibodies performance, we analyzed whether histological tumor types differed for any markers in Tregs or Teffs in any locations. In most cases, no apparent differences were found, and most markers were evaluated only in patients with adenocarcinoma and squamous cell carcinoma, due to random flow cytometry grouping and low prevalence of "other cancers" group within our patients. However, we have found that in cases of "other cancers", expression of CTLA4, GITR, CCR4 and CXCR5 seemed to be affected, so we excluded those data from the final reports at Figure 7, but they are presented at Supplemental Figures 9, 11, 14 and 20. Only 2 markers tended to differ between adenocarcinoma and squamous cells carcinoma, GARP and LAP, so we presented their expression in adenocarcinoma samples exclusively in Figure 7 A, E, but provided the full data about their expression in Supplemental Figures 10 and 13.

For flow cytometry, we used live/dead fixable reagent, then washed cells, applied FC blocking reagent (Human TruStain FcX, Biolegend) for 5-10 min at room temperature, then stained for surface markers for 40-50 min, 4°C in pre-titrated concentrations, then washed, performed Fixation/Permeabilization step using Transcription Factor Buffer Set (BD Biosciences) and stained for intranuclear and intracellular antibodies for 60 min, 4°C. We evaluated cells using CyAn Dako or CytoFLEX flow cytometers and analyzed data with FlowJo. Compensation was performed using single stains and fluorescent minus one (FMO) controls. We applied gating on cells negative for live/dead fixable reagent (in all experiments) and also gated on CD45hi+ population (in some experiments) to exclude dead, apoptotic and non-hematopoietic cells and therefore to markedly decrease

non-specific signals. Further gating strategies for particular markers are shown in Supplemental Figures 1 and 6-40. We applied antibodies to FOXP3, Helios, CTLA4 and Ki-67 after Fixation/Permeabilization. To evaluate expression of GARP, LAP, Tim3 and CD40L, we used stimulation for 2 days with CD3/28 beads at 1/1 ratio in T cell media. The same conditions, but overnight stimulation, were used to evaluate PD1 expression, as levels of PD1 in non-stimulated cells were low. As we used cells after their overnight incubation in the plastic flasks (see details above in "Preparation of a single-cell suspension and lymphocytes isolation"), we collected mostly the non-adherent cells. Therefore, axis labels "% in all cells" refer to non-adherent, SSC-FSC viable lymphocytes gated, (CD45+) and live/dead fixable reagent gated cells.

PrimeFlow assay

We used PrimeFlow RNA Assay method (cat#88-18009-204, Affimetrix), that employs a fluorescent in-situ hybridization technique enabling simultaneous detection of up to 3 RNA transcripts in a single cell using a standard flow cytometer. RNA detection may be combined with intracellular, intranuclear and superficial antibodies staining (18-20). We applied live/dead fixable reagent, then FC blocking, followed by superficial antibodies staining (CD4, CD45), then performed Fixation/Permeabilization according to manufacturer's instruction, then stained for FOXP3 for 1 hour, washed and proceeded with target genes and housekeeping genes (RPL13A, NM_012423) hybridization according to protocol in Human PrimeFlow RNA kit. Target genes probes included:

VA1-15518-204	FOXP3, human, type 1
VA6-12565-204	FOXP3, human, type 6
VA6-13816-204	GATA1, human, type 6
VA4-18923-204	IKZF4, human, type 4
VA6-18867-204	IRF4, human, type 6
VA4-18412-204	SATB1, human, type 4
VA4-12619-06	LEF1, human, type 4
VA1-16969-06	HDAC6, human, type 4

Controls included: i) use of all reagents and the whole procedure, including amplification, but in absence of mRNA probes (Supplemental Figure 41C); ii) target genes amplified with and without co-staining with flow cytometry antibodies; iii) housekeeping genes with all three types of fluorescent labels (Supplemental Figure 41B), iv) evaluation of dot plots with housekeeping genes expression vs. live/dead co-staining (Supplemental Figure 41A); and v) FMO controls (Supplemental Figure 41D). When indicated, cells were incubated for 3 days with 50% of their T cell media replaced by tumor conditioned media (TCM) or normal lung conditioned media (NCM). For gene mRNAs expression and FOXP3 protein per cell data, we used median of fluorescence (MOF) instead of mean of fluorescence because i) it is not easily influenced by outliers, and ii) most fluorescence data were not normally distributed. For mRNA and protein expression in single cell levels, we gated CD4+FOXP3+ (i.e. by antibodies) Tregs on fully compensated data, and saved those new *.fcs files separately. Then we exported fluorescent data for required channels as CSV-Scale values, performed log transformation of data and used them for statistics as illustrated at Figure 11, A-C.

Human TSDR FOXP3 methylation assay

We isolated genomic DNA from 80-170x10^3 CD4+ CD25+ beads-isolated Tregs using Gentra Puregene Cell Kit (Qiagen), according to the manufacturer's instructions. We added GlycoBlue (ThermoFisher Scientific) to locate pellets that were otherwise not visible due to low cell numbers. We evaluated DNA quantity using Qubit dsDNA HS Assay (ThermoFisher Scientific). Then, according to manufacturer's instruction (EpiTect II DNA Methylation Enzyme Kit, Qiagen, formerly SABiosciences), we exposed isolated DNA to two restriction enzymes, one methylation-sensitive and the other is methylation dependent. Next, we used DNA digests, four from each DNA sample, to conduct DNA methylation PCR array, in triplicates, with custom FOXP3 primers corresponding to the Treg-specific demethylated region (TSDR) of human FOXP3, and RT² SYBR Green/ROX qPCR Mastermix (both Qiagen, formerly SABiosciences). We used internal control digests along with the tested samples, and calculated % of methylated CpG islands in TSDR region of FOXP3, in Excel template file provided with the kit. We defined 0–5% of methylation as "unmethylated FOXP3". Percentages of

unmethylated TSDR FOXP3 in female Tregs were calculated as (UM TSDR*2), where UM is % unmethylated TSDR FOXP3. Aliquots of Tregs used for TSDR FOXP3 methylation assay were cryopreserved to evaluate their FOXP3+ expression by flow cytometry, and the same Treg samples were used in Treg suppression assay to evaluate and confirm their function. Healthy donor Tregs DNAs with previously characterized (and confirmed by commercial pyrosequencing) demethylated TSDR FOXP3 were included in ongoing experiments to ensure quality of data.

RT-qPCR

We isolated RNA from single cell suspensions using QIAshredder and RNeasy Mini Kit (both Qiagen), evaluate RNA qualities and quantities and reverse transcribed RNA to cDNA with TaqMan Reverse Transcription Reagents (N8080234, ThermoFisher Scientific). Then we run TaqMan gene expression assay with primers to TGFb, IL-10, CTNNB1 (beta-catenin), IDO1 (indoleamine-2,3-dioxygenase 1), COX-2 (cyclooxygenase-2), HIF1a (hypoxia-inducible factor-1α), CA9 (carbonic anhydrase IX) and CXCL13. Differences in cDNA input were corrected by normalizing signals for 18S rRNA (all ThermoFisher Scientific). We normalized genes expression using ΔΔCT method with distant lungs as controls. In case of CXCL13 expression, lung LNs served as controls.

Treg suppression assays with adjusted FOXP3+ Treg purity

Tregs were isolated after overnight incubation of all samples in T cell media, which allowed cells to recover their CD25 expression. We used magnetic beads (#130-091-301, CD4+CD25+Treg isolation kit, Miltenyi-Biotec). After counting and evaluation with Trypan blue, most Tregs were immediately used for suppression assays, while small aliquots were frozen for flow cytometry to control FOXP3+ purity after isolation. If sample had efficient number of cells, the portion of 80-170x10^3 Treg was cryopreserved for TSDR FOXP3 methylation assay. To ensure suppression assays reflected effects of tumors on Tregs and not conventional T effector (Teff) cells, the same healthy donor CFSE-labeled PBMC cells were used in each assay. In preliminary studies, these cells were tested with different healthy donor Tregs to ensure absence of variability due to HLA differences (data not shown). We also evaluated Tregs in suppression assays with autologous patient CFSE-labeled CD3-stimulated CD4+CD25- Teff cells, and in suppression assays based on MLR, as described (21). Tumor Tregs had superior suppressive activity in all types of suppression assays, so we used the one with standardized conditions and healthy donors PBMC in all leftover experiments and in following calculations.

When multiple experiments with samples from one patient were performed (as two different lung LNs, central vs. peripheral tumor parts, two starting cell numbers, two types of stimulations, different final volumes in wells, different modifications of Treg isolation, U-bottom vs. V-bottom wells, duplicates and triplicates etc.), then results of only one, the most "standard" modification, were included in calculations presented at Figure 5B. Aliquots of isolated Tregs were stained for CD45, CD4, CD25, CD127, CTLA4, FOXP3 and fixable live/dead reagent. We used CD45, CD25, CD127 and CTLA4 in some, while CD4, FOXP3 and fixable live/dead reagent in all Treg samples. Tregs isolated from PBMC of lung cancer, LT and healthy donors (Figure 5C) had comparable FOXP3+ purity after isolation, so no adjustments for results of their suppressive function were required. Lung cancer patients Tregs isolated from tumors, PBMC and LNs also had comparable FOXP3+ purity, but lung Tregs FOXP3+ purity was significantly worse, making direct comparison non-reliable in most cases. To resolve this problem, we run experiments with 5 tested Tregs, 3 tumors and 2 healthy donors' ones. Prior to suppression assays, Tregs were diluted with CD4+CD25+FOXP3- autologous Teffs mimicking their decreased FOXP3+ purity, in concentrations of 100 to 40% of original Tregs (Supplemental Table 1). Then we run linear regression assays to evaluate how Tregs decreased their suppressive function when their FOXP3+ purity decreased, and found that all resulting regression lines have little variability between each other. So we combined those lines and received 2 regression analyses equations (Figures 5D, Supplemental Figure 5B, Supplemental Table 2). Then we run suppressive assays with two more Tregs samples, one healthy donor and one lung cancer distant lung Tregs, using the same dilutions with their own Teffs, to evaluate predictive errors of our equations. Prediction errors were just 1% and 10% (CD4 and CD8 responders, correspondingly) for healthy donor Treg sample isolated with 48% FOXP3+ purity, and 15% and 18% for lung Tregs, isolated with

very low Treg purity (22%) (Supplemental Figure 5C-D and Supplemental Table 3). Then we adjusted the results of suppression assays according to their FOXP3+ Tregs purities.

In vitro pTreg (iTreg) conversion assay

We applied CD25+ beads from Treg isolation kit (#130-091-301, Miltenyi-Biotec) to overnight rested cells, 10 uL of microbeads per each $7x10^6$ cells in 90 uL of MACs buffer, incubated for 20 min, and then we depleted cells of CD25+ Tregs using LD columns. We evaluated the small aliquots of each sample to ensure very low and equal % of leftover Tregs in all CD25-depleted samples (Figure 3C). We stimulated cell suspensions with CD3/28 beads (1:10 cells ratio), TGFb 10ng/mL and IL2 100 U/mL for 7 days with fresh TGFb 1 and IL2 every other day, and then evaluated % of pTregs by flow cytometry.

Statistics

We applied parametric tests if data were normally distributed and non-parametric tests if not. The tests included: Student's t-test (or Mann–Whitney U-test) to compare 2 groups of samples; one-way ANOVA (or Kruskal–Wallis) tests for comparison of 3 and more groups, with Tukey's, Sidak's (or Dunn's) multiple comparisons post-hoc tests. For some flow cytometry experiments, where indicated, we used 2-ways ANOVA with Tukey's (rows) and Sidak's (columns) tests. When we performed multiple paired comparisons of data from different experiments, but the same aliquots of samples, we used one unpaired t-test per row with FDR (False discovery rate) set up as 1%. For repeated measurements, we used Friedman test with Dunn's multiple comparisons post-hoc test. For correlation, we used Pearson's (or Spearman's) assays, and we applied partial correlation analyses where indicated. For testing associations in two-way tables, we used chi-square or Fisher exact test. Data are shown as mean ± SEM. A two-tailed p value of <0.05 was considered statistically significant. We used GraphPad Prism 6.0 and SPSS 17.0.

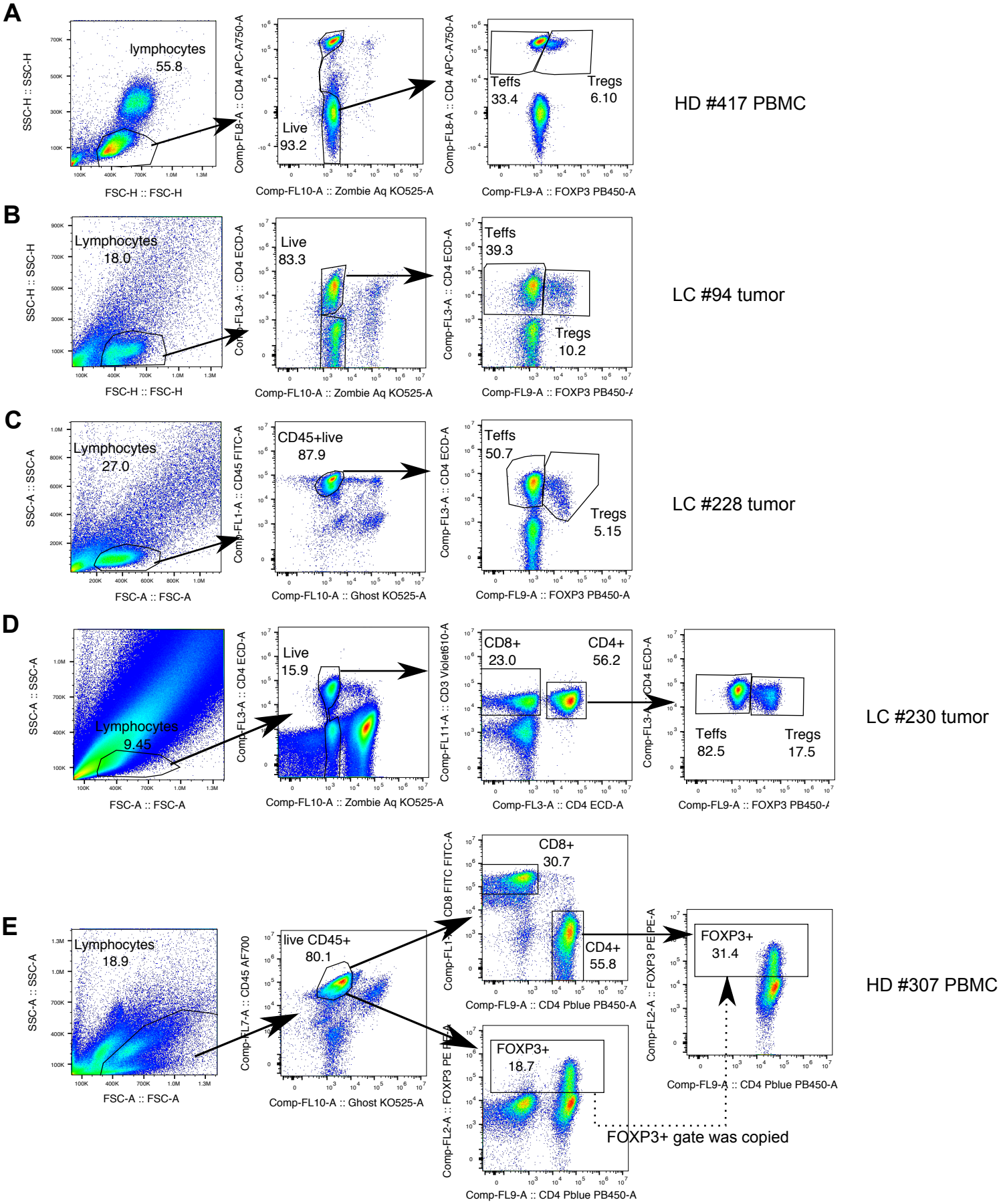

Supplemental Figure 1. Gating strategy to identify Tregs.
(A-D) non-stimulated cells were gated on lymphocyte subsets by FSC-SSC properties when possible (A, B, C). Tumors with high protein and necrotic loads (D) and stimulated cells (E) were gated on FSC-SSC properties of viable cells. Then viable CD4- and CD4+hi (A, B, D) or CD45+hi (C, E) cells were gated, and Tregs were identified as CD4+FOXP3 + cells. (A) healthy donor PBMC, (B, C) tumors with low and (D) high necrotic rates, and (E) healthy donor PBMC incubated for 8 days in conditions of iTregs conversion.

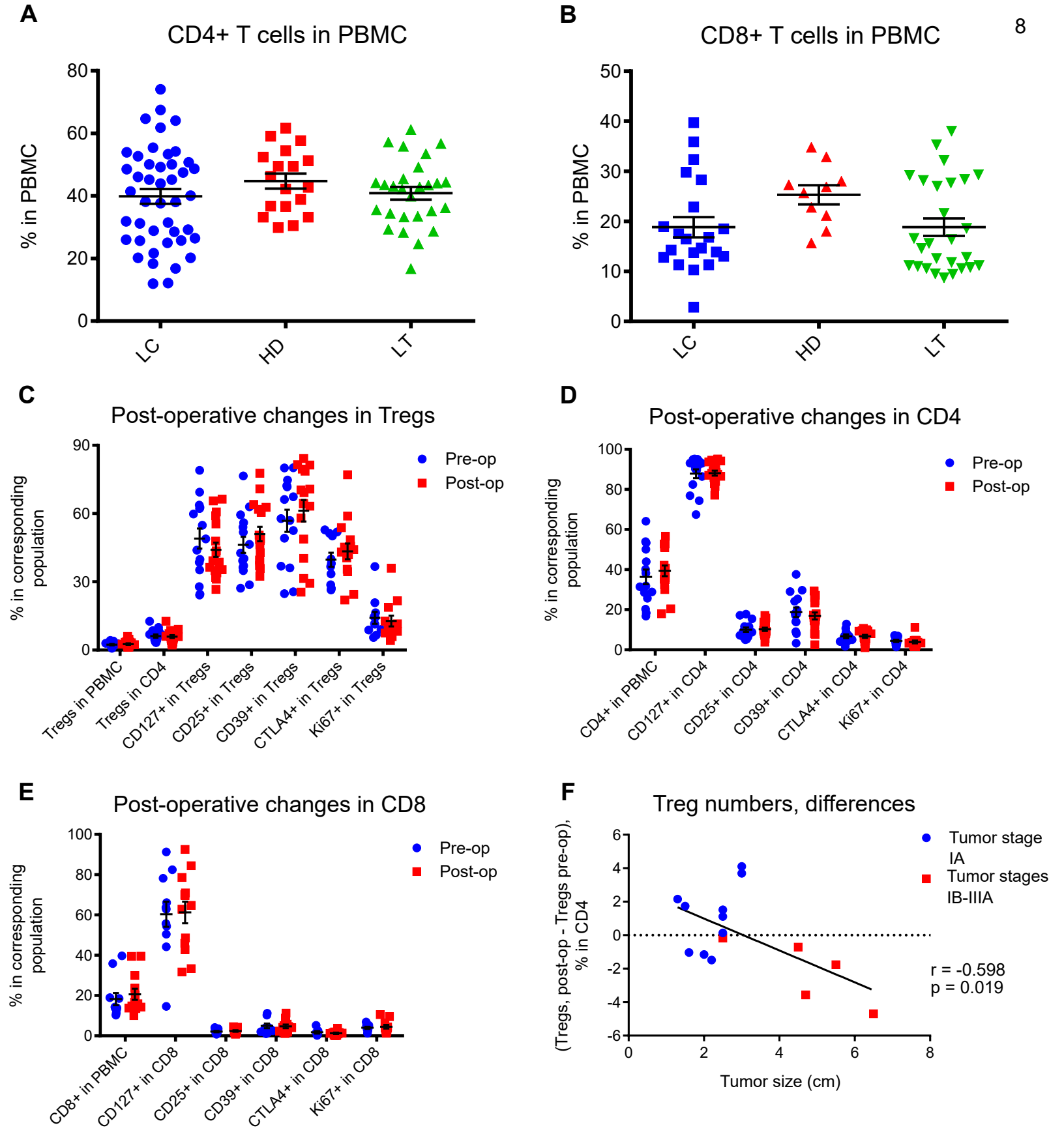

Supplemental Figure 2. Characteristics of blood Tregs in LC patients.
The frequencies of (A) CD4+ and (B) CD8+ cells were evaluated in PBMC from LC, LT and HD groups, at least 11 samples per group. Expression of Treg-associated markers was evaluated in (C) Tregs, (D) CD4+ and (E) CD8+ T cells pre- and postoperatively at 3 months post-op. Each marker was evaluated at least 11 times. (F) Percent of FOXP3+ Tregs in CD4+ subset were compared within each individual (n = 15), and differences in Treg numbers post- vs. pre-operatively demonstrated correlation with the size of tumors removed. This data suggest that number of peripheral Tregs dropped more when larger tumors were removed. "LC" - lung cancer, "HD" - healthy donors, "LT" lung diseased pre-transplant patients. Statistics used: A, B - Kruskal-Wallis tests, p values were >0.05. C-E Multiple t-tests with false discovery rate set to 1%, all p values were >0.05. F - Spearman correlation assay.

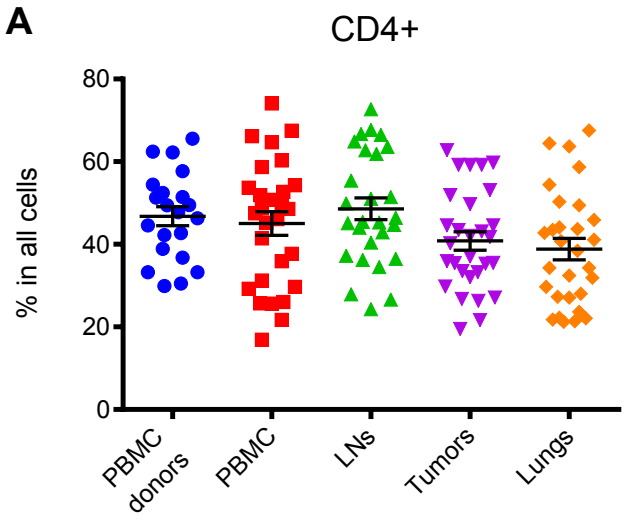

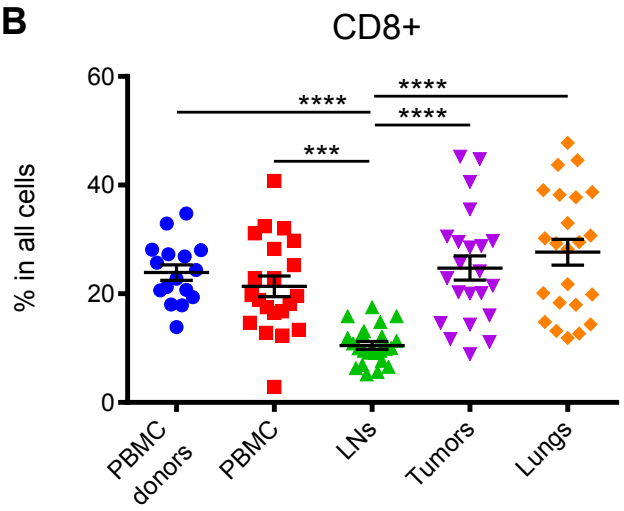

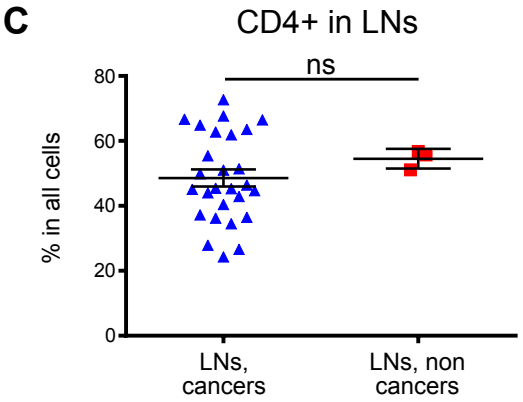

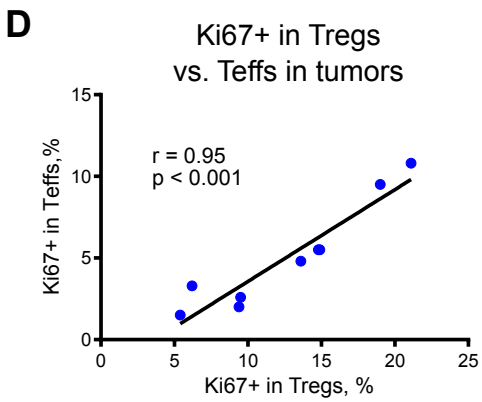

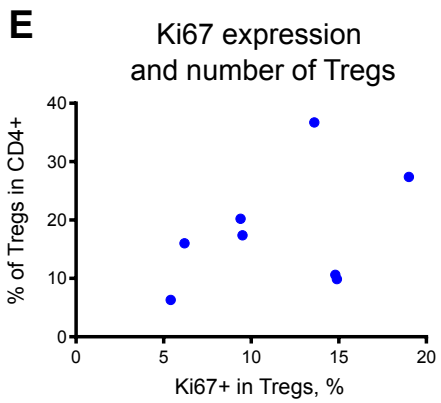

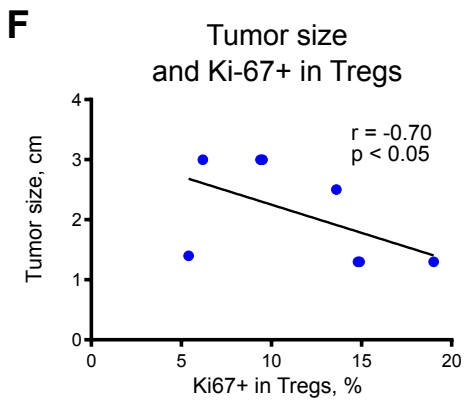

Supplemental Figure 3. Evaluation of lung cancer T cells and division of intratumoral Tregs
The frequencies of (A) CD4+ and (B) CD8+ cells were evaluated in healthy donors, and in LC PBMC, LNs, tumors and distant lungs, with at least 16 samples per group. (C) CD4+ cells were compared in lung cancer LNs (n = 30) versus LNs from three non-cancer patients (with diaphragmal hernia, sarcoidosis and interstitial lung disease, "LNs, non cancers"). Ki67 expression in intratumoral Tregs correlated with (D) Ki67 expression in intratumoral CD4+FOXP3- Teffs (n = 9), (E) had no correlations with frequency of intratumoral Tregs in CD4+ subsets (n = 8), and (F) inversely correlated with tumor size (n = 8). "ns", no significant differences; ***p<0.001; ****p<0.0001. Statistics used: A, B, Kruskal-Wallis test with post-hoc Dunn's multiple comparisons test; C, Mann Whitney test; D, E, F, Spearman correlation assay.

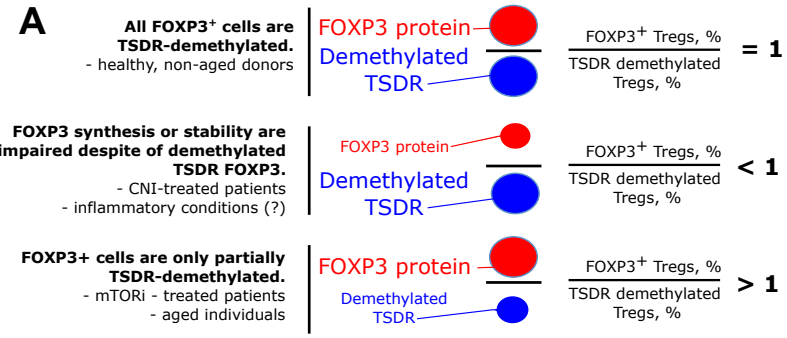

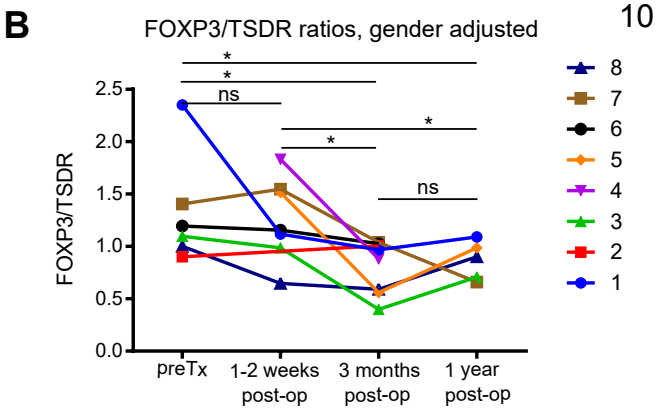

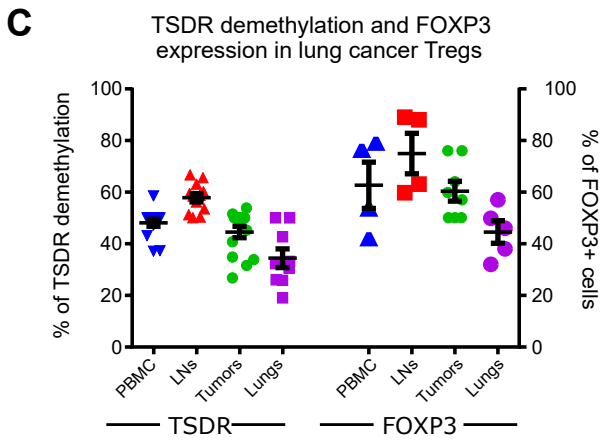

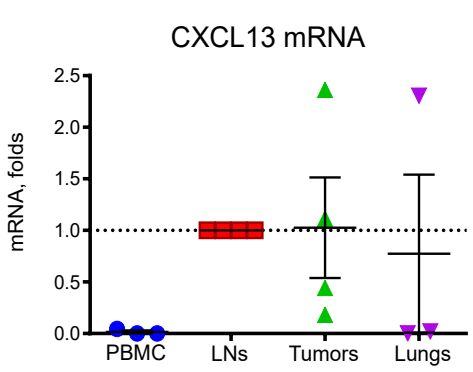

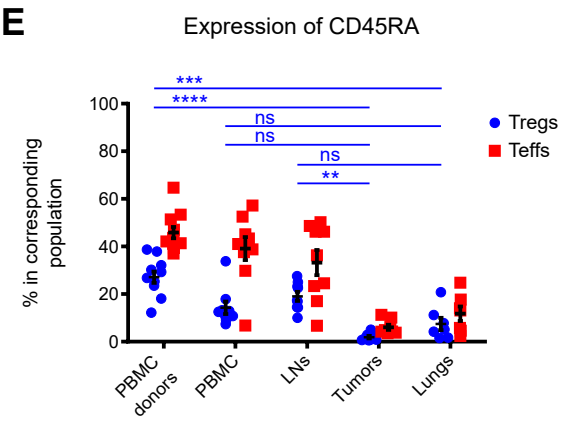

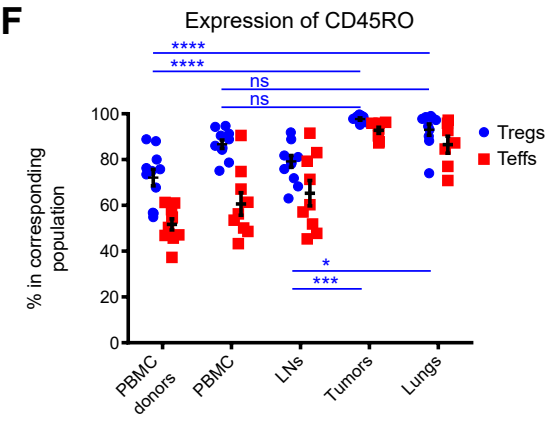

Supplemental Figure 4. Demethylation of TSDR FOXP3 in Tregs, trafficking and maturation of Tregs and Teffs. (A) FOXP3/TSDR ratio as a measure of iTreg and tTres subsets. Top: in healthy donors, majority of Tregs are cells expressing FOXP3 and completely demethylated at the TSDR. Middle: calcineurin inhibitors therapy (CNI) may disrupt NFAT signaling, leading to impaired FOXP3 promoter activation and decreased FOXP3 synthesis (22). Bottom: increased percent of partially methylated TSDR FOXP3 Tregs moves FOXP3/TSDR ratio up, as we showed previously in mTOR-inhibitor (Rapamycin) treated patients (23). Similarly, age-related thymic involution may lead to FOXP3/TSDR>1 in Tregs. (B) Ratios of FOXP3+ expression in isolated suppressive Tregs to percent of demethylated TSDR of FOXP3 (FOXP3/TSDR) in the same Treg cells were calculated for 8 liver transplant patients who were observed pre-operatively and 1-2 weeks, 3 months and 1 year after Tx. After Tx, all patients received calcineurin inhibitors therapy (CNI). Use of CNI corresponded with gradual decrease of FOXP3/TSDR ratios in Tregs. (C) Suppressive Tregs from LC samples were evaluated for their expression of FOXP3 (right) and percent of demethylated TSDR of FOXP3 was evaluated in the same samples (left part of the graph). At least 4 samples were included into each group. (D) RT-qPCR data for mRNA expression of CXCL13 in single cell suspensions of indicated samples. mRNA expression in LNs were set up as 1. At least three samples were evaluated for each mRNA. Expression of CD45RA (E) and CD45RO (F) were evaluated in Tregs vs. Teffs in different samples as indicated, at least in 7 samples in each group. "ns", no significant differences; *p<0.05; **p<0.01; ***p<0.001; ****p<0.0001. "Tx", transplantation. Statistics used: B, Friedman test with Dunn's test. Missing data (6 variables out of 32) were replaced by means of their group to increase statistical power of repeated measures data. E, F, Two-way ANOVA with Tukey's multiple comparisons test for row factor, a location of either Tregs or Teffs (PBMC vs. LNs vs. tumors etc.), and with Sidak's multiple comparisons test for column factor, to compare expression in Tregs vs. Teffs. Only p values in row factor in tumor and lung Tregs are shown in figures, and full data presented at Supplemental Table 9.

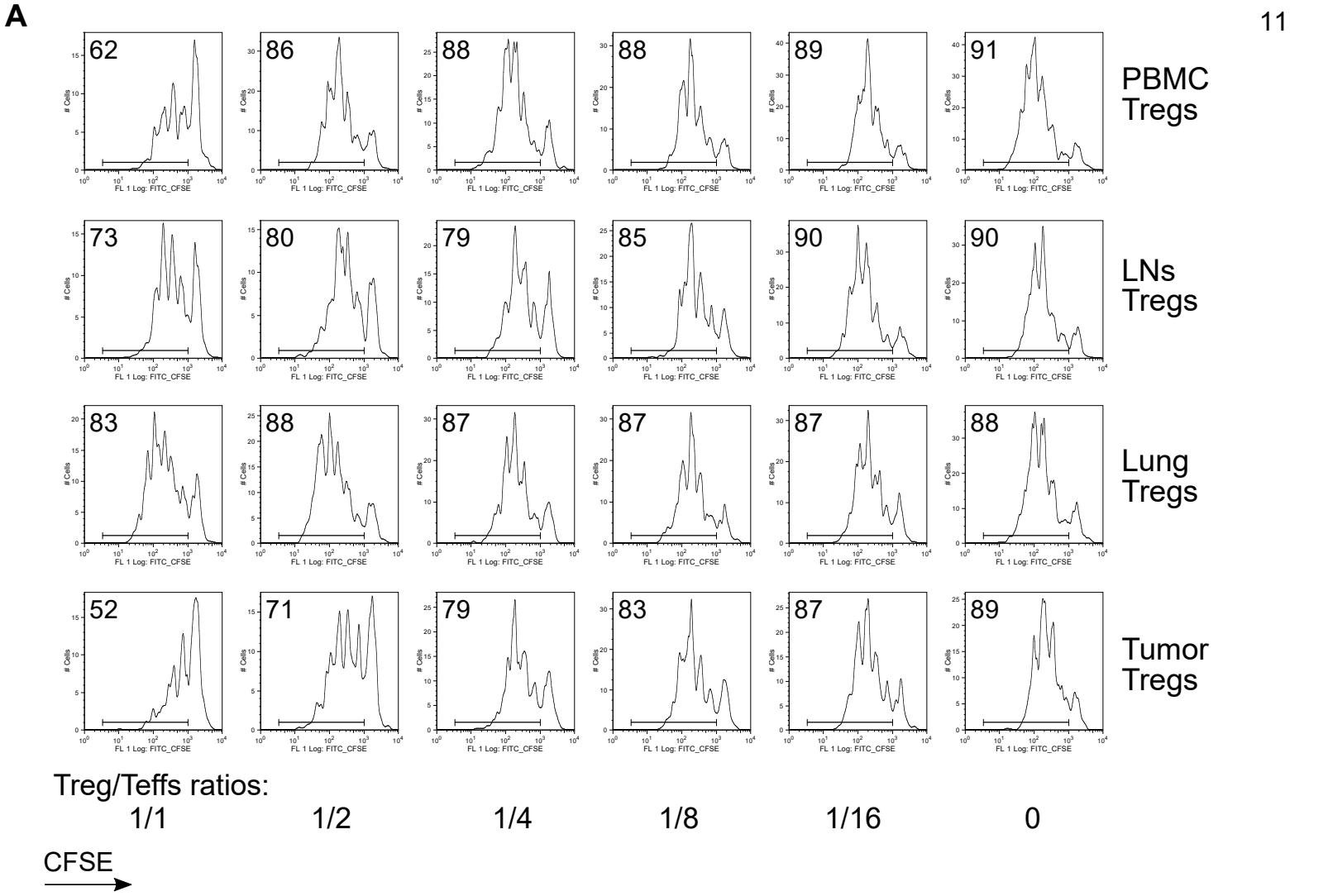

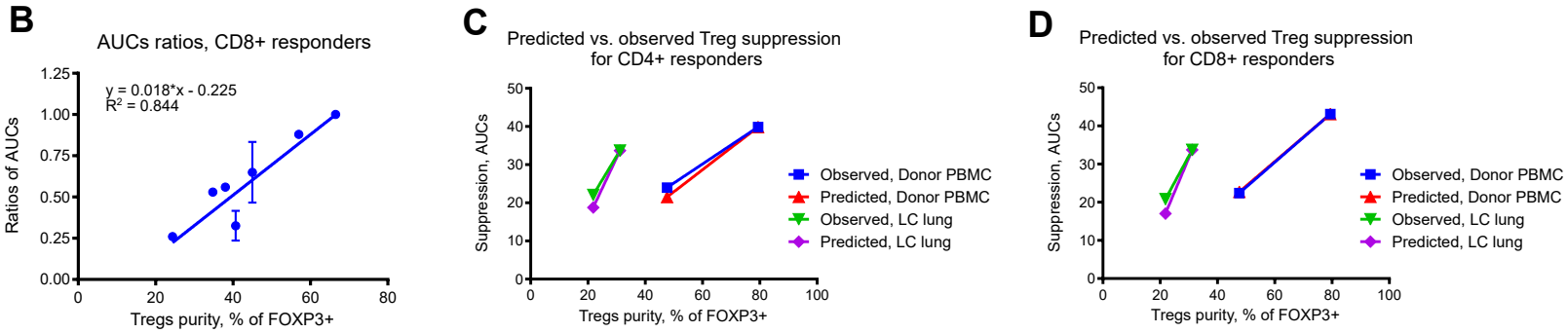

Supplemental Figure 5. Suppressive function of Tregs.
(A) Suppressive function of Tregs with CFSE+CD8+ healthy donor responders. One representative experiment out of 45 is shown. The suppressive function of the same Tregs towards CD4+ responders is illustrated at Figure 5A. (B) Resulting equation of regression analysis performed with 5 Treg samples with different FOXP3+ purities as described in Results. This equation shows how Treg lose their capability to suppressive CD8+ responders when they were isolated with decreased FOXP3+ purity. The corresponding data for CD4+ responders are presented at Figure 5D. Observed vs. predicted suppressive function of Tregs for (C) CD4+ and (D) CD8+ responders, evaluated for one healthy donor and one lung cancer, distant lung Tregs, to validate equations of regression analyses shown at (B) and Figure 5D. Statistics used: B - linear regression analysis.

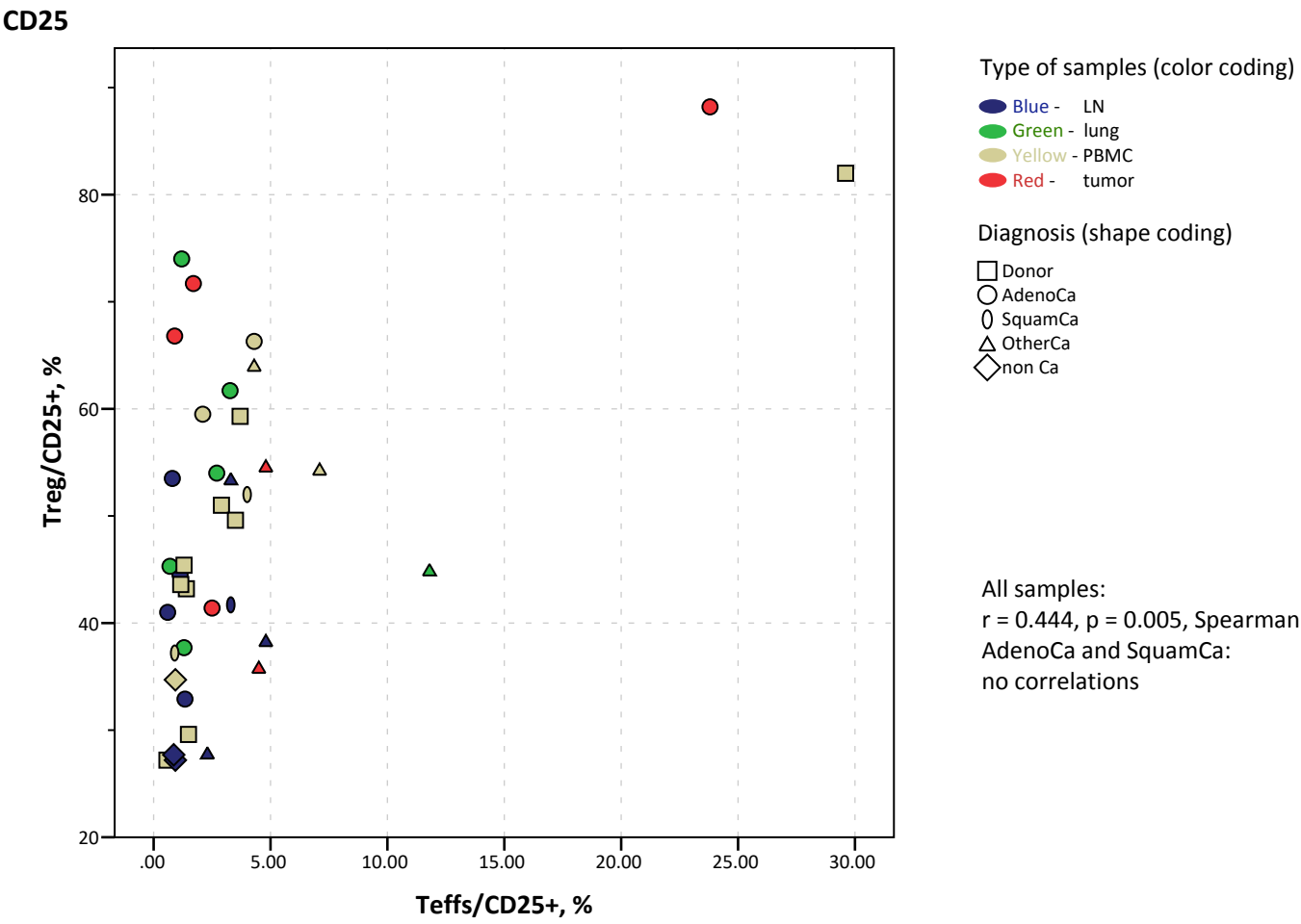

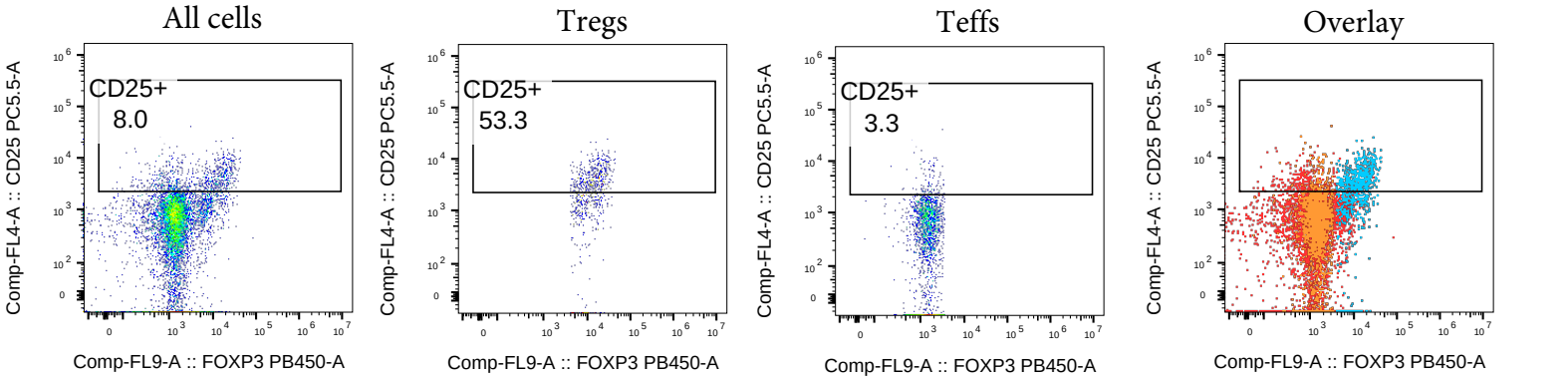

Subset Name	Median : Comp-FL4-A
Tregs	2541.8
CD4+Teffs	130.5
live	439.0

Supplemental Figure 6. CD25 expression in Tregs versus Teffs.
Top: correlation of CD25+ expression in CD4+FOXP3+ Tregs (y) and in CD4+FOXP3- Teffs (x), Spearman's correlation assay, n = 38. Different type of samples are coded by color, as indicated in legend. Shapes of symbols represent diagnostic categories, as indicated in legend. When adenocarcinoma and squamous cells carcinoma samples were analyzed separately, expression of CD25 in Tregs and Teffs had no correlations. Bottom: gating strategy and the representative expression of CD25+ in Tregs and Teffs are shown, with corresponding MOF for CD25 in all viable cells (red), CD4+FOXP3+ Tregs (blue) and CD4+FOXP3- Teffs (orange). "Donor" - healthy donors, "AdenoCa" - adenocarcinoma, "SquamCa" - squamous cell carcinoma, "OtherCa" - other types of cancers: large cell neuroendocrine carcinoma, lung metastasis of colon adenocarcinoma, high grade carcinoma or melanoma. "Non Ca" - non-cancer patients with diaphragmatic hernia, sarcoidosis or interstitial lung disease.

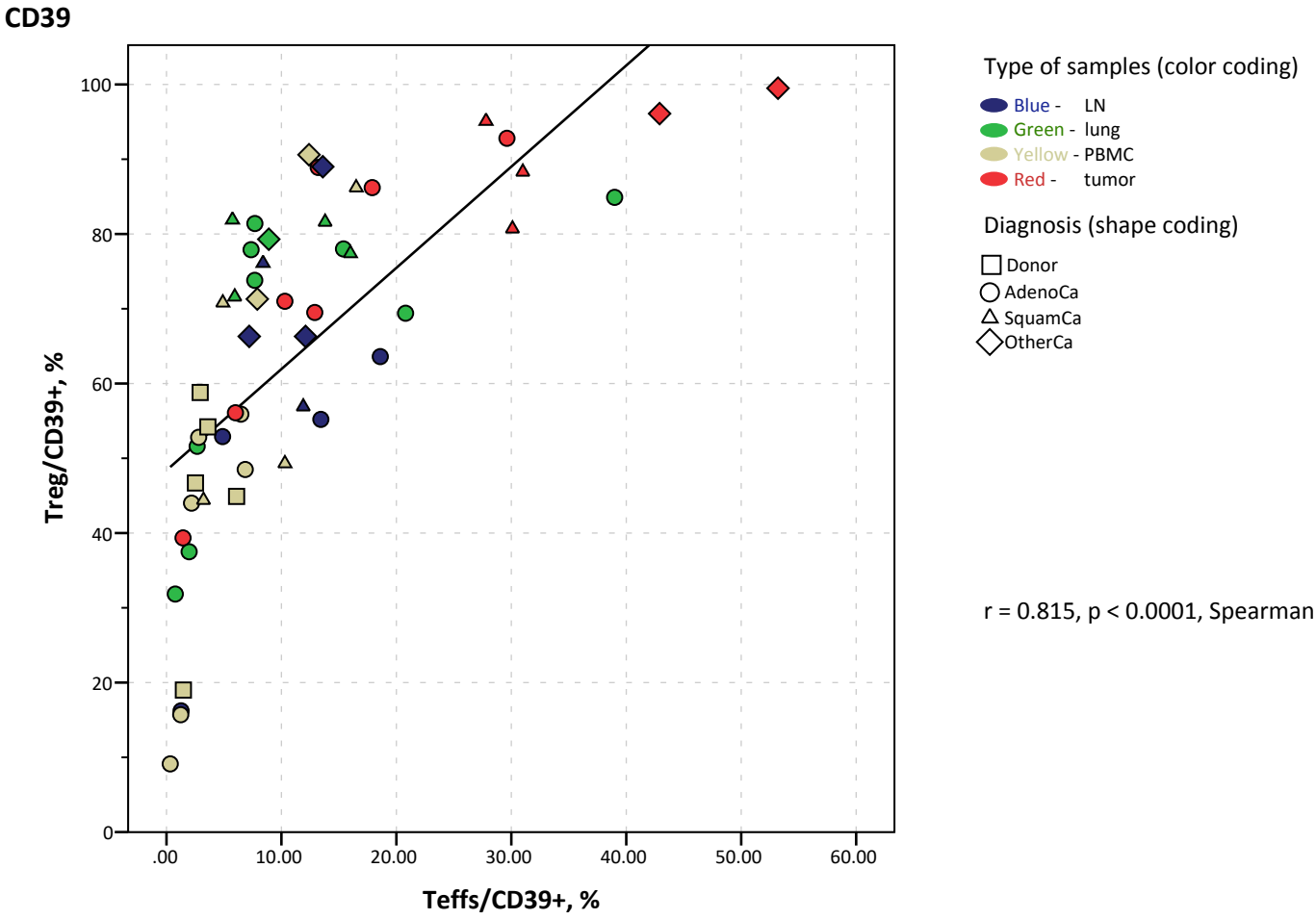

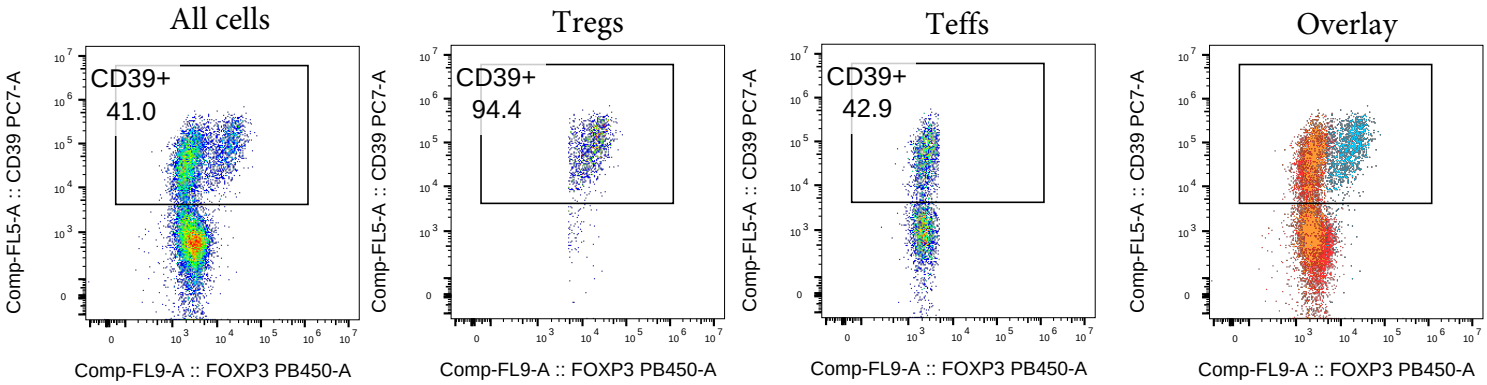

	Subset Name	Median : Comp-FL5-A
	Tregs	75510.5
	CD4+Teffs	2181.5
	live	1474.7

Supplemental Figure 7. CD39 expression in Tregs versus Teffs.
Top: correlation of CD39+ expression in CD4+FOXP3+ Tregs (y) and in CD4+FOXP3- Teffs (x), Spearman's correlation assay, n = 54. Different type of samples are coded by color, as indicated in legend. Shapes of symbols represent diagnostic categories, as indicated in legend. Bottom: gating strategy and the representative expression of CD39+ in Tregs and Teffs are shown, with corresponding MOF for CD39 in all viable cells (red), CD4+FOXP3+ Tregs (blue) and CD4+FOXP3- Teffs (orange). "Donor" - healthy donors, "AdenoCa" - adenocarcinoma, "SquamCa" - squamous cell carcinoma, "OtherCa" - other types of cancers: large cell neuroendocrine carcinoma, lung metastasis of colon adenocarcinoma, high grade carcinoma or melanoma.

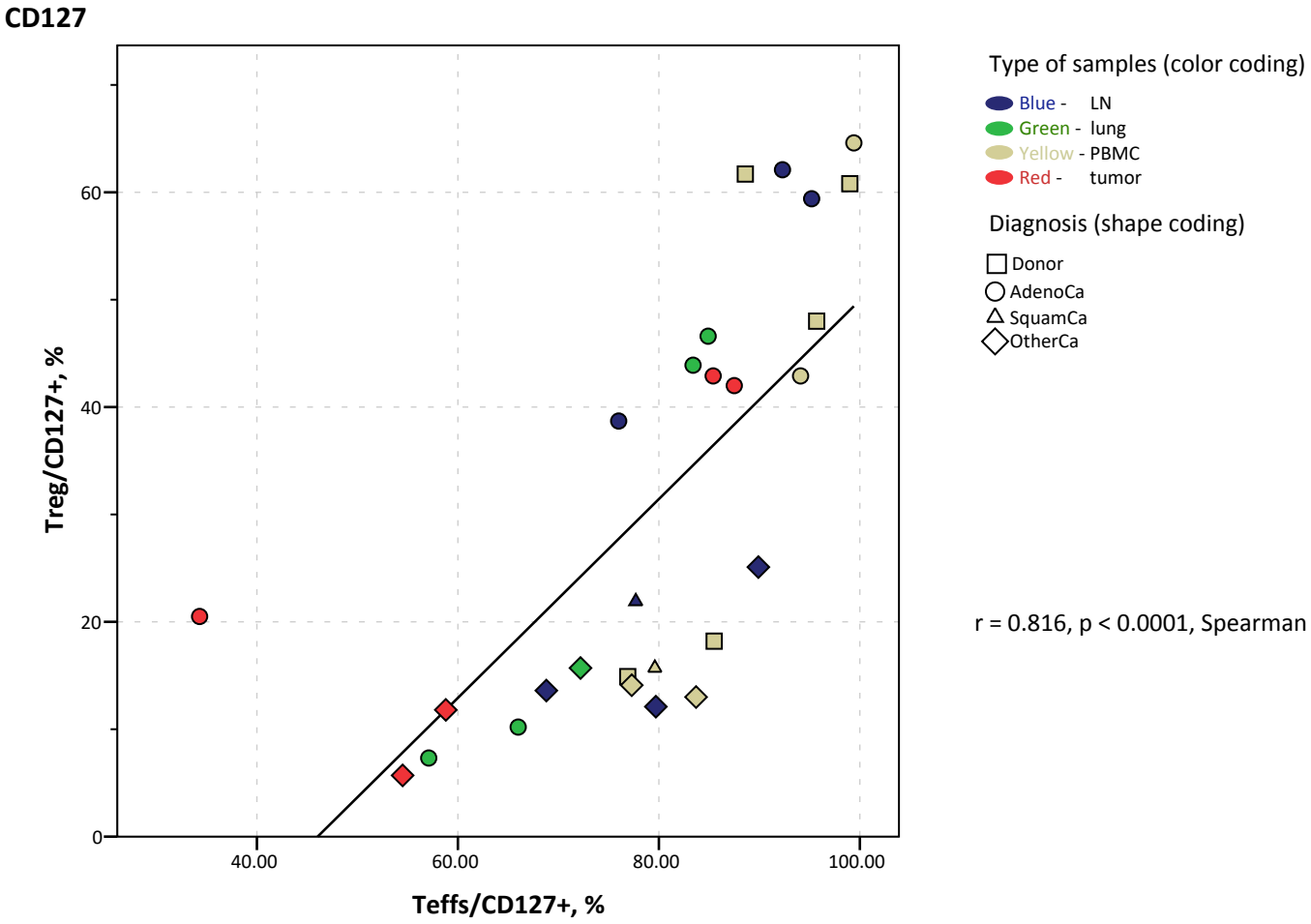

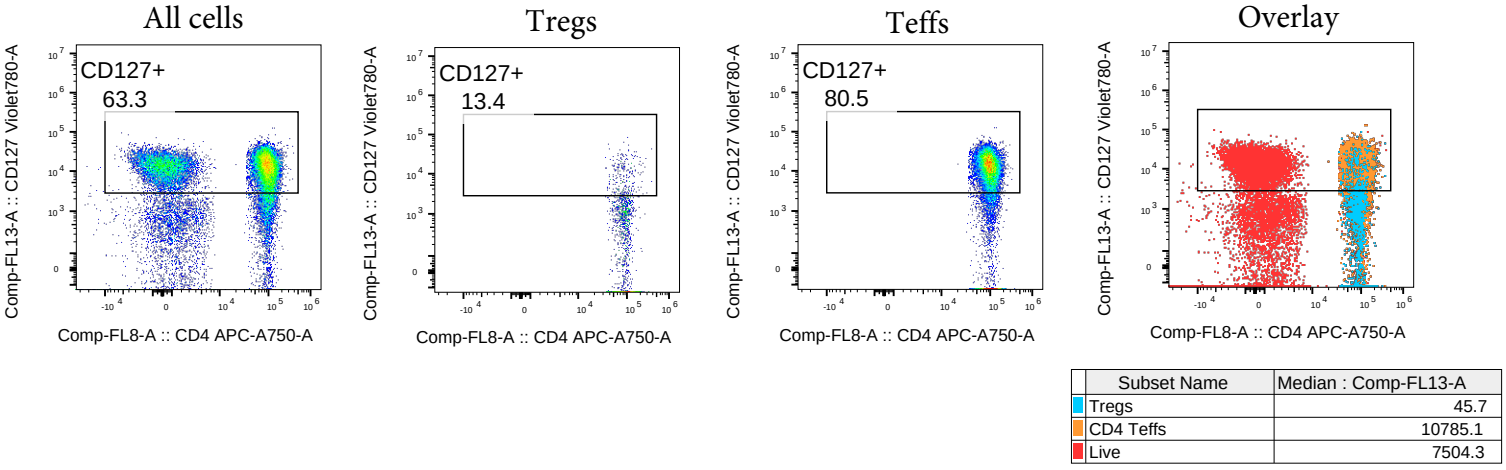

Subset Name	Median : Comp-FL13-A
Tregs	45.7
CD4 Teffs	10785.1
Live	7504.3

Supplemental Figure 8. CD127 expression in Tregs versus Teffs.
Top: correlation of CD127+ expression in CD4+FOXP3+ Tregs (y) and in CD4+FOXP3- Teffs (x), Spearman's correlation assay, n = 27. Different type of samples are coded by color, as indicated in legend. Shapes of symbols represent diagnostic categories, as indicated in legend. Bottom: gating strategy and the representative expression of CD127+ in Tregs and Teffs are shown, with corresponding MOF for CD127 in all viable cells (red), CD4+FOXP3+ Tregs (blue) and CD4+FOXP3- Teffs (orange). "Donor" - healthy donors, "AdenoCa" - adenocarcinoma, "SquamCa" - squamous cell carcinoma, "OtherCa" - other types of cancers: large cell neuroendocrine carcinoma, lung metastasis of colon adenocarcinoma, high grade carcinoma or melanoma.

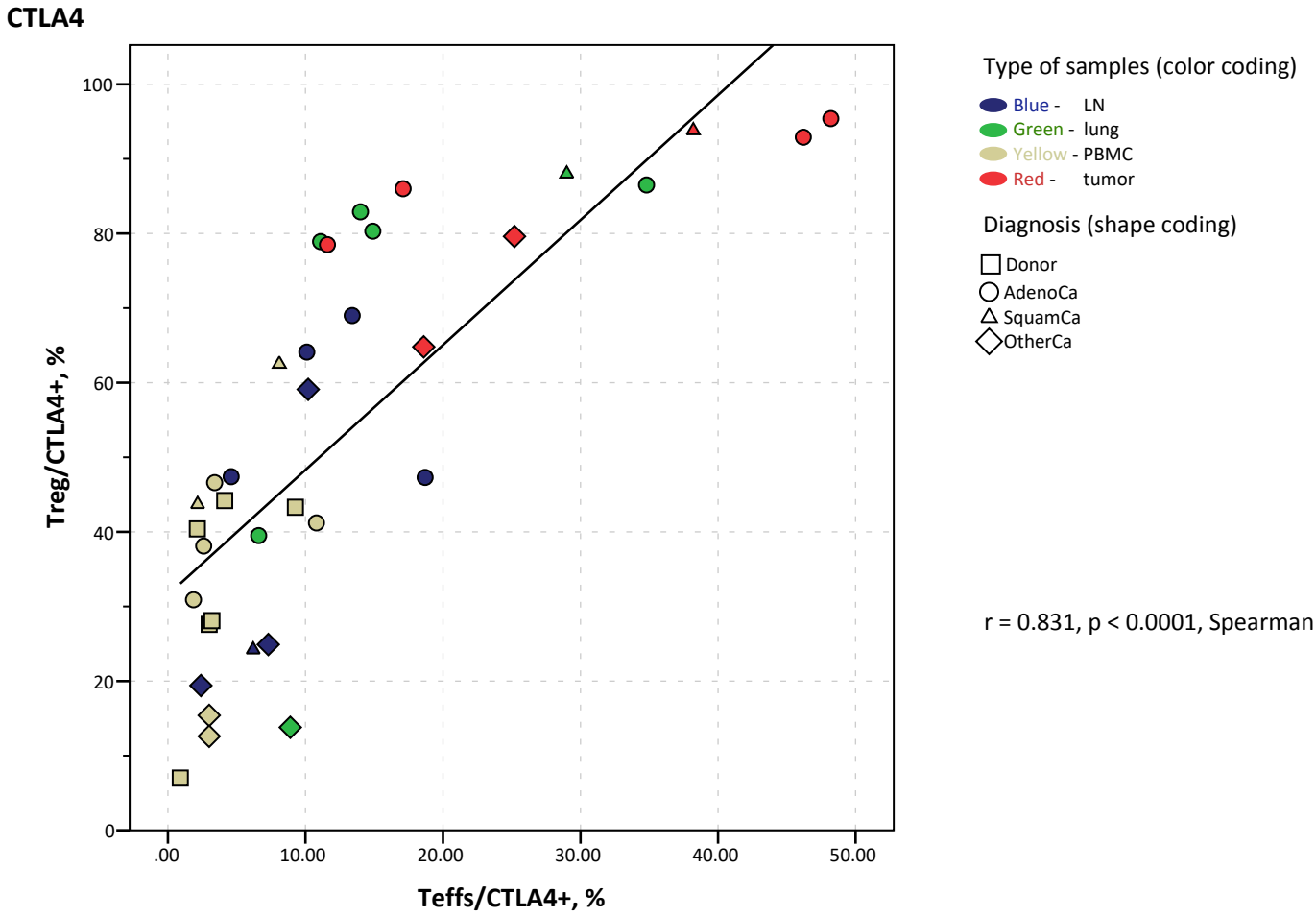

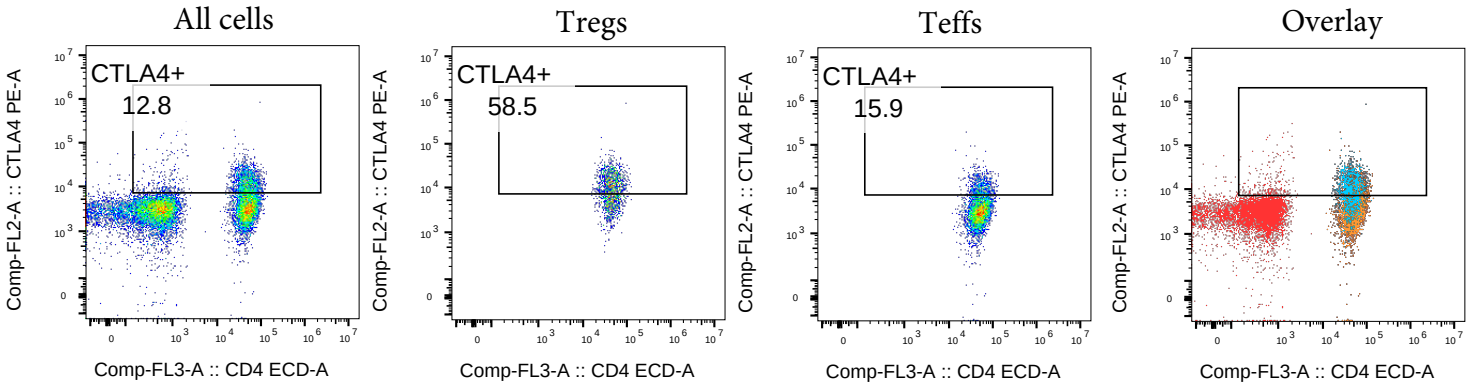

Subset Name	Median : Comp-FL2-A
Tregs	9010.2
CD4+Teffs	3246.0
live	3246.0

Supplemental Figure 9. CTLA4 expression in Tregs versus Teffs.
Top: correlation of CTLA4+ expression in CD4+FOXP3+ Tregs (y) and in CD4+FOXP3- Teffs (x), Spearman's correlation assay, n = 38. Different type of samples are coded by color, as indicated in legend. Shapes of symbols represent diagnostic categories, as indicated in legend. Bottom: gating strategy and the representative expression of CTLA4+ in Tregs and Teffs are shown, with corresponding MOF for CTLA4 in all viable cells (red), CD4+FOXP3+ Tregs (blue) and CD4+FOXP3- Teffs (orange). CTLA4 was evaluated by intracellular staining of fixed and permeabilized cells. "Donor" - healthy donors, "AdenoCa" - adenocarcinoma, "SquamCa" - squamous cell carcinoma, "OtherCa" - other types of cancers: large cell neuroendocrine carcinoma, lung metastasis of colon adenocarcinoma, high grade carcinoma or melanoma.

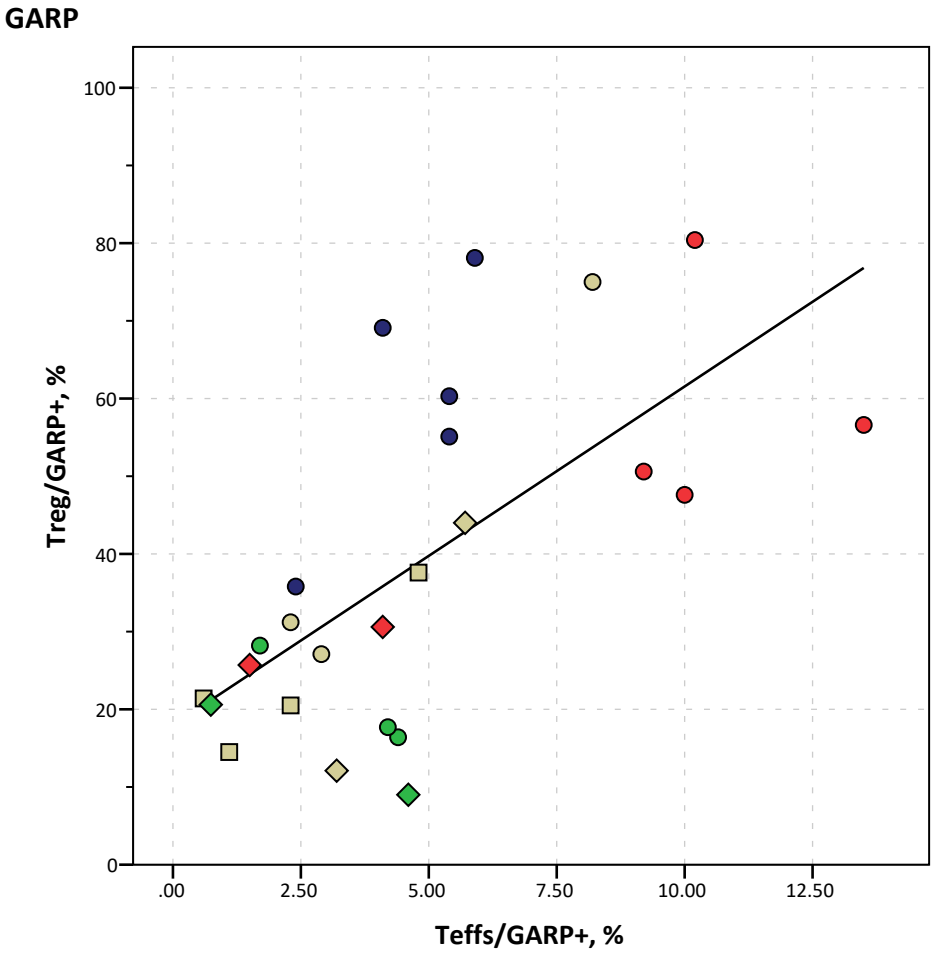

Type of samples (color coding)

- Blue - LN
- Green - lung
- Yellow - PBMC
- Red - tumor

Diagnosis (shape coding)

- Donor
- AdenoCa
- SquamCa

All samples:
r = 0.665, p < 0.0001, Spearman
AdenoCa and Donors:
r = 0.715, p = 0.01, Spearman

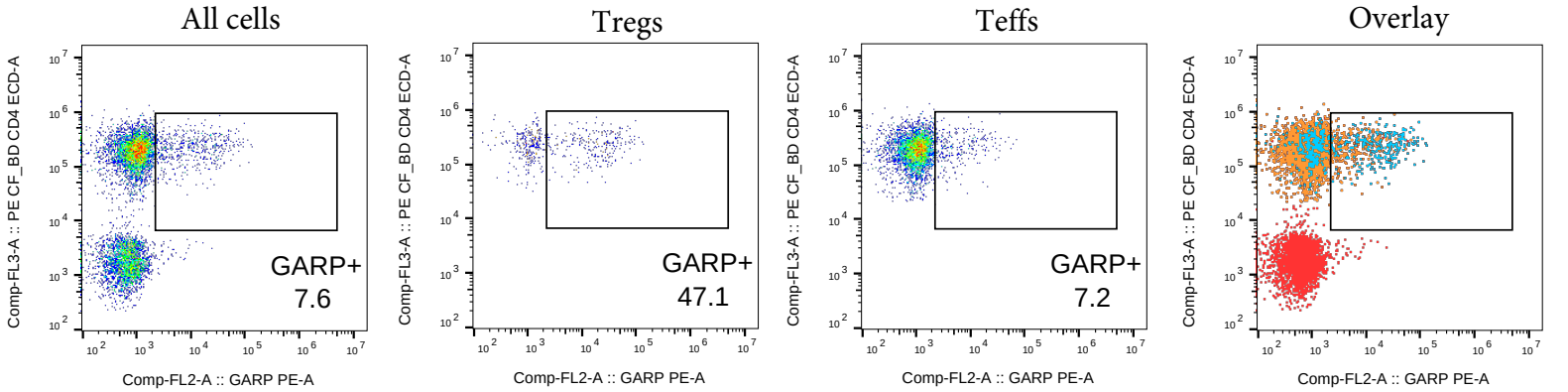

Subset Name	Median : Comp-FL2-A
FOXP3+	1778.5
CD4+Teffs	1057.5
live	923.9

LC235 PBMC A1.fcs
live
7420.0

LC235 PBMC A1.fcs
FOXP3+
561.0

LC235 PBMC A1.fcs
CD4+Teffs
4029.0

Supplemental Figure 10. GARP expression in Tregs versus Teffs.
Top: correlation of GARP+ expression in CD4+FOXP3+ Tregs (y) and in CD4+FOXP3- Teffs (x), Spearman's correlation assay, n = 25. Different types of samples are coded by color, as indicated in legend. Shapes of symbols represent diagnostic categories, as indicated in legend. Bottom: gating strategy and the representative expression of GARP+ in Tregs and Teffs are shown, with corresponding MOF for GARP in all viable cells (red), CD4+FOXP3+ Tregs (blue) and CD4+FOXP3- Teffs (orange). GARP was evaluated after stimulation for 2 days with CD3/28 beads at 1/1 ratio in T cell media. "Donor" - healthy donors, "AdenoCa" - adenocarcinoma, "SquamCa" - squamous cell carcinoma.

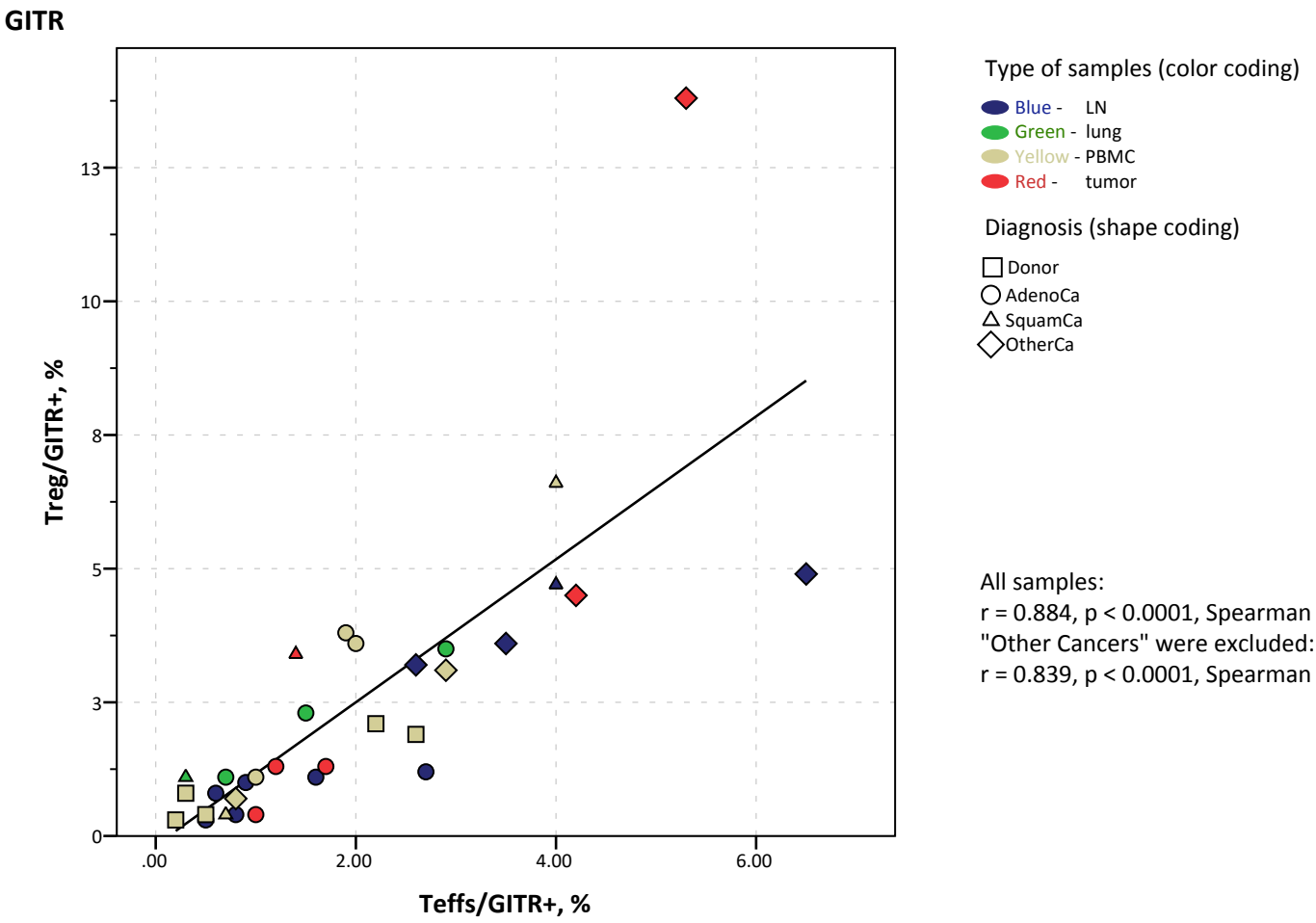

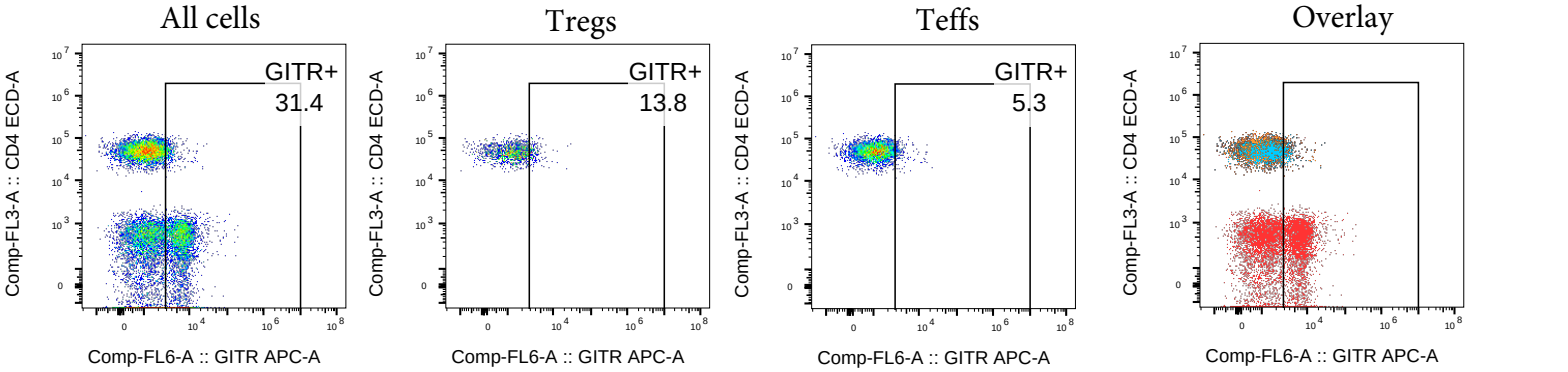

	Subset Name	Median : Comp-FL6-A
	Tregs	1399.5
	CD4+Teffs	1146.2
	live	1582.7

Supplemental Figure 11. GITR expression in Tregs versus Teffs.
Top: correlation of GITR+ expression in CD4+FOXP3+ Tregs (y) and in CD4+FOXP3- Teffs (x), Spearman's correlation assay, n = 32. Different types of samples are coded by color, as indicated in legend. Shapes of symbols represent diagnostic categories, as indicated in legend. Bottom: gating strategy and the representative expression of GITR+ in Tregs and Teffs are shown, with corresponding MOF for GITR in all viable cells (red), CD4+FOXP3+ Tregs (blue) and CD4+FOXP3- Teffs (orange). "Donor" - healthy donors, "AdenoCa" - adenocarcinoma, "SquamCa" - squamous cell carcinoma, "OtherCa" - other types of cancers: large cell neuroendocrine carcinoma, lung metastasis of colon adenocarcinoma, high grade carcinoma or melanoma.

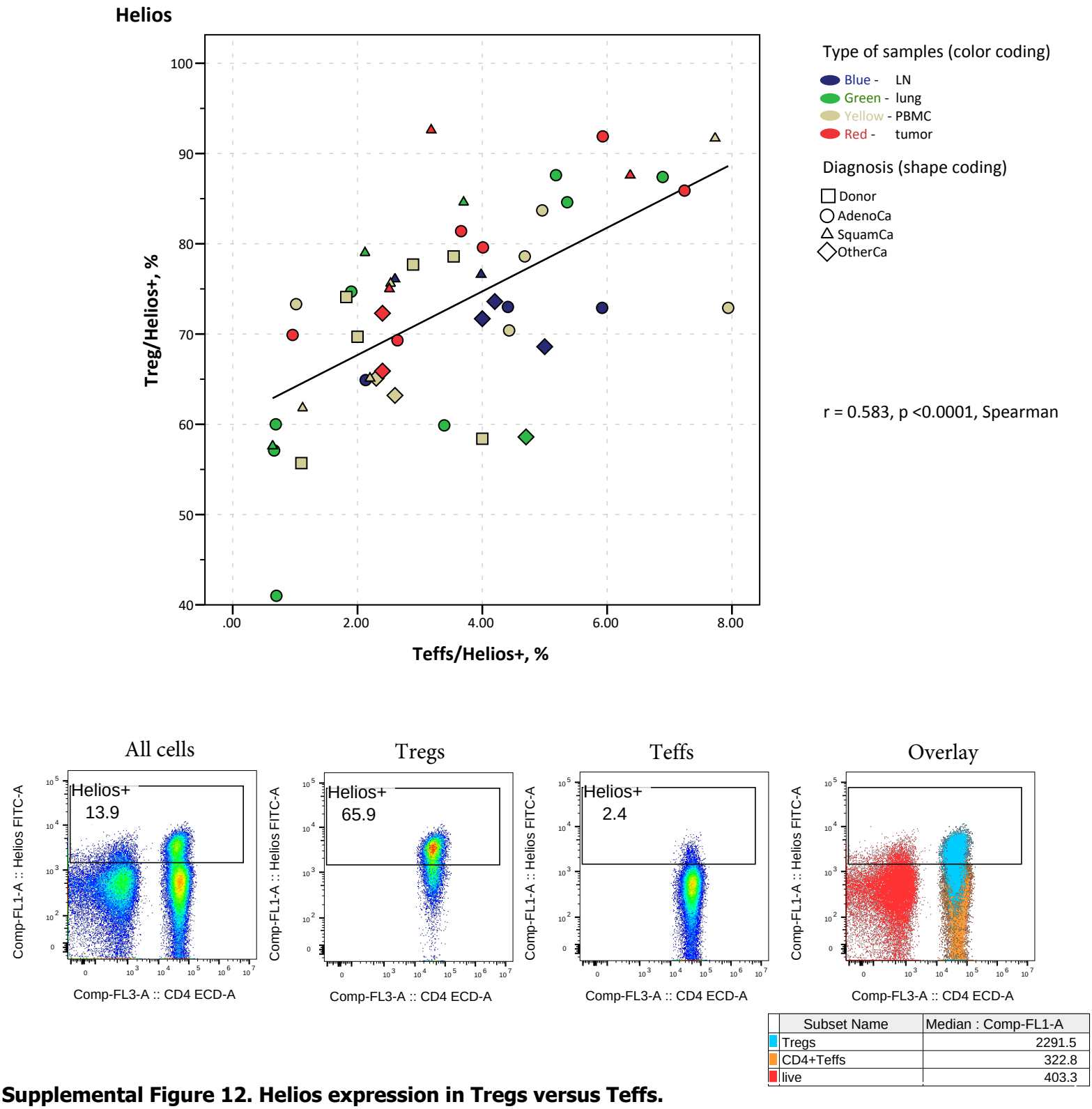

Supplemental Figure 12. Helios expression in Tregs versus Teffs.
Top: correlation of Helios+ expression in CD4+FOXP3+ Tregs (y) and in CD4+FOXP3- Teffs (x), Spearman's correlation assay, n = 49. Different types of samples are coded by color, as indicated in legend. Shapes of symbols represent diagnostic categories, as indicated in legend. Bottom: gating strategy and the representative expression of Helios+ in Tregs and Teffs are shown, with corresponding MOF for Helios in all viable cells (red), CD4+FOXP3+ Tregs (blue) and CD4+FOXP3- Teffs (orange). Helios was evaluated by intranuclear staining of fixed and permeabilized cells. "Donor" - healthy donors, "AdenoCa" - adenocarcinoma, "SquamCa" - squamous cells carcinoma, "OtherCa" - other types of cancers: large cell neuroendocrine carcinoma, lung metastasis of colon adenocarcinoma, high grade carcinoma or melanoma.

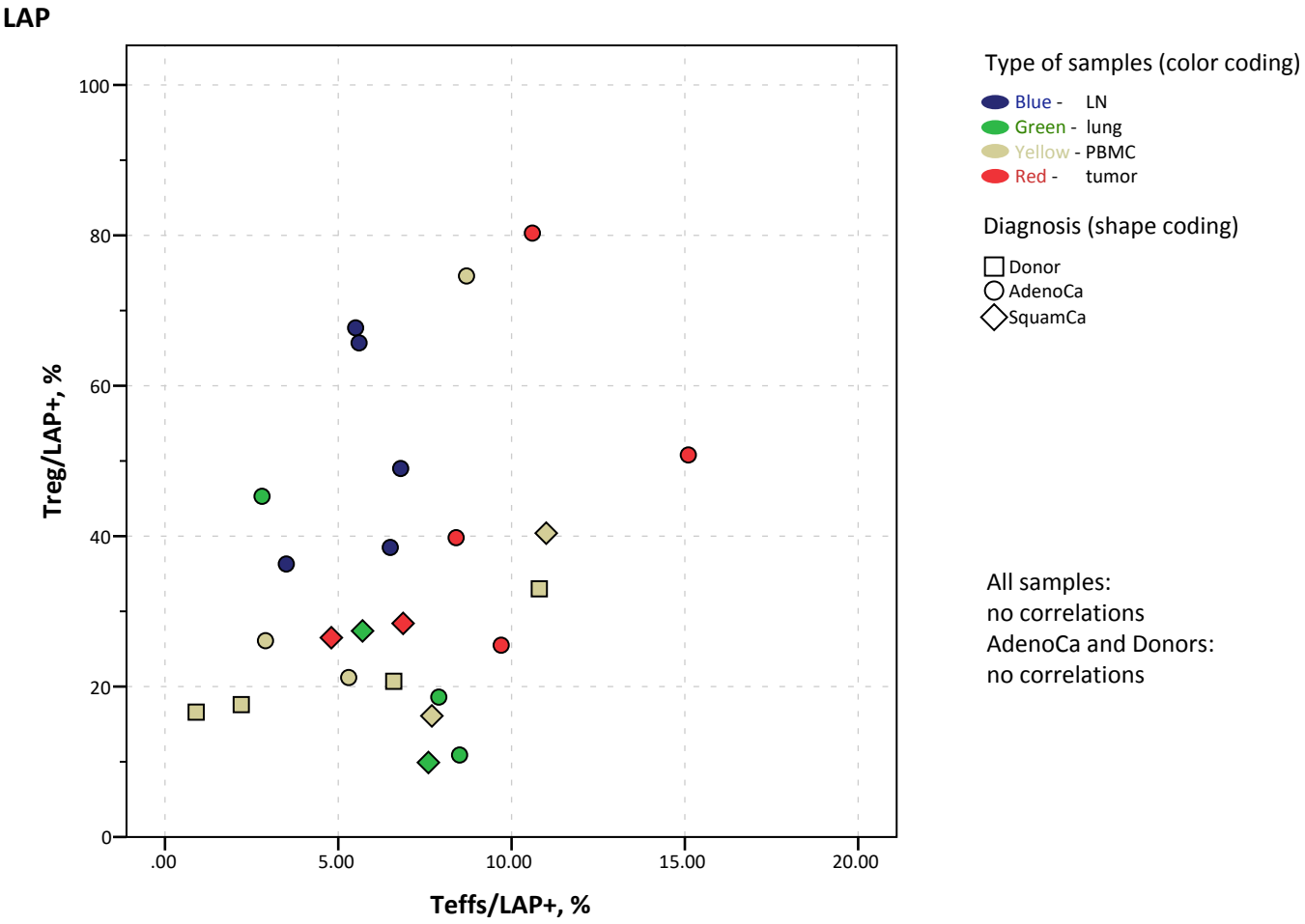

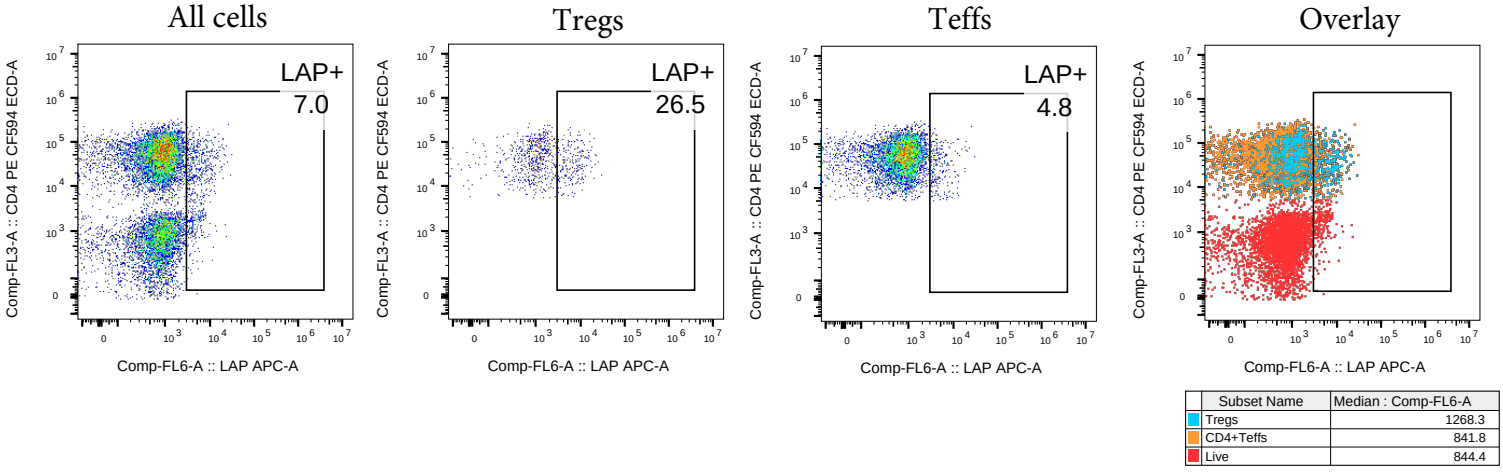

Supplemental Figure 13. LAP expression in Tregs versus Teffs.
Top: correlation of LAP+ expression in CD4+FOXP3+ Tregs (y) and in CD4+FOXP3- Teffs (x), Spearman's correlation assay, n = 25. Different types of samples are coded by color, as indicated in legend. Shapes of symbols represent diagnostic categories, as indicated in legend. Bottom: gating strategy and the representative expression of LAP+ in Tregs and Teffs are shown, with corresponding MOF for LAP in all viable cells (red), CD4+FOXP3+ Tregs (blue) and CD4+FOXP3- Teffs (orange). LAP was evaluated after stimulation for 2 days with CD3/28 beads at 1/1 ratio in T cell media. Tregs and Teffs have no correlations in their expression of LAP. "Donor" - healthy donors, "AdenoCa" - adenocarcinoma, "SquamCa" - squamous cells carcinoma.

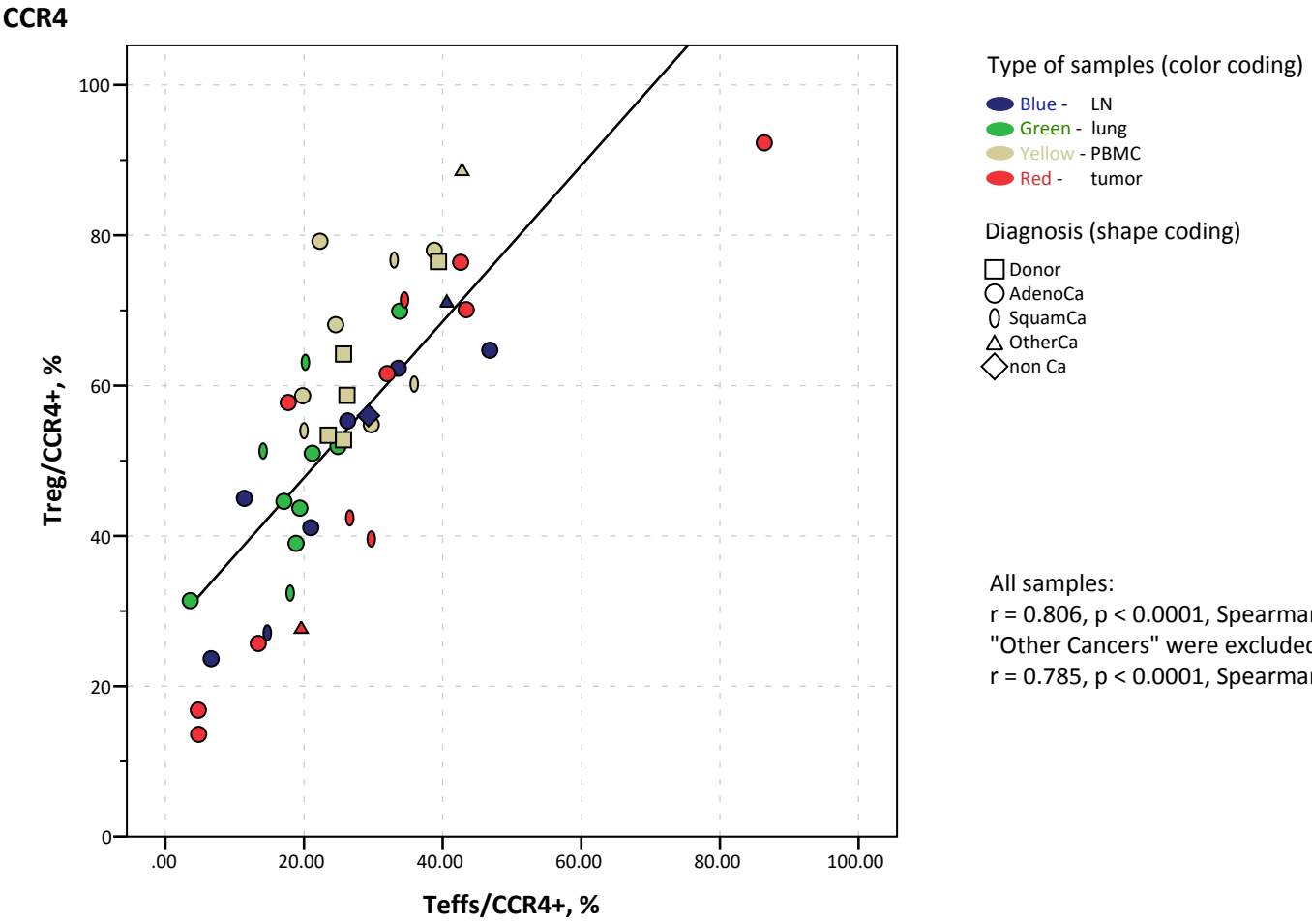

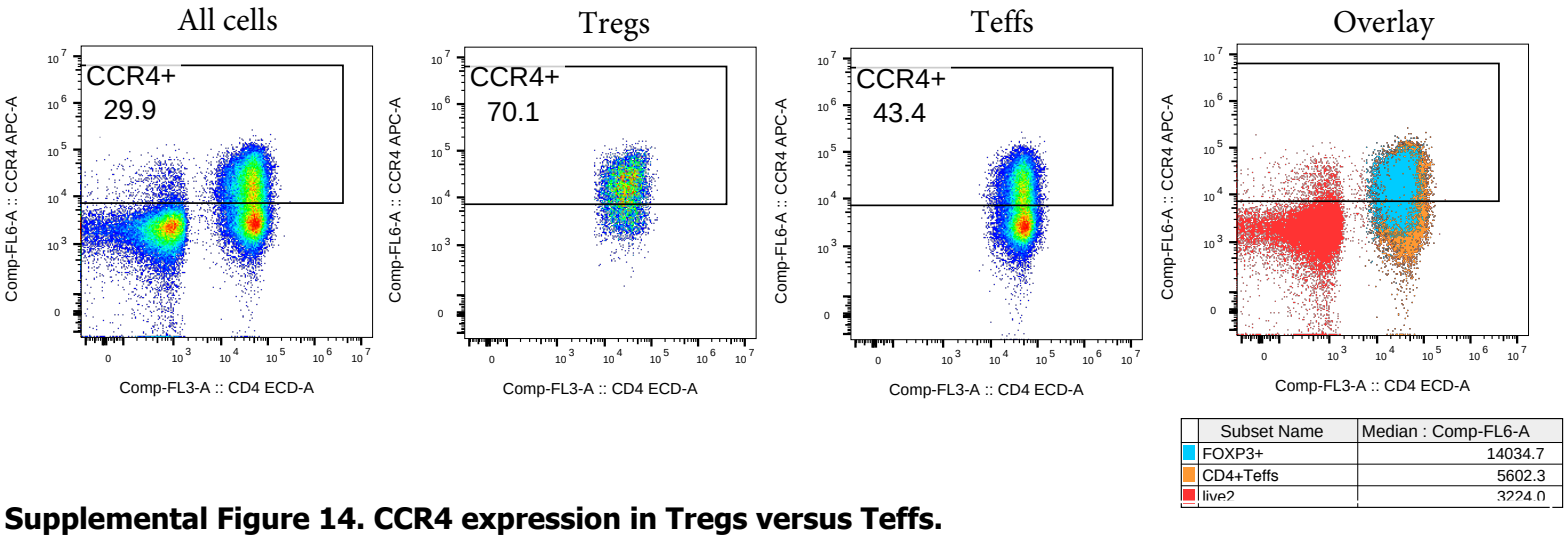

Supplemental Figure 14. CCR4 expression in Tregs versus Teffs.
Top: correlation of CCR4+ expression in CD4+FOXP3+ Tregs (y) and in CD4+FOXP3- Teffs (x), Spearman's correlation assay, n = 45. Different types of samples are coded by color, as indicated in legend. Shapes of symbols represent diagnostic categories, as indicated in legend. Bottom: gating strategy and the representative expression of CCR4+ in Tregs and Teffs are shown, with corresponding MOF for CCR4 in all viable cells (red), CD4+FOXP3+ Tregs (blue) and CD4+FOXP3- Teffs (orange). "Donor" - healthy donors, "AdenoCa" - adenocarcinoma, "SquamCa" - squamous cells carcinoma, "OtherCa" - other types of cancers: large cell neuroendocrine carcinoma, lung metastasis of colon adenocarcinoma, high grade carcinoma or melanoma. "Non Ca" - non-cancer patients with diaphragmal hernia, sarcoidosis or interstitial lung disease.

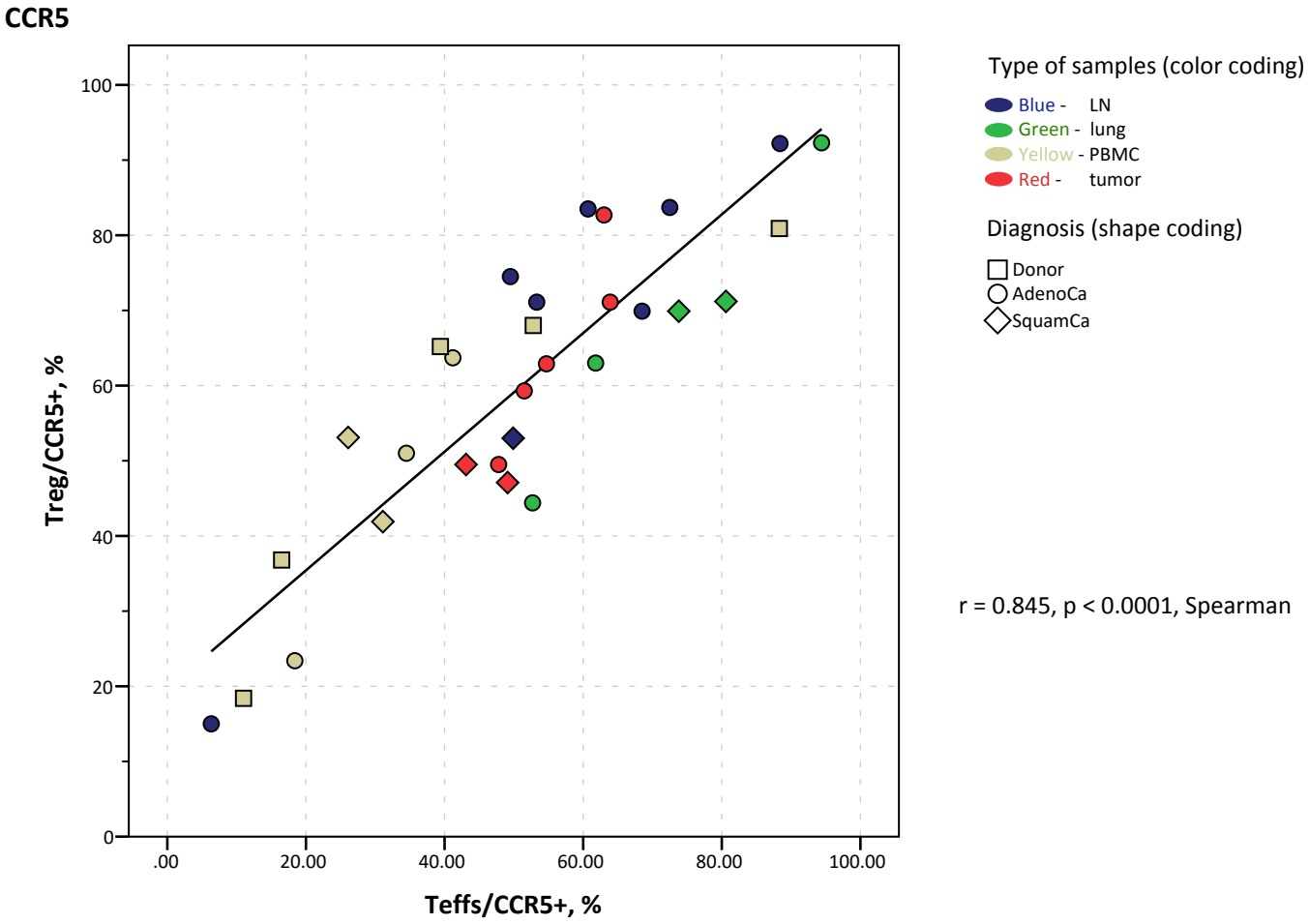

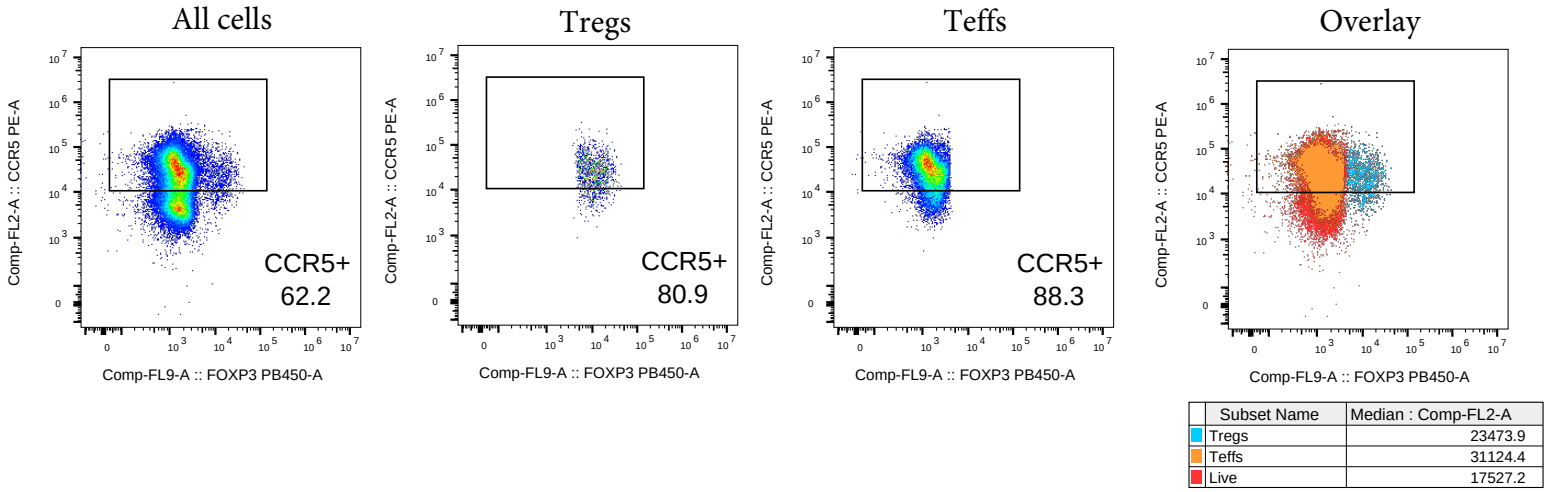

Subset Name	Median : Comp-FL2-A
Tregs	23473.9
Teffs	31124.4
Live	17527.2

Supplemental Figure 15. CCR5 expression in Tregs versus Teffs.
Top: correlation of CCR5+ expression in CD4+FOXP3+ Tregs (y) and in CD4+FOXP3- Teffs (x), Spearman's correlation assay, n = 30. Different types of samples are coded by color, as indicated in legend. Shapes of symbols represent diagnostic categories, as indicated in legend. Bottom: gating strategy and the representative expression of CCR5+ in Tregs and Teffs are shown, with corresponding MOF for CCR5 in all viable cells (red), CD4+FOXP3+ Tregs (blue) and CD4+FOXP3- Teffs (orange). "Donor" - healthy donors, "AdenoCa" - adenocarcinoma, "SquamCa" - squamous cell carcinoma.

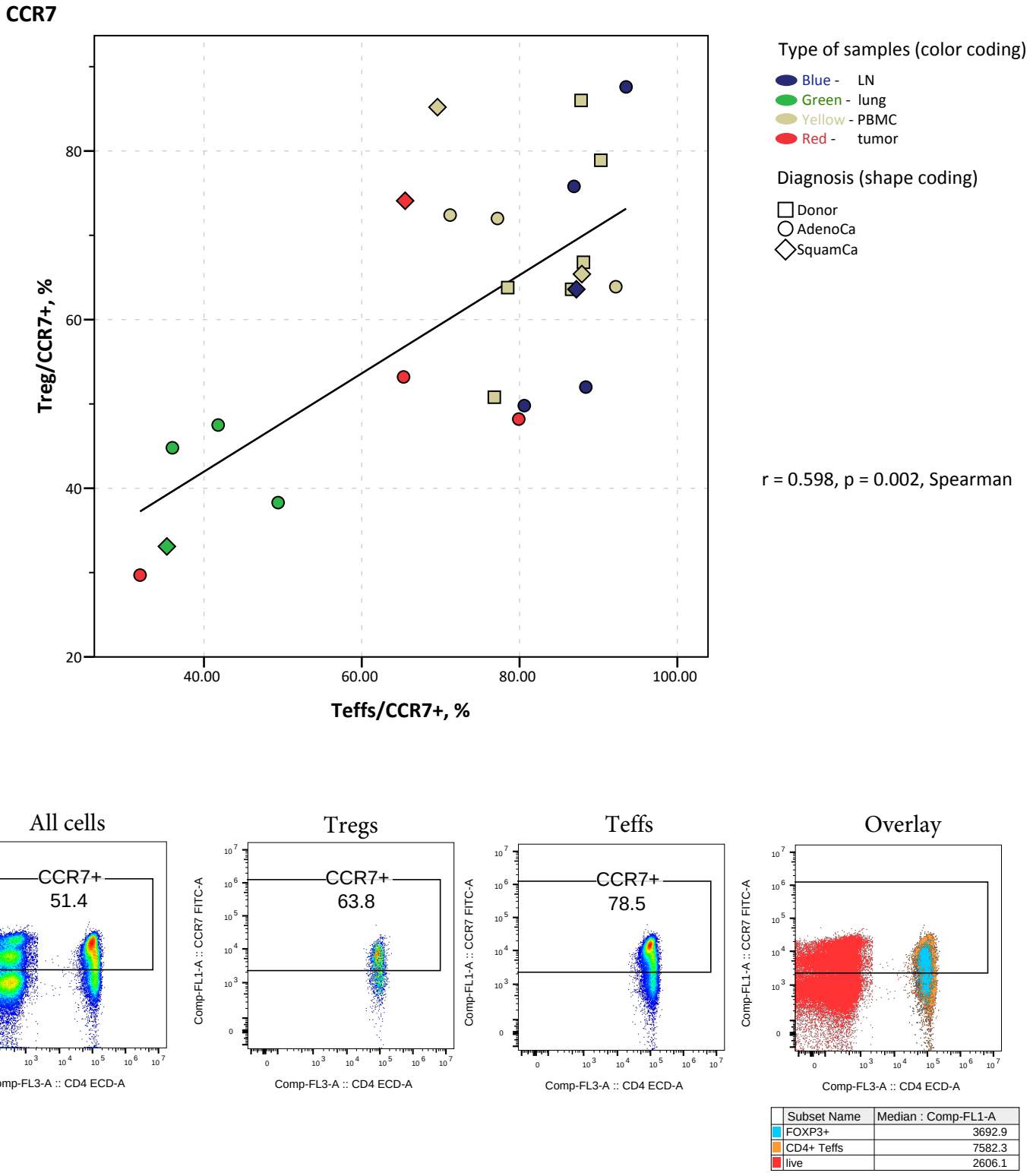

Supplemental Figure 16. CCR7 expression in Tregs versus Teffs.
Top: correlation of CCR7+ expression in CD4+FOXP3+ Tregs (y) and in CD4+FOXP3- Teffs (x), Spearman's correlation assay, n = 24. Different types of samples are coded by color, as indicated in legend. Shapes of symbols represent diagnostic categories, as indicated in legend. Bottom: gating strategy and the representative expression of CCR7+ in Tregs and Teffs are shown, with corresponding MOF for CCR7 in all viable cells (red), CD4+FOXP3+ Tregs (blue) and CD4+FOXP3- Teffs (orange). "Donor" - healthy donors, "AdenoCa" - adenocarcinoma, "SquamCa" - squamous cell carcinoma.

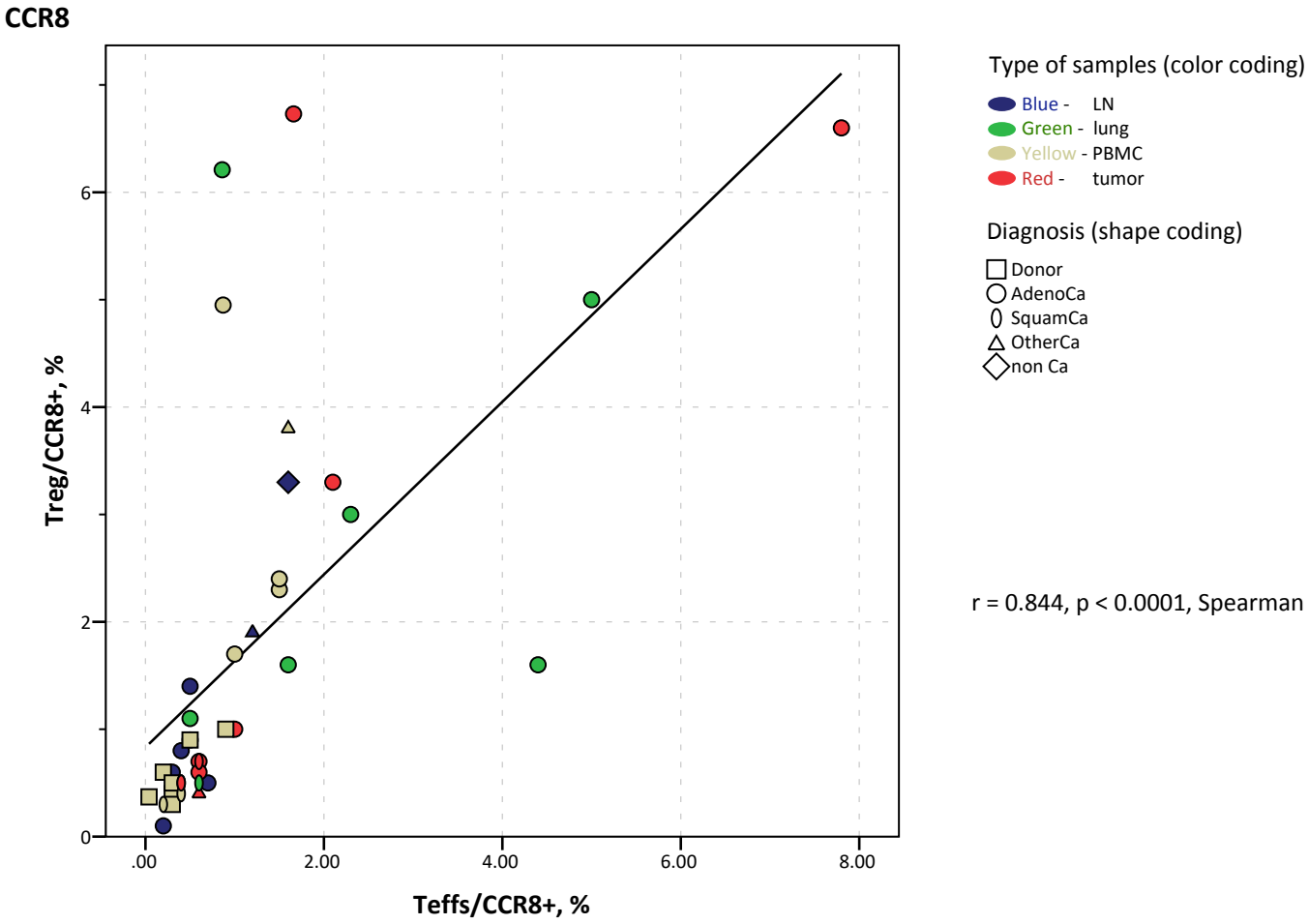

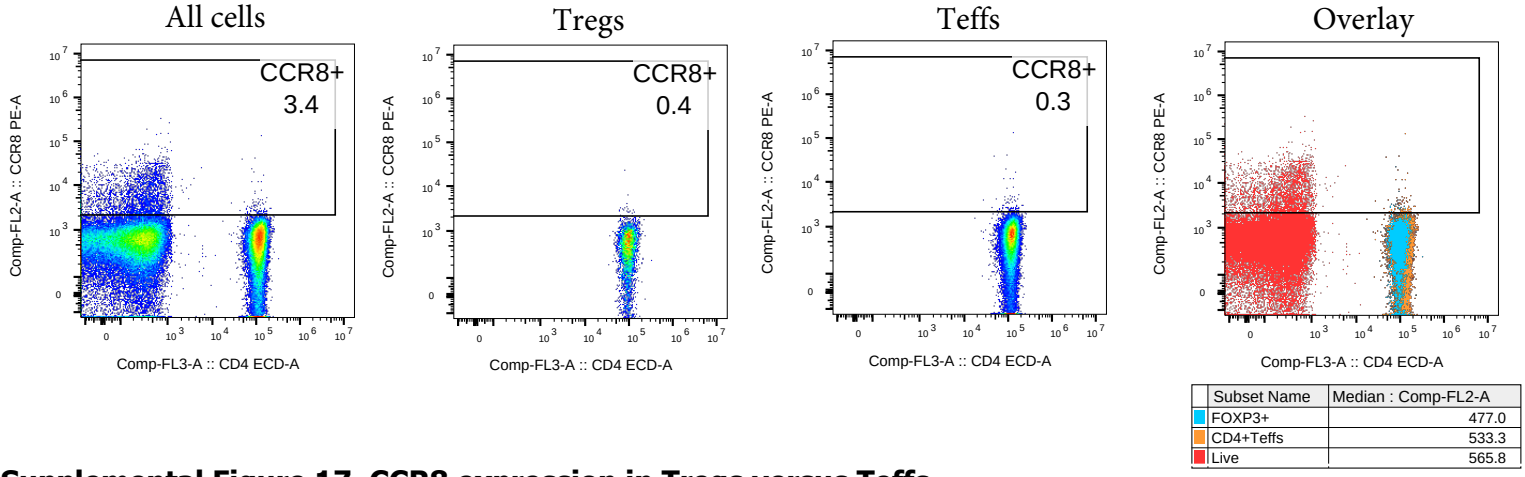

Supplemental Figure 17. CCR8 expression in Tregs versus Teffs.
Top: correlation of CCR8+ expression in CD4+FOXP3+ Tregs (y) and in CD4+FOXP3- Teffs (x), Spearman's correlation assay, n = 39. Different types of samples are coded by color, as indicated in legend. Shapes of symbols represent diagnostic categories, as indicated in legend. Bottom: gating strategy and the representative expression of CCR8+ in Tregs and Teffs are shown, with corresponding MOF for CCR8 in all viable cells (red), CD4+FOXP3+ Tregs (blue) and CD4+FOXP3- Teffs (orange). "Donor" - healthy donors, "AdenoCa" - adenocarcinoma, "SquamCa" - squamous cell carcinoma. "OtherCa" - other types of cancers: large cell neuroendocrine carcinoma, lung metastasis of colon adenocarcinoma, high grade carcinoma or melanoma. "Non Ca" - non-cancer patients with diaphragmatic hernia, sarcoidosis or interstitial lung disease.

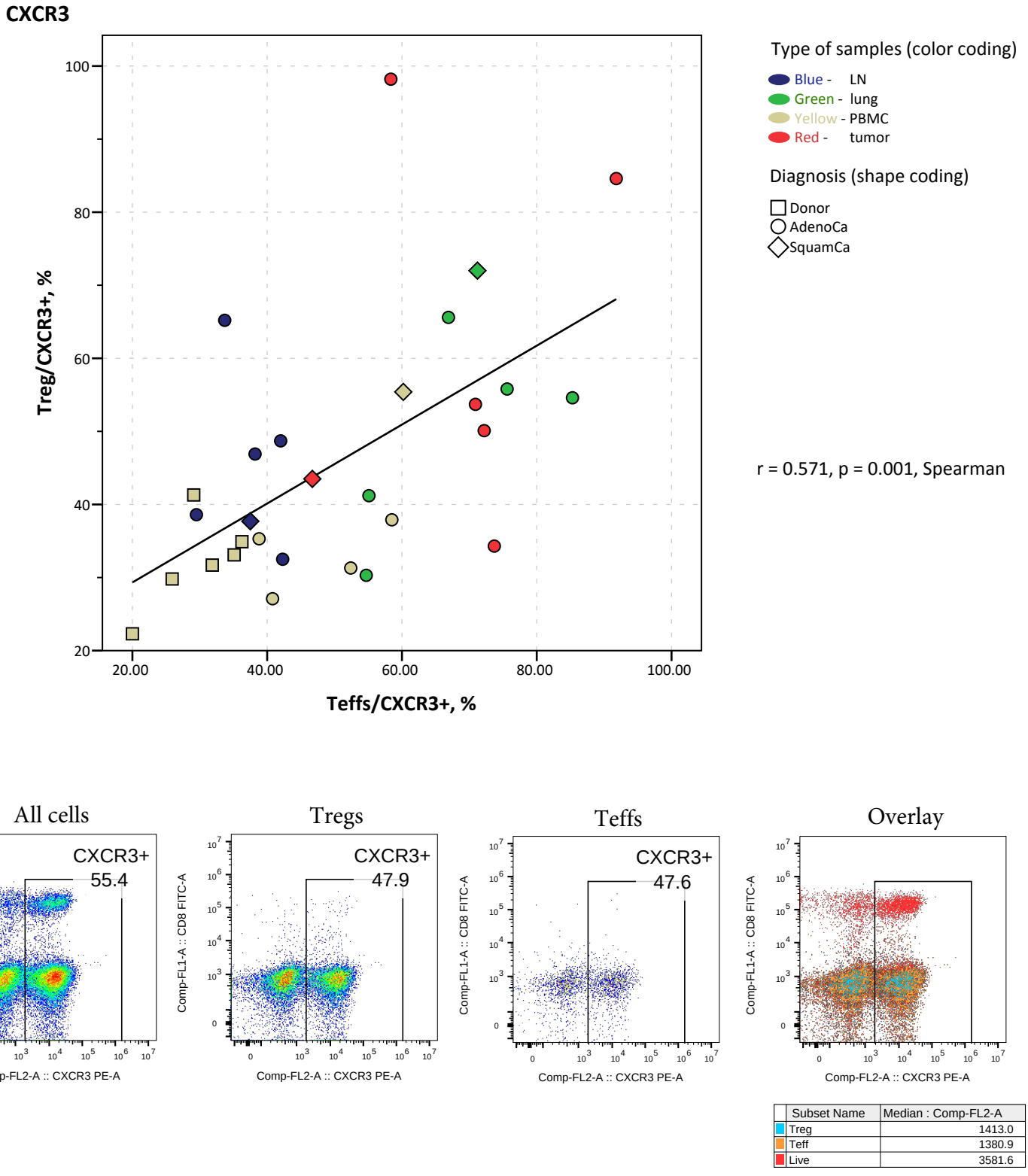

Supplemental Figure 18. CXCR3 expression in Tregs versus Teffs.
Top: correlation of CXCR3+ expression in CD4+FOXP3+ Tregs (y) and in CD4+FOXP3- Teffs (x), Spearman's correlation assay, n = 29. Different type of samples are coded by color, as indicated in legend. Shapes of symbols represent diagnostic categories, as indicated in legend. Bottom: gating strategy and the representative expression of CXCR3+ in Tregs and Teffs are shown, with corresponding MOF for CXCR3 in all viable cells (red), CD4+FOXP3+ Tregs (blue) and CD4+FOXP3- Teffs (orange). "Donor" - healthy donors, "AdenoCa" - adenocarcinoma, "SquamCa" - squamous cells carcinoma.

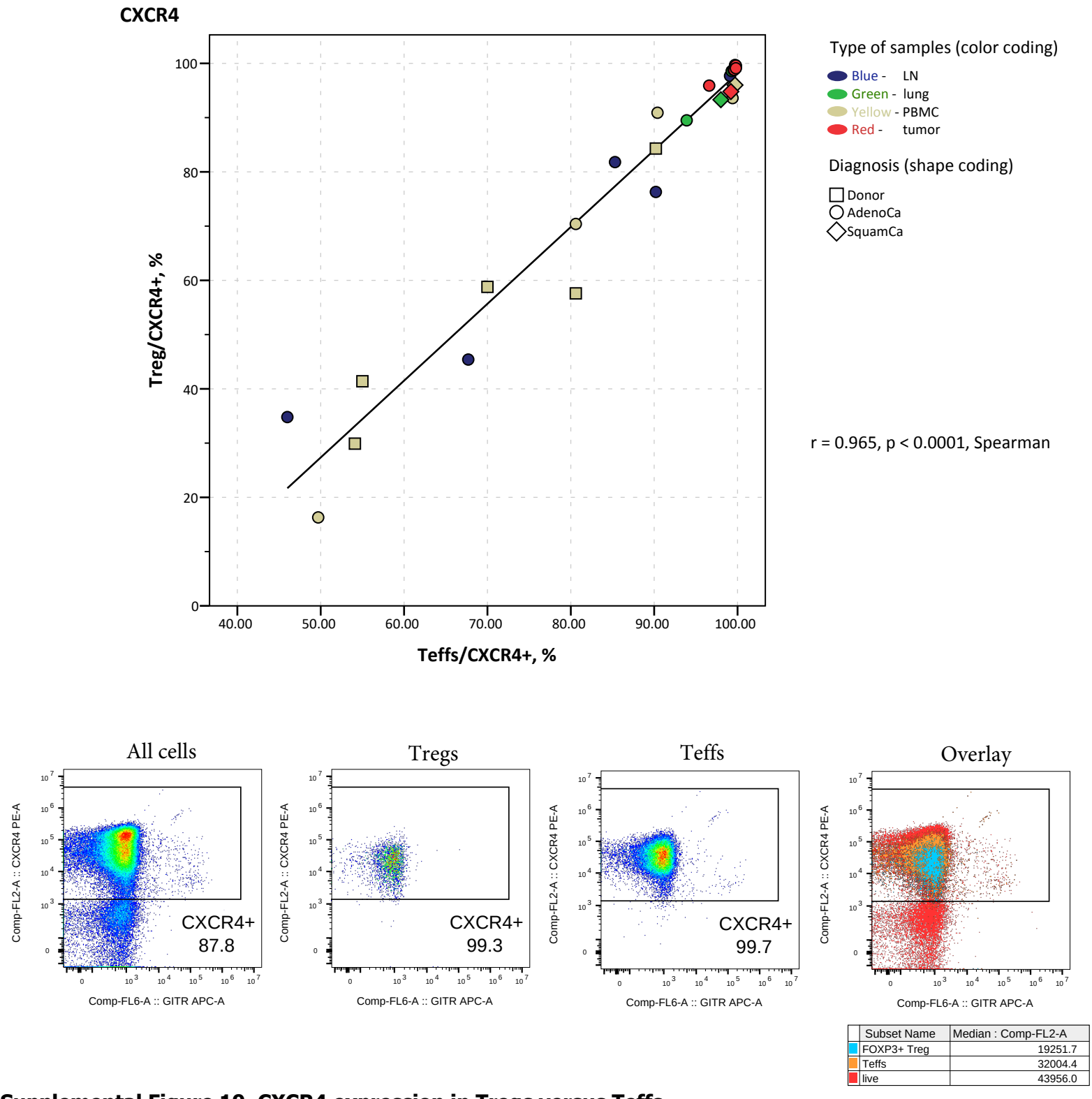

Supplemental Figure 19. CXCR4 expression in Tregs versus Teffs.
Top: correlation of CXCR4+ expression in CD4+FOXP3+ Tregs (y) and in CD4+FOXP3- Teffs (x), Spearman's correlation assay, n = 29. Different types of samples are coded by color, as indicated in legend. Shapes of symbols represent diagnostic categories, as indicated in legend. Bottom: gating strategy and the representative expression of CXCR4+ in Tregs and Teffs are shown, with corresponding MOF for CXCR4 in all viable cells (red), CD4+FOXP3+ Tregs (blue) and CD4+FOXP3- Teffs (orange). "Donor" - healthy donors, "AdenoCa" - adenocarcinoma, "SquamCa" - squamous cells carcinoma.

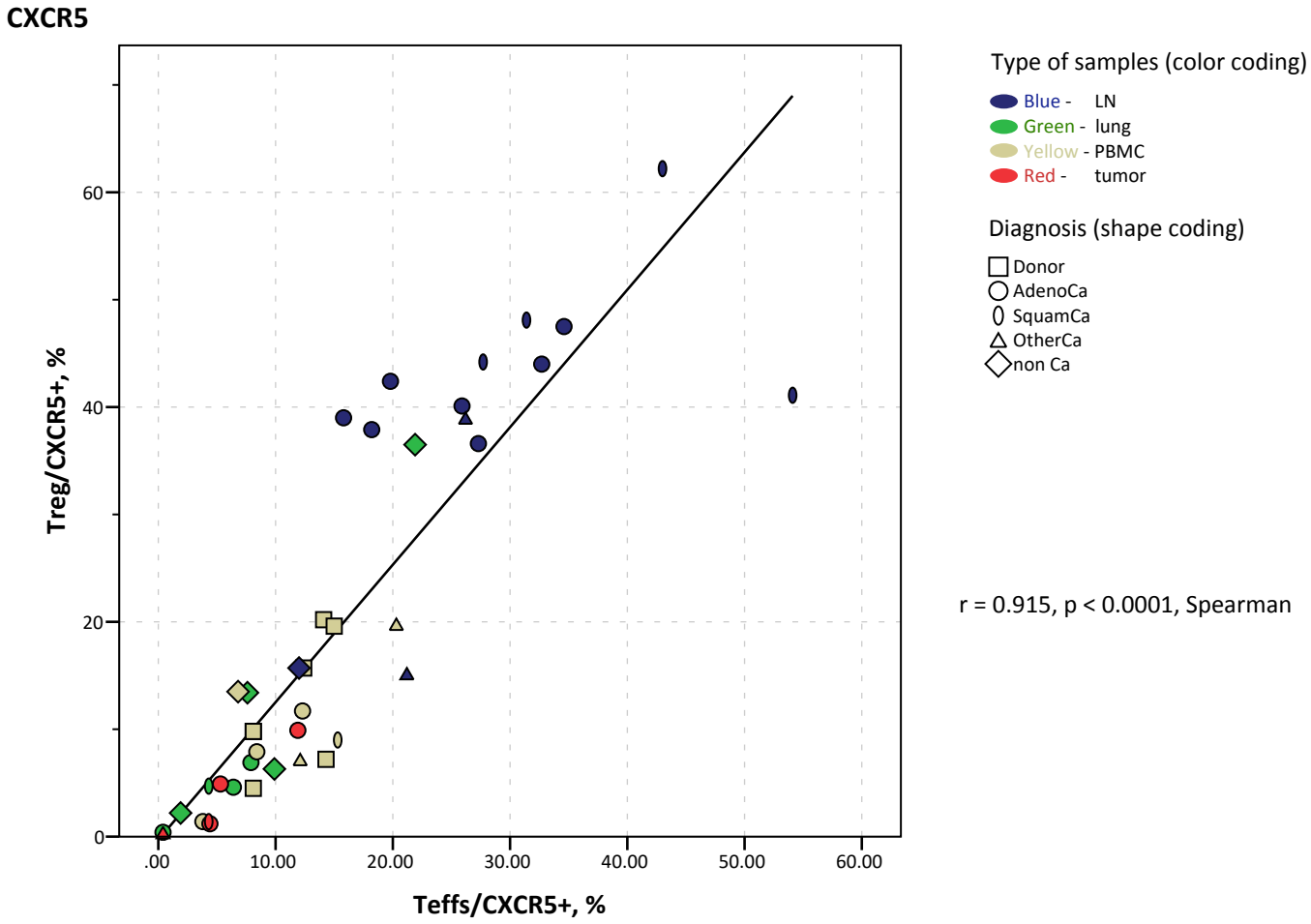

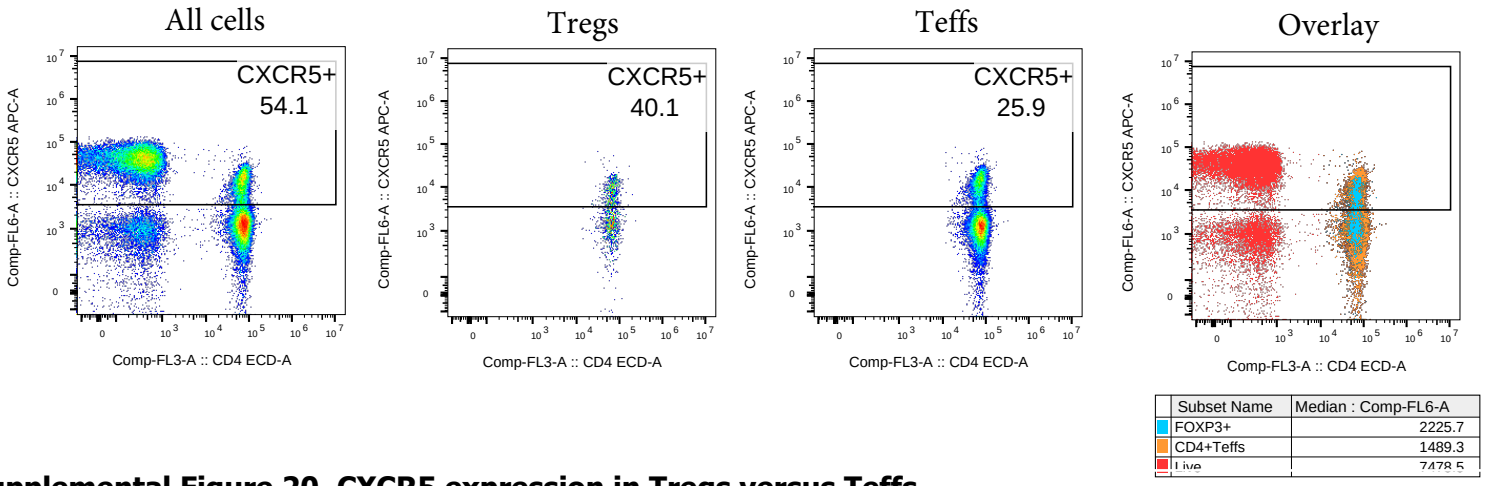

Supplemental Figure 20. CXCR5 expression in Tregs versus Teffs.
Top: correlation of CXCR5+ expression in CD4+FOXP3+ Tregs (y) and in CD4+FOXP3- Teffs (x), Spearman's correlation assay, n = 41. Different types of samples are coded by color, as indicated in legend. Shapes of symbols represent diagnostic categories, as indicated in legend. Bottom: gating strategy and the representative expression of CXCR5+ in Tregs and Teffs are shown, with corresponding MOF for CXCR5 in all viable cells (red), CD4+FOXP3+ Tregs (blue) and CD4+FOXP3- Teffs (orange). "Donor" - healthy donors, "AdenoCa" - adenocarcinoma, "SquamCa" - squamous cells carcinoma, "OtherCa" - other types of cancers: large cell neuroendocrine carcinoma, lung metastasis of colon adenocarcinoma, high grade carcinoma or melanoma. "Non Ca" - non-cancer patients with diaphragmatic hernia, sarcoidosis or interstitial lung disease.

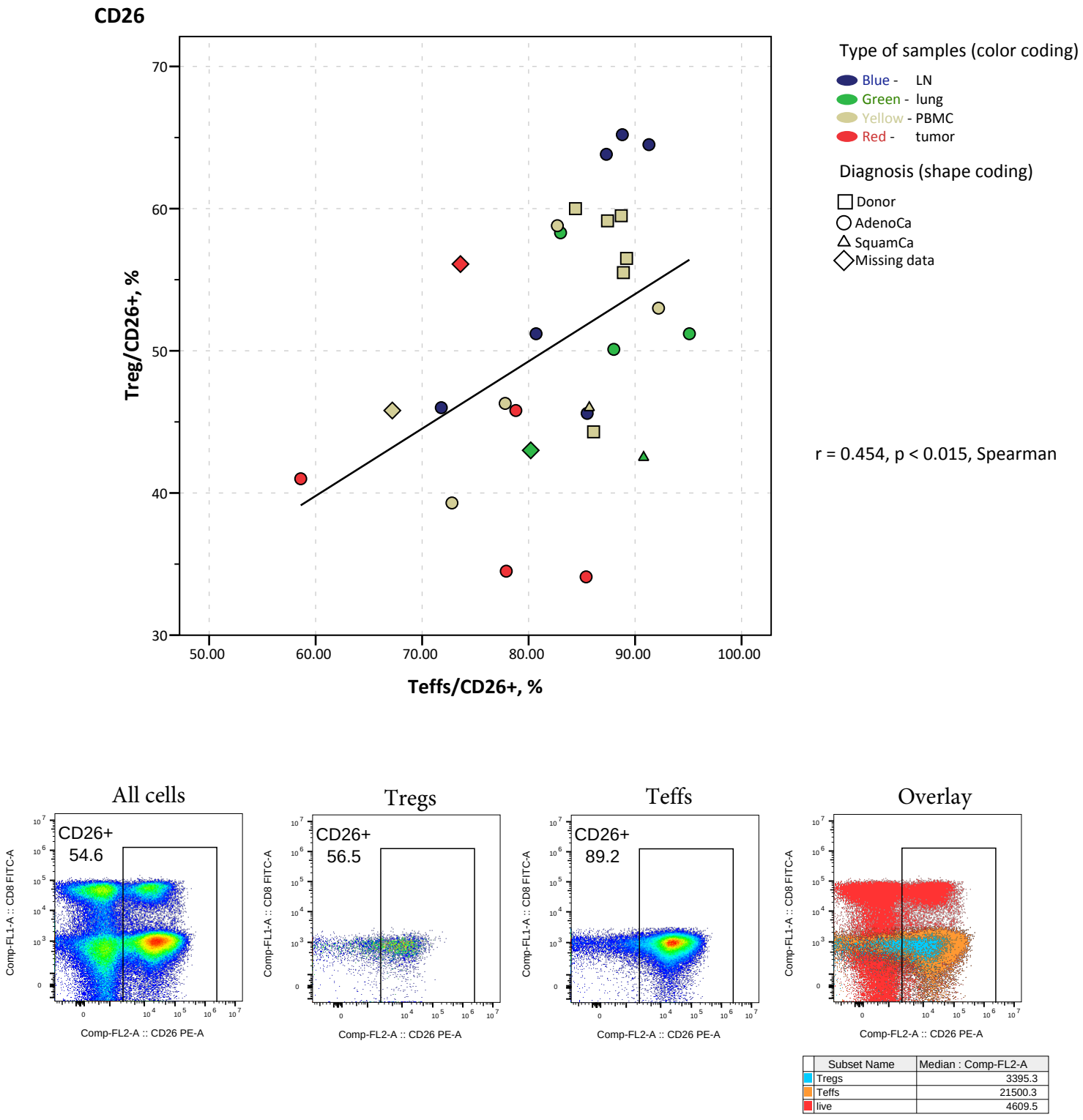

Supplemental Figure 21. CD26 expression in Tregs versus Teffs.
Top: correlation of CD26+ expression in CD4+FOXP3+ Tregs (y) and in CD4+FOXP3- Teffs (x), Spearman's correlation assay, n = 28. Different types of samples are coded by color, as indicated in legend. Shapes of symbols represent diagnostic categories, as indicated in legend. Bottom: gating strategy and the representative expression of CD26+ in Tregs and Teffs are shown, with corresponding MOF for CD26 in all viable cells (red), CD4+FOXP3+ Tregs (blue) and CD4+FOXP3- Teffs (orange). "Donor", healthy donors; "AdenoCa", adenocarcinoma; "SquamCa", squamous cell carcinoma; "Missing data", patients had confirmed lung cancer, but details of histologic type are unknown.

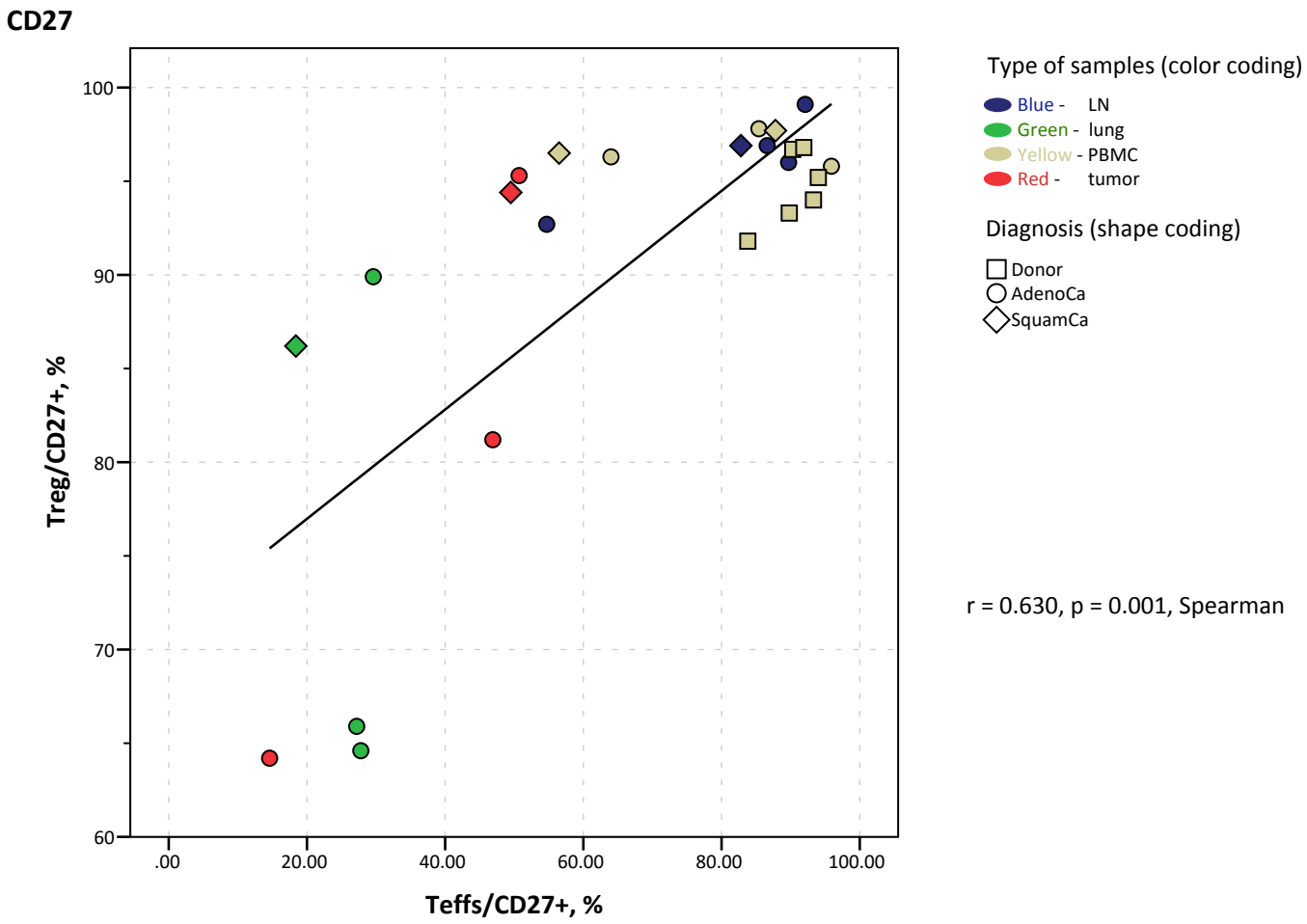

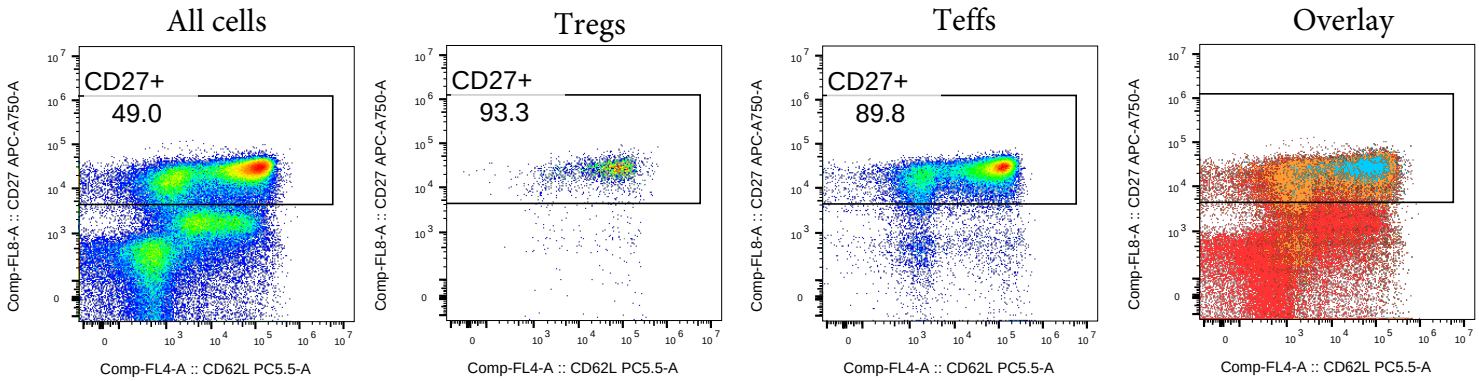

	Subset Name	Median : Comp-FL8-A
	FOXP3+	23555.7
	CD4+ Teffs	23230.1
	live	3807.7

Supplemental Figure 22. CD27 expression in Tregs versus Teffs.
Top: correlation of CD27+ expression in CD4+FOXP3+ Tregs (y) and in CD4+FOXP3- Teffs (x), Spearman's correlation assay, n = 24. Different types of samples are coded by color, as indicated in legend. Shapes of symbols represent diagnostic categories, as indicated in legend. Bottom: gating strategy and the representative expression of CD27+ in Tregs and Teffs are shown, with corresponding MOF for CD27 in all viable cells (red), CD4+FOXP3+ Tregs (blue) and CD4+FOXP3- Teffs (orange). "Donor", healthy donors; "AdenoCa", adenocarcinoma; "SquamCa", squamous cell carcinoma.

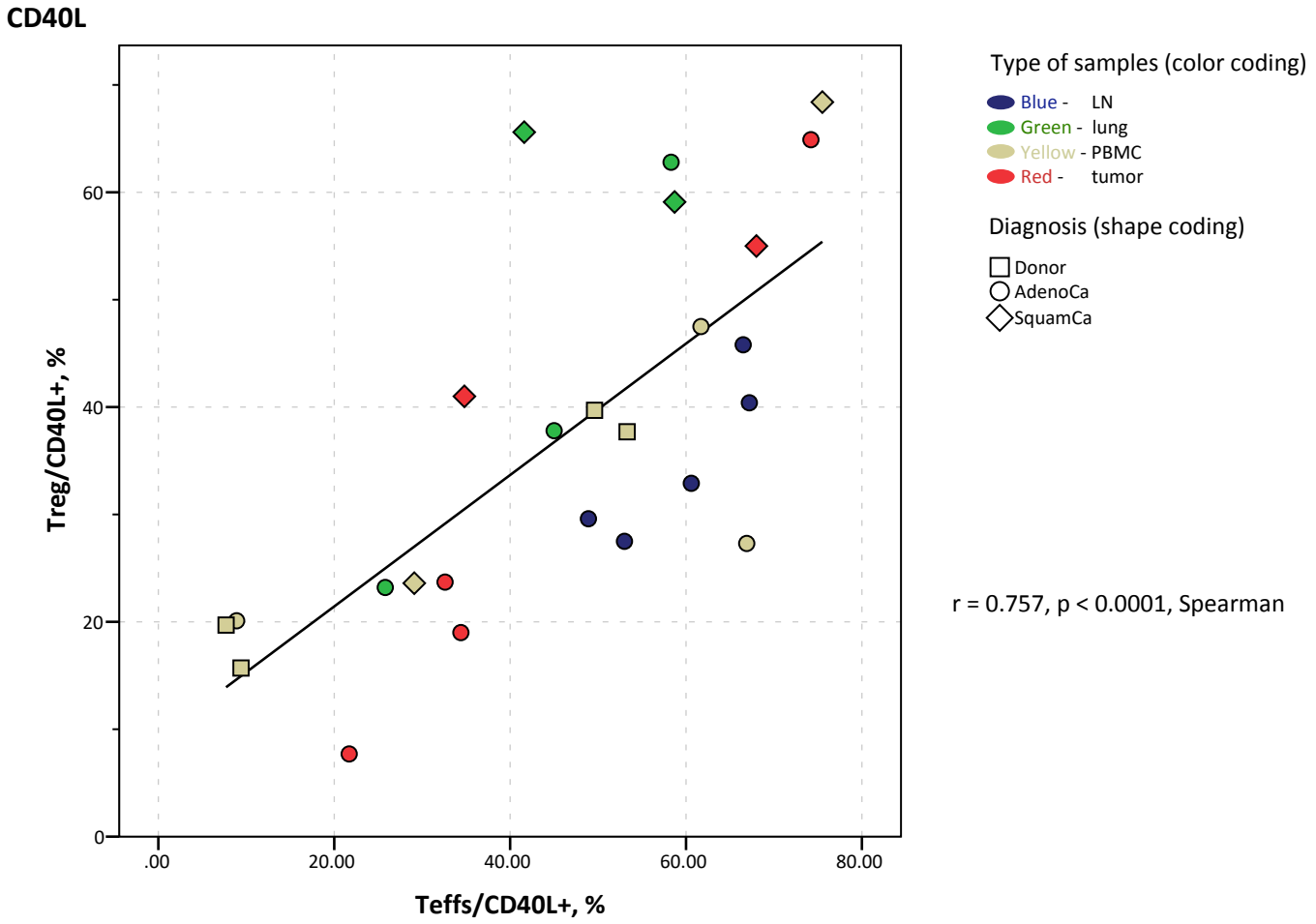

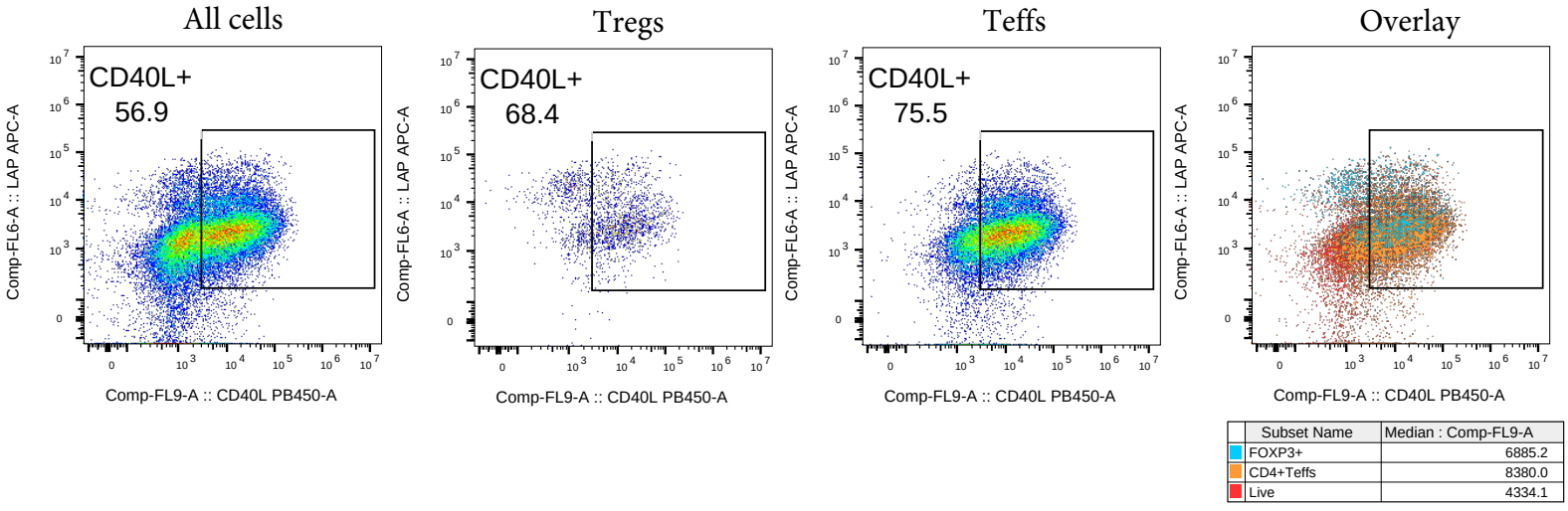

Supplemental Figure 23. CD40L expression in Tregs versus Teffs.
Top: correlation of CD40L+ expression in CD4+FOXP3+ Tregs (y) and in CD4+FOXP3- Teffs (x), Spearman's correlation assay, n = 25. Different types of samples are coded by color, as indicated in legend. Shapes of symbols represent diagnostic categories, as indicated in legend. Bottom: gating strategy and the representative expression of CD40L+ in Tregs and Teffs are shown, with corresponding MOF for CD40L in all viable cells (red), CD4+FOXP3+ Tregs (blue) and CD4+FOXP3- Teffs (orange). CD40L was evaluated after stimulation for 2 days with CD3/28 beads at 1/1 ratio in T cell media. "Donor", healthy donors; "AdenoCa", adenocarcinoma; "SquamCa", squamous cell carcinoma.

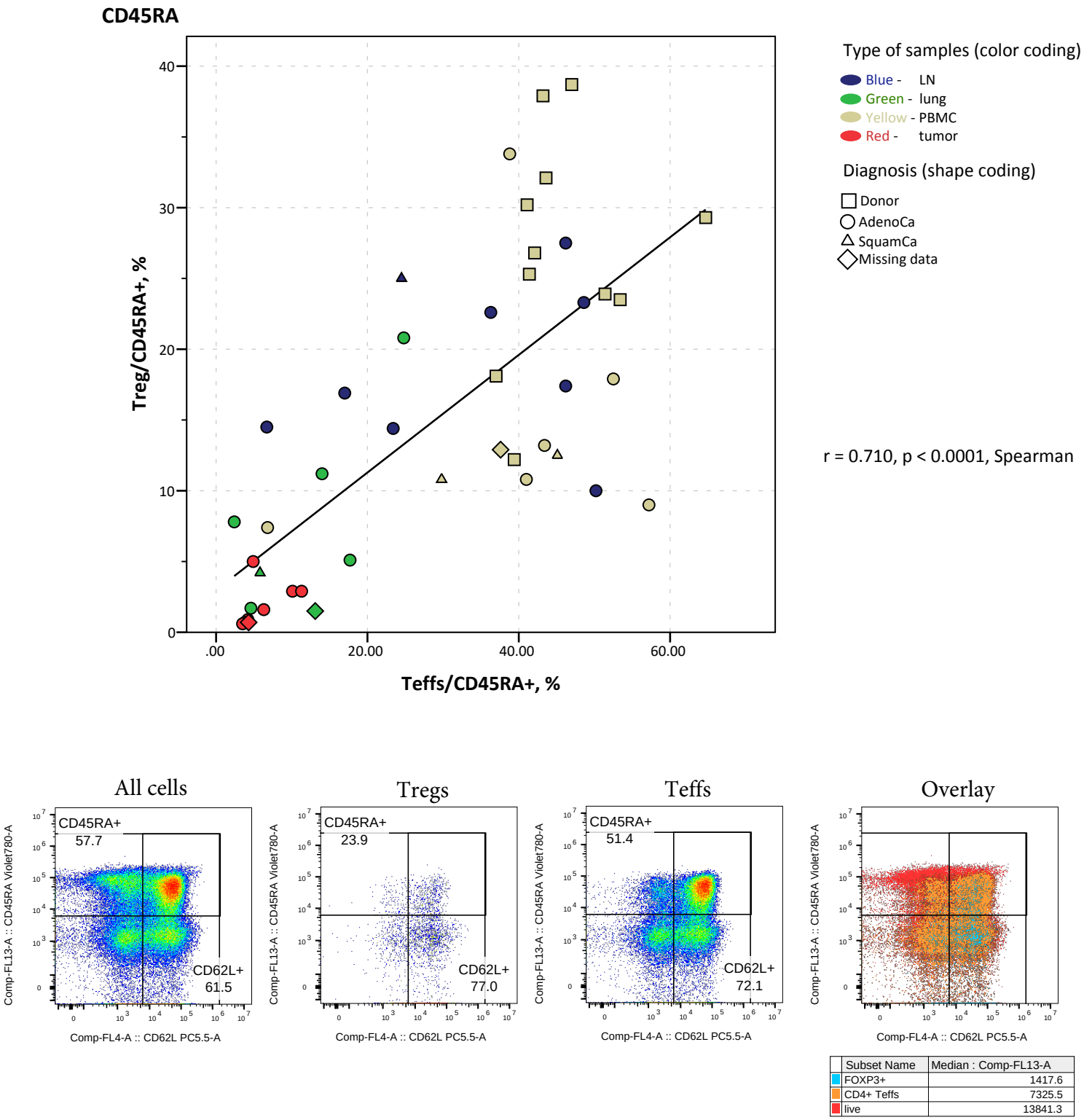

Supplemental Figure 24. CD45RA expression in Tregs versus Teffs.
Top: correlation of CD45RA+ expression in CD4+FOXP3+ Tregs (y) and in CD4+FOXP3- Teffs (x), Spearman's correlation assay, n = 44. Different types of samples are coded by color, as indicated in legend. Shapes of symbols represent diagnostic categories, as indicated in legend. Bottom: gating strategy and the representative expression of CD45RA+ in Tregs and Teffs are shown, with corresponding MOF for CD45RA in all viable cells (red), CD4+FOXP3+ Tregs (blue) and CD4+FOXP3- Teffs (orange). "Donor", healthy donors; "AdenoCa", adenocarcinoma; "SquamCa", squamous cell carcinoma; "Missing data" patients had confirmed lung cancer, but of unknown histological type.

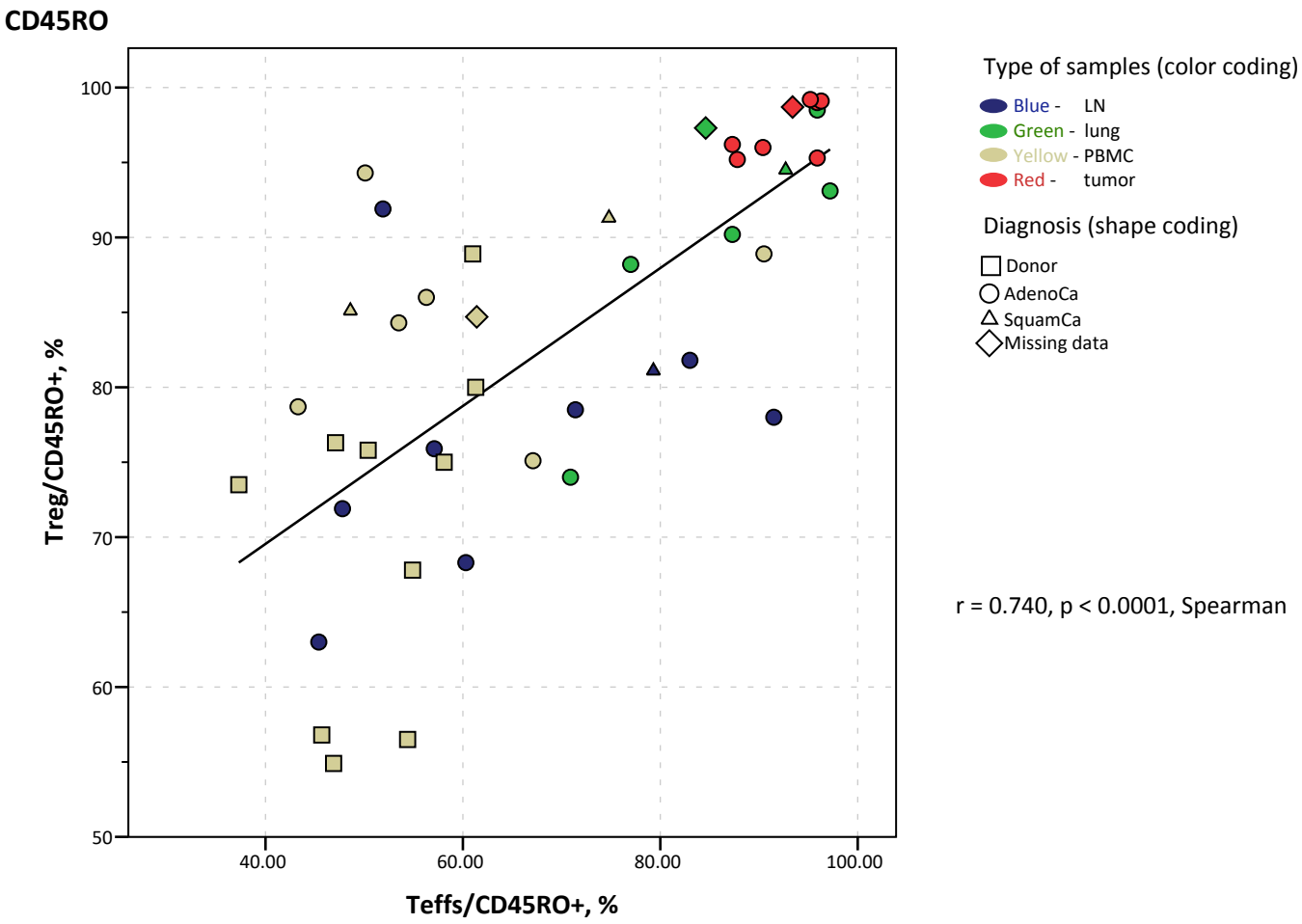

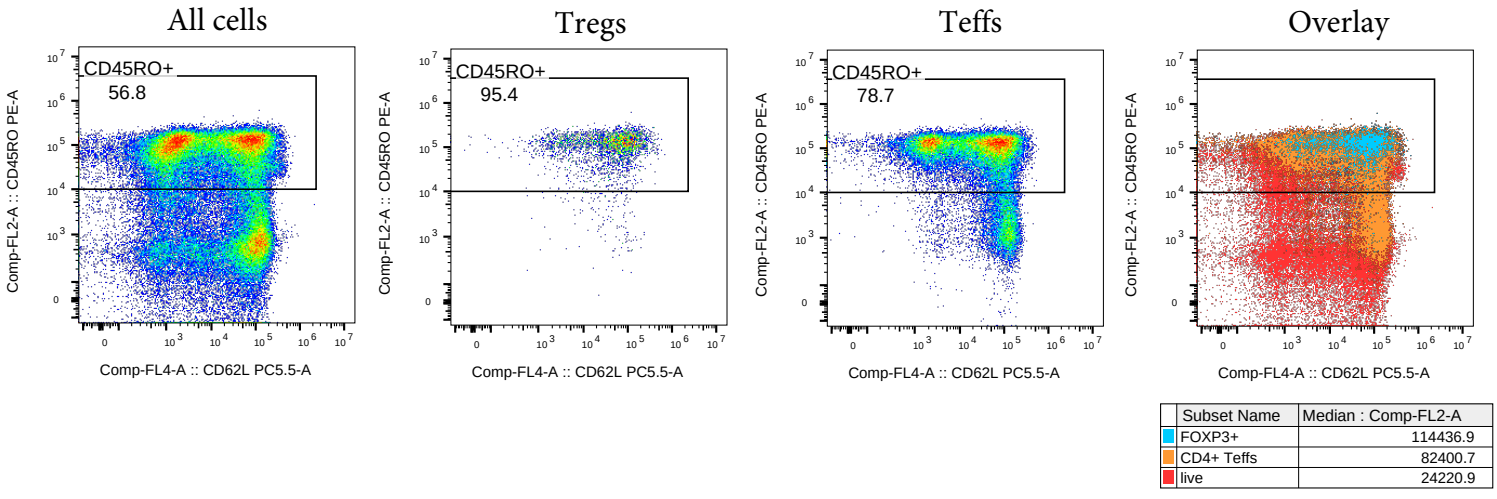

Supplemental Figure 25. CD45RO expression in Tregs versus Teffs.
Top: correlation of CD45RO+ expression in CD4+FOXP3+ Tregs (y) and in CD4+FOXP3- Teffs (x), Spearman's correlation assay, n = 43. Different types of samples are coded by color, as indicated in legend. Shapes of symbols represent diagnostic categories, as indicated in legend. Bottom: gating strategy and the representative expression of CD45RO+ in Tregs and Teffs are shown, with corresponding MOF for CD45RO in all viable cells (red), CD4+FOXP3+ Tregs (blue) and CD4+FOXP3- Teffs (orange). "Donor", healthy donors; "AdenoCa", adenocarcinoma; "SquamCa", squamous cell carcinoma; "Missing data" patients had confirmed lung cancer, but of unknown histological type.

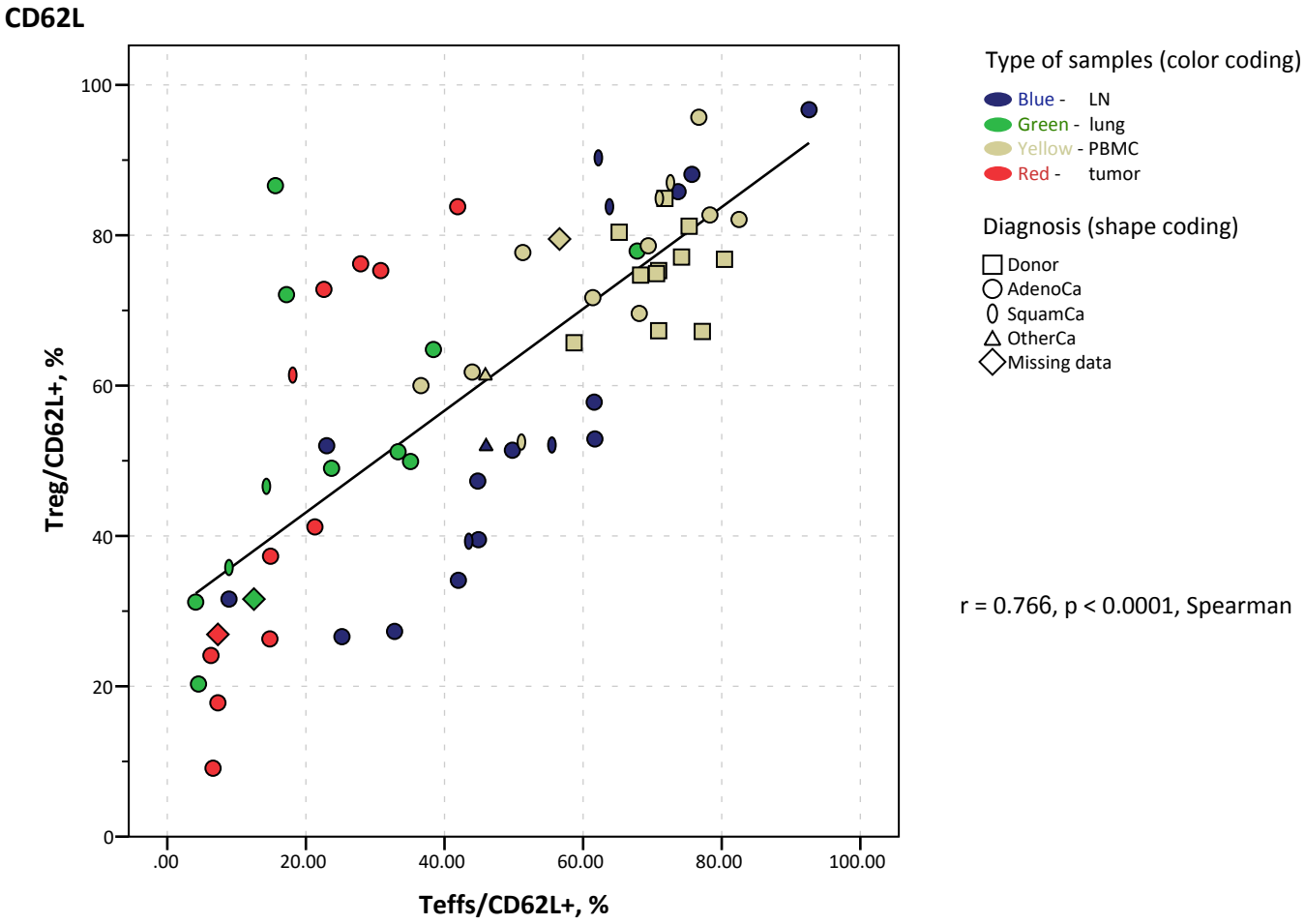

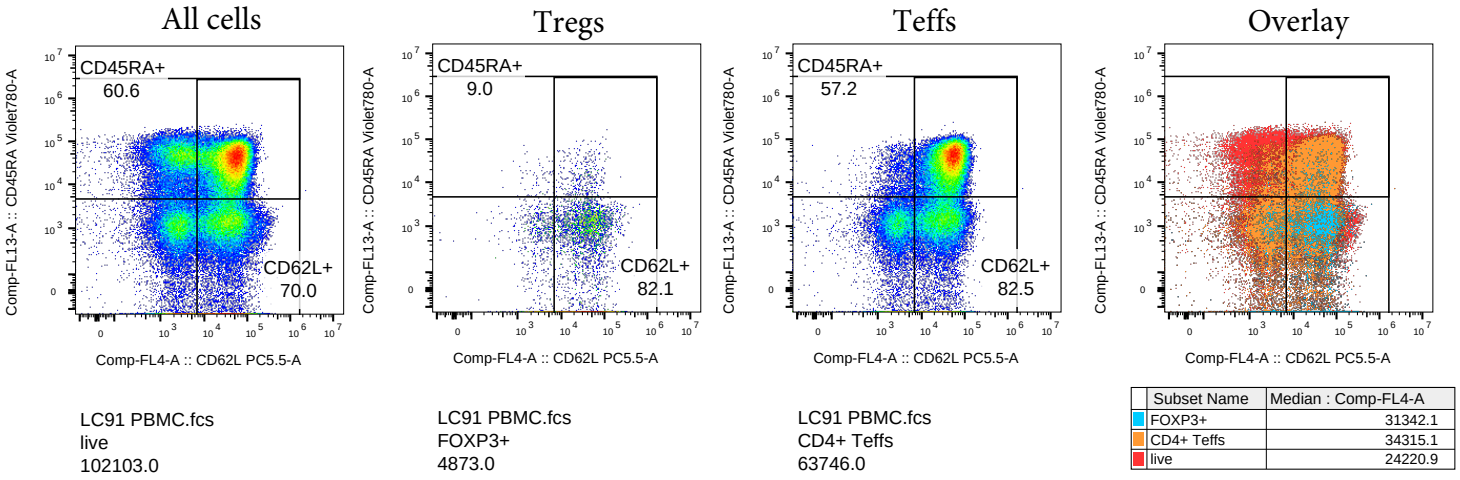

Supplemental Figure 26. CD62L expression in Tregs versus Teffs.
Top: correlation of CD62L+ expression in CD4+FOXP3+ Tregs (y) and in CD4+FOXP3- Teffs (x), Spearman's correlation assay, n = 67. Different types of samples are coded by color, as indicated in legend. Shapes of symbols represent diagnostic categories, as indicated in legend. Bottom: gating strategy and the representative expression of CD62L+ in Tregs and Teffs are shown, with corresponding MOF for CD62L in all viable cells (red), CD4+FOXP3+ Tregs (blue) and CD4+FOXP3- Teffs (orange). "Donor" - healthy donors, "AdenoCa" - adenocarcinoma, "SquamCa" - squamous cell carcinoma, "OtherCa" - other types of cancers: large cell neuroendocrine carcinoma, lung metastasis of colon adenocarcinoma, high grade carcinoma or melanoma, "Missing data" patients had confirmed lung cancer, but details of its histological type are unknown.

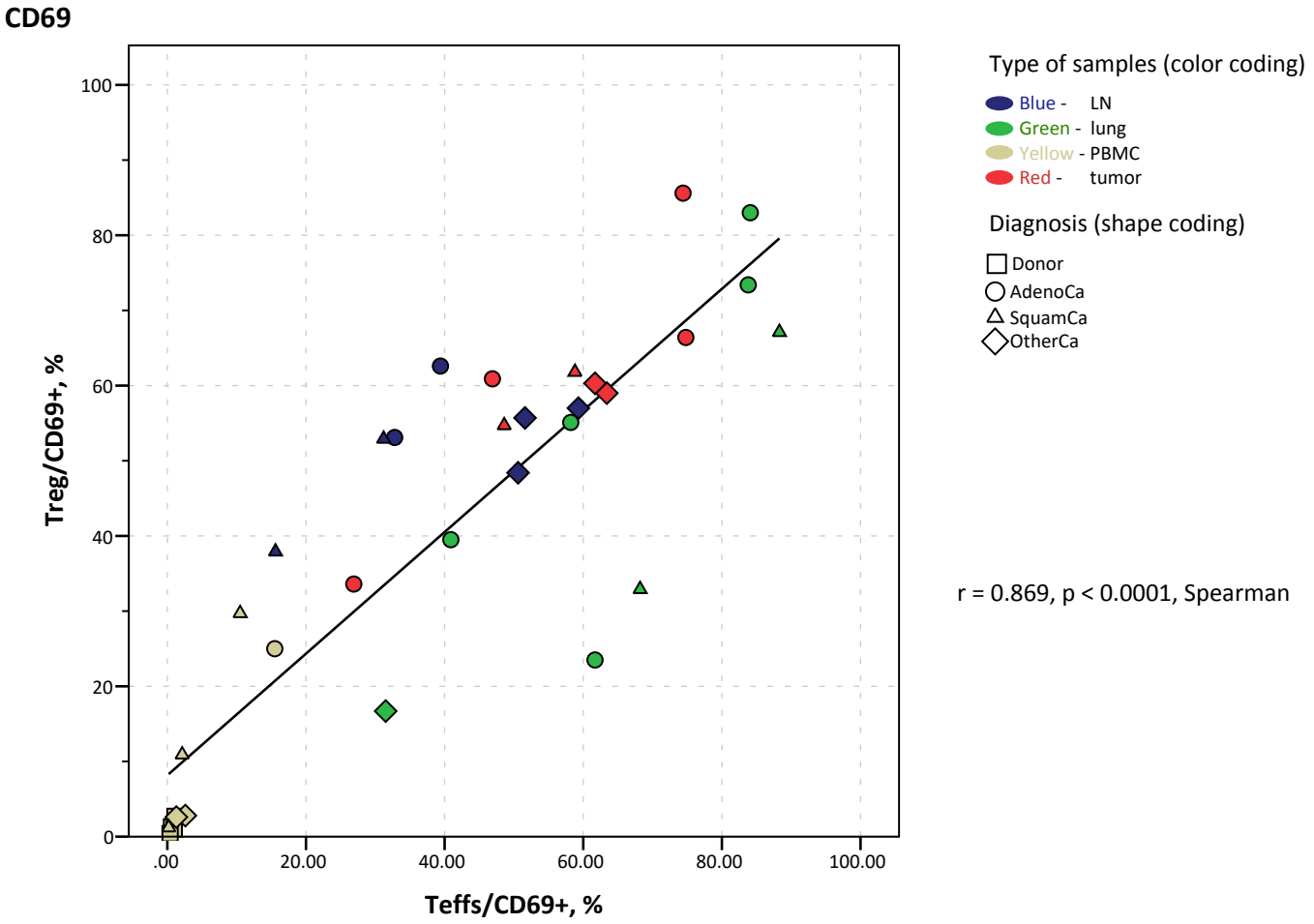

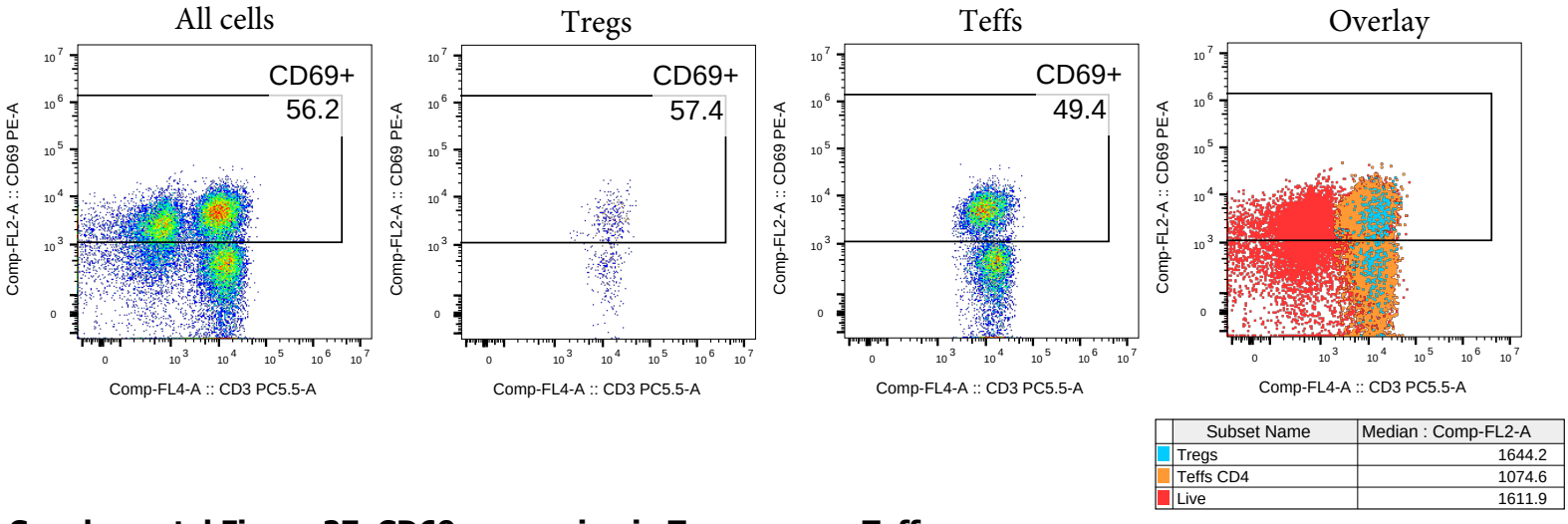

Subset Name	Median : Comp-FL2-A
Tregs	1644.2
Teffs CD4	1074.6
Live	1611.9

Supplemental Figure 27. CD69 expression in Tregs versus Teffs.
Top: correlation of CD69+ expression in CD4+FOXP3+ Tregs (y) and in CD4+FOXP3- Teffs (x), Spearman's correlation assay, n = 34. Different type of samples are coded by color, as indicated in legend. Shapes of symbols represent diagnostic categories, as indicated in legend. Bottom: gating strategy and the representative expression of CD69+ in Tregs and Teffs are shown, with corresponding MOF for CD69 in all viable cells (red), CD4+FOXP3+ Tregs (blue) and CD4+FOXP3- Teffs (orange). "Donor" - healthy donors, "AdenoCa" - adenocarcinoma, "SquamCa" - squamous cells carcinoma, "OtherCa" - other types of cancers: large cell neuroendocrine carcinoma, lung metastasis of colon adenocarcinoma, high grade carcinoma or melanoma.

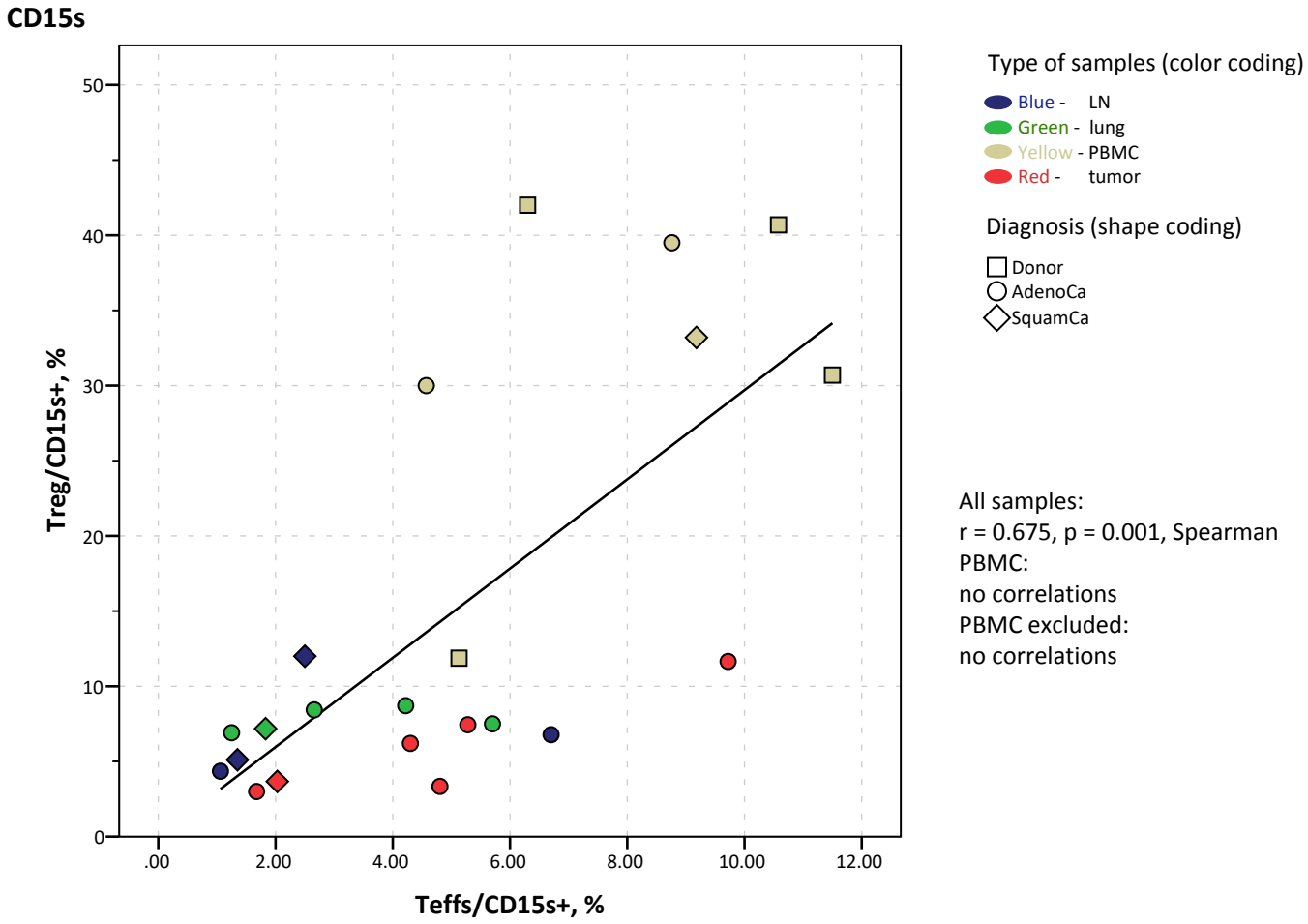

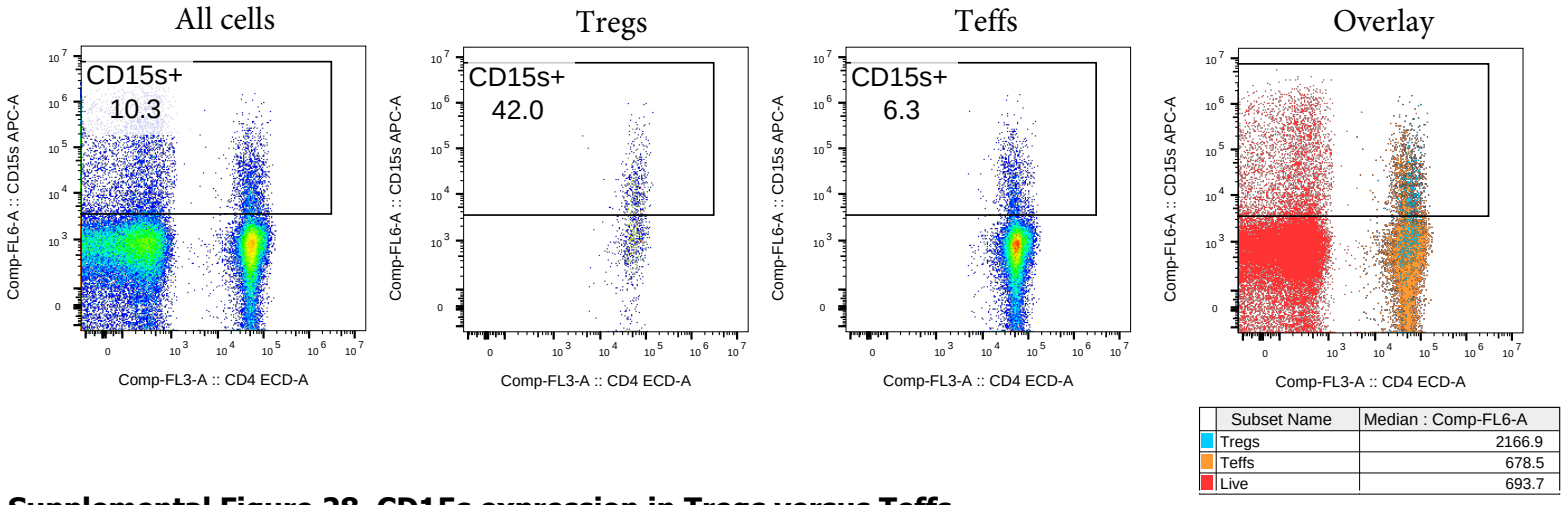

Supplemental Figure 28. CD15s expression in Tregs versus Teffs.
Top: correlation of CD15s+ expression in CD4+FOXP3+ Tregs (y) and in CD4+FOXP3- Teffs (x), Spearman's correlation assay, n = 22. Different type of samples are coded by color, as indicated in legend. Shapes of symbols represent diagnostic categories, as indicated in legend. When CD15s expression in PBMC samples was analyzed separately, no correlations between CD15s+ Tregs and Teffs existed. Similarly, when leftover samples were analyzed with PBMC data excluded, CD15s in Tregs and in Teffs did not correlate. Bottom: gating strategy and the representative expression of CD15s+ in Tregs and Teffs are shown, with corresponding MOF for CD15s in all viable cells (red), CD4+FOXP3+ Tregs (blue) and CD4+FOXP3- Teffs (orange). "Donor", healthy donors; "AdenoCa", adenocarcinoma; "SquamCa", squamous cell carcinoma.

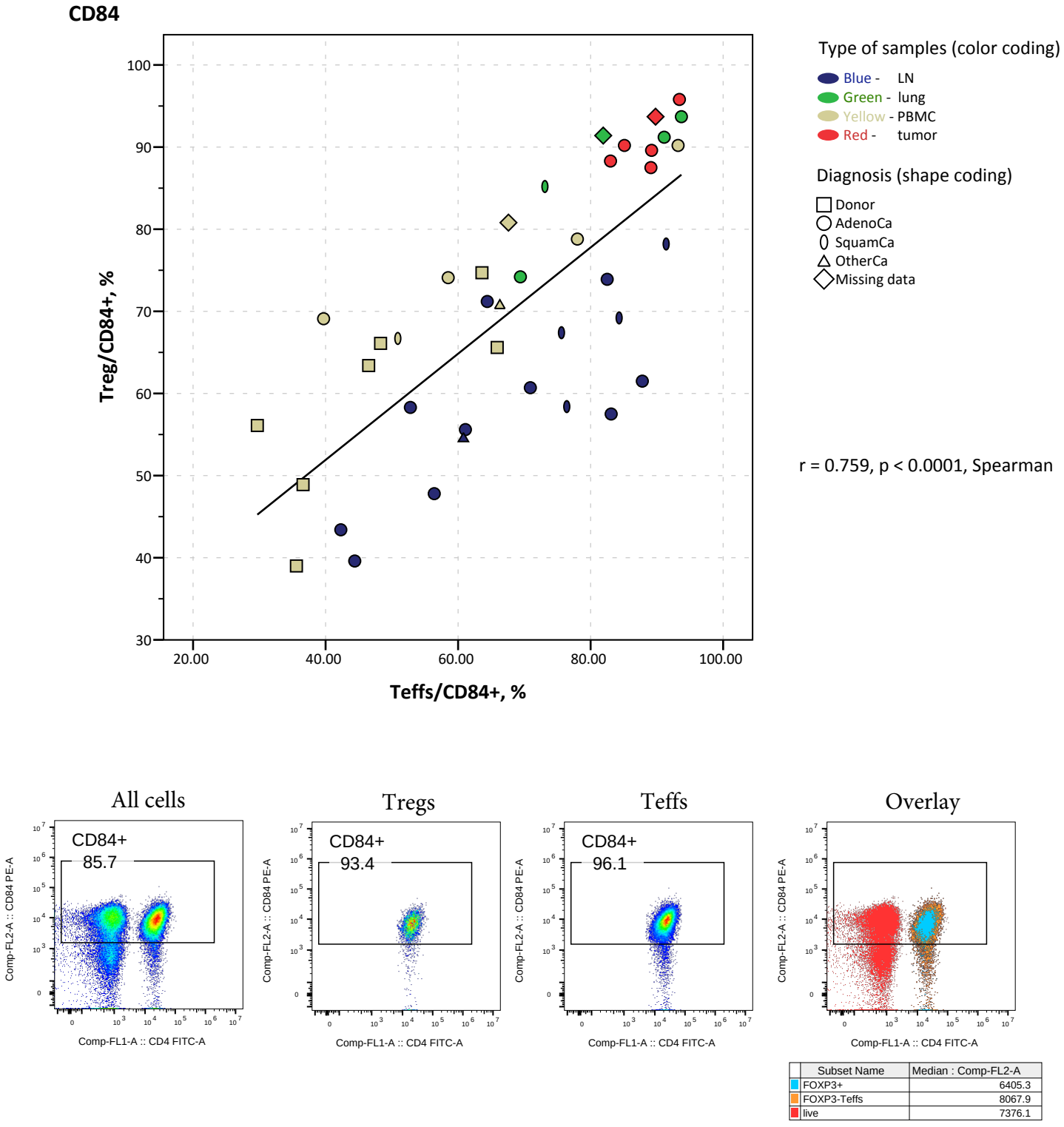

Supplemental Figure 29. CD84 expression in Tregs versus Teffs.
Top: correlation of CD84+ expression in CD4+FOXP3+ Tregs (y) and in CD4+FOXP3- Teffs (x), Spearman's correlation assay, n = 46. Different type of samples are coded by color, as indicated in legend. Shapes of symbols represent diagnostic categories, as indicated in legend. Bottom: gating strategy and the representative expression of CD84+ in Tregs and Teffs are shown, with corresponding MOF for CD84 in all viable cells (red), CD4+FOXP3+ Tregs (blue) and CD4+FOXP3- Teffs (orange). "Donor" - healthy donors, "AdenoCa" - adenocarcinoma, "SquamCa" - squamous cells carcinoma, "OtherCa" - other types of cancers: large cell neuroendocrine carcinoma, lung metastasis of colon adenocarcinoma, high grade carcinoma or melanoma, "Missing data" patients had confirmed lung cancer, but details of its histological type are unknown.

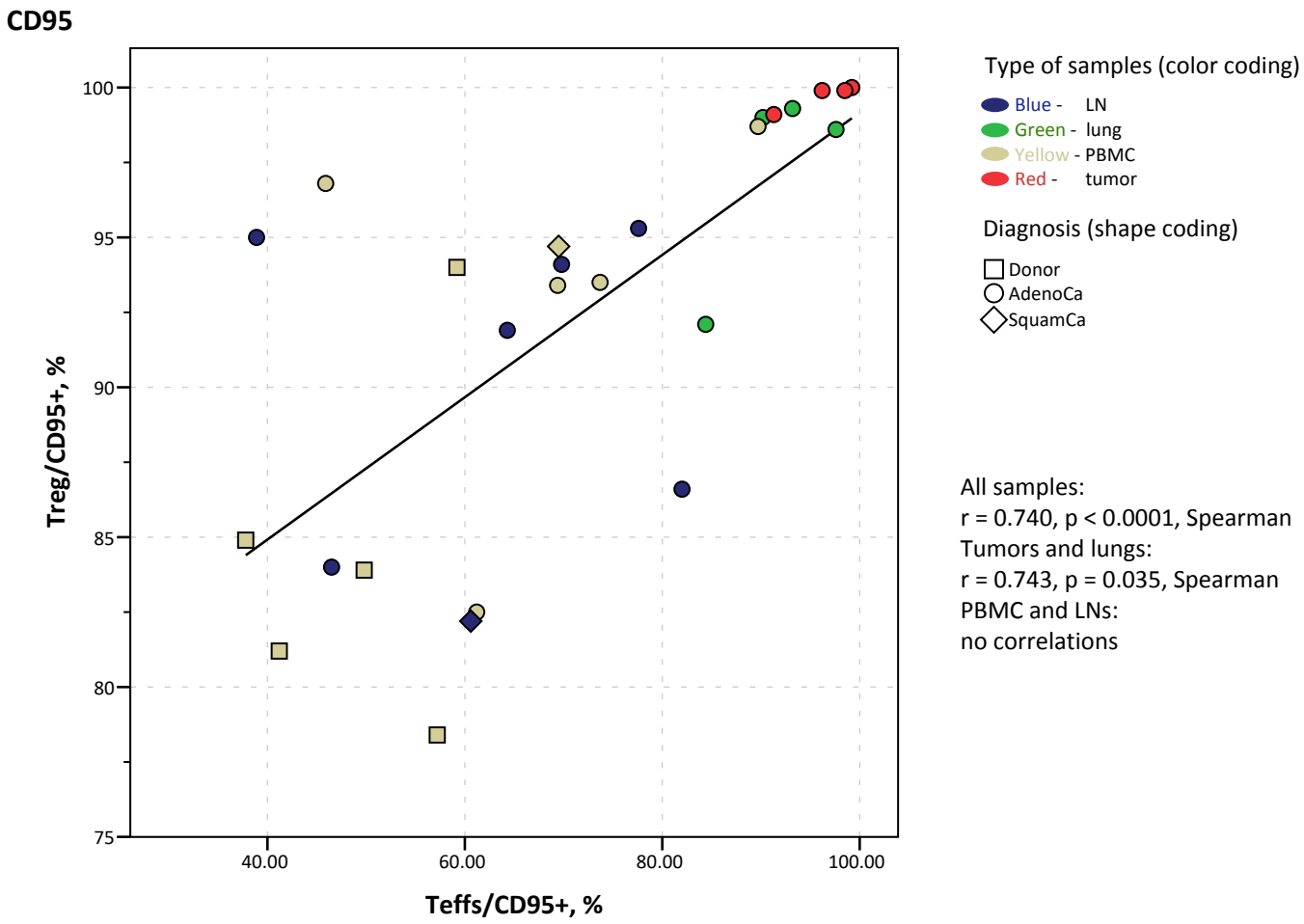

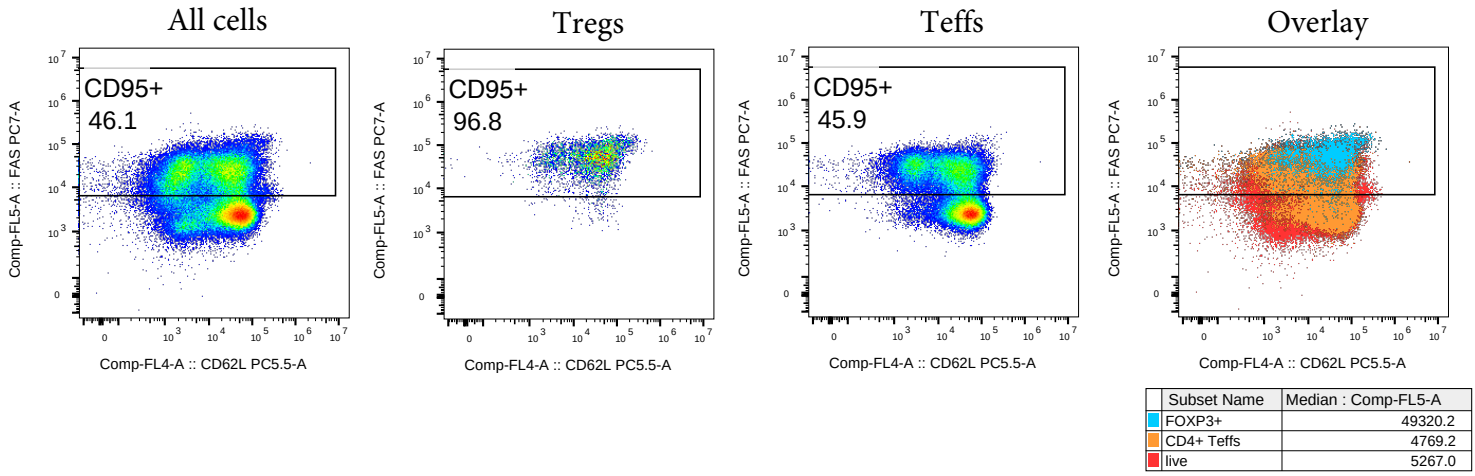

Supplemental Figure 30. CD95 expression in Tregs versus Teffs.
Top: correlation of CD95+ expression in CD4+FOXP3+ Tregs (y) and in CD4+FOXP3- Teffs (x), Spearman's correlation assay, n = 26. Different type of samples are coded by color, as indicated in legend. Shapes of symbols represent diagnostic categories, as indicated in legend. When CD95 expression in PBMC and LNs was analyzed separately, no correlation of CD95 in Tregs vs. Teffs existed. Bottom: gating strategy and the representative expression of CD95+ in Tregs and Teffs are shown, with corresponding MOF for CD95 in all viable cells (red), CD4+FOXP3+ Tregs (blue) and CD4+FOXP3- Teffs (orange). "Donor", healthy donors; "AdenoCa", adenocarcinoma; "SquamCa", squamous cell carcinoma.

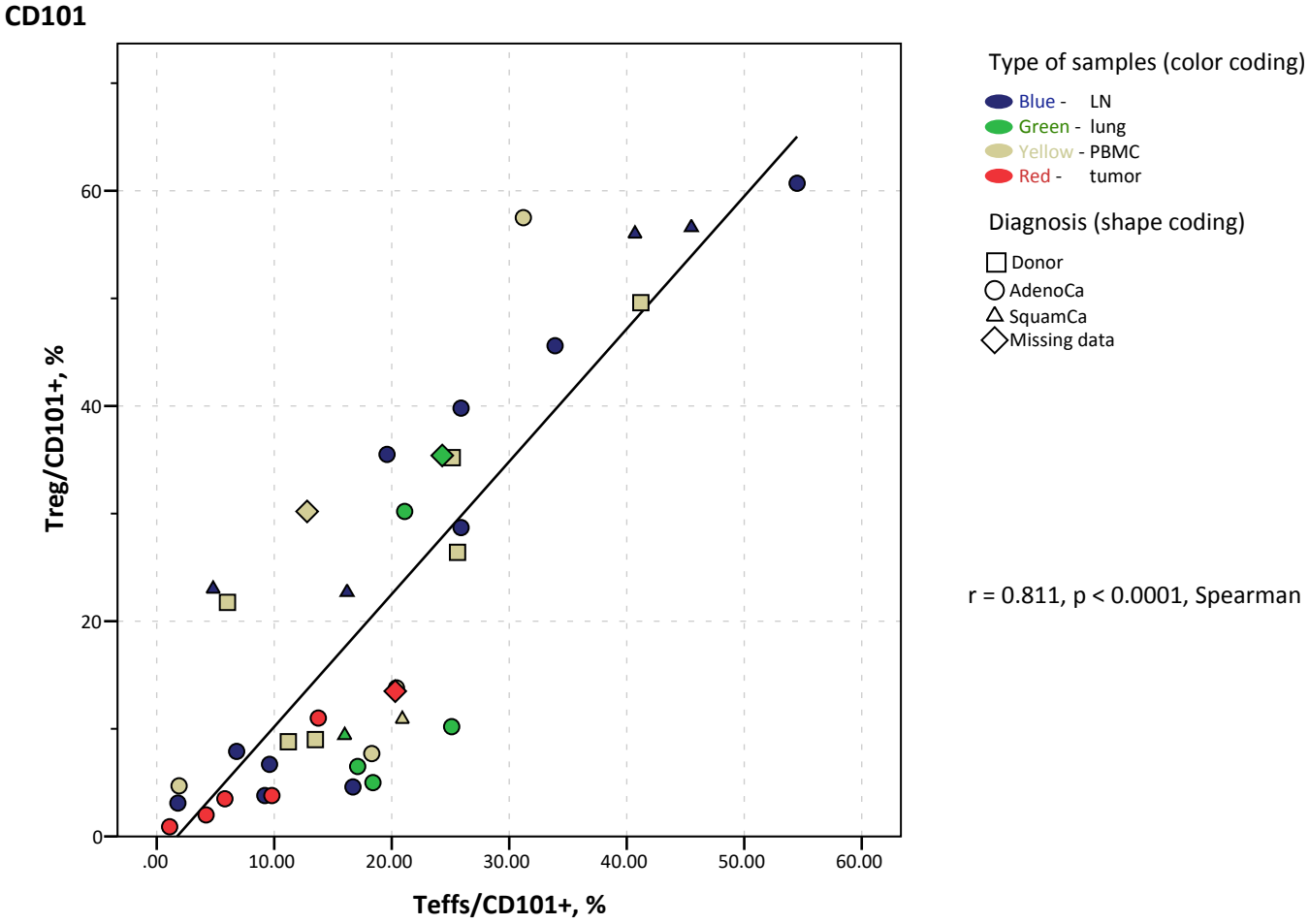

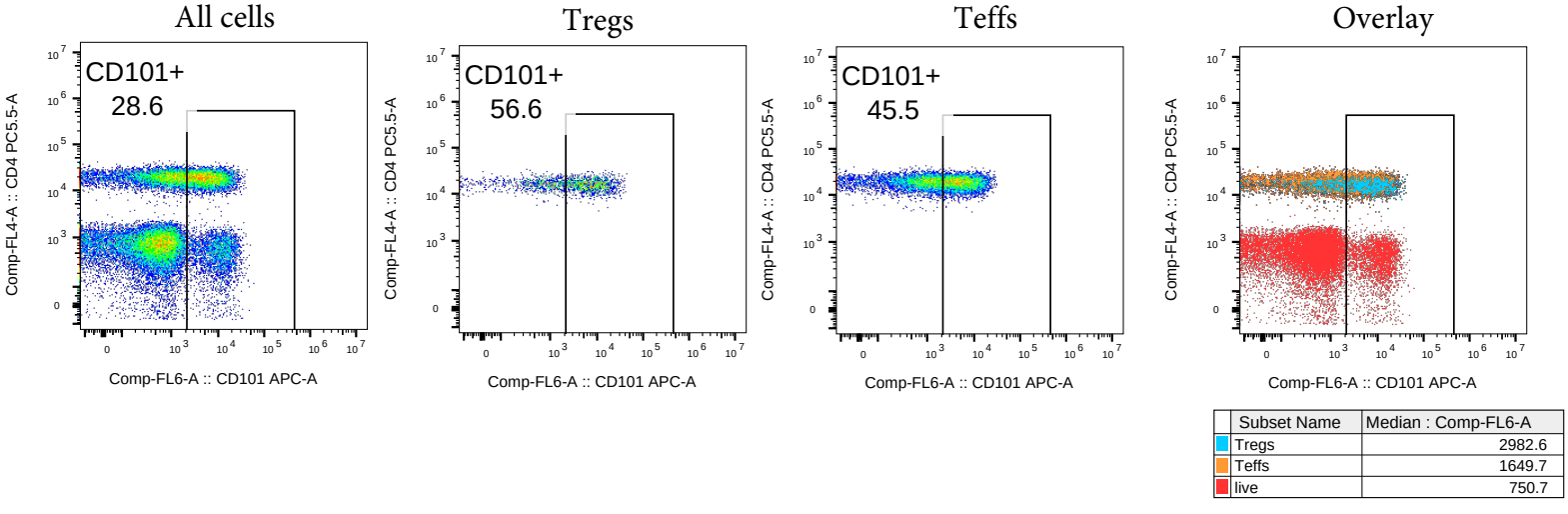

Supplemental Figure 31. CD101 expression in Tregs versus Teffs.
Top: correlation of CD101+ expression in CD4+FOXP3+ Tregs (y) and in CD4+FOXP3- Teffs (x), Spearman's correlation assay, n = 38. Different type of samples are coded by color, as indicated in legend. Shapes of symbols represent diagnostic categories, as indicated in legend. Bottom: gating strategy and the representative expression of CD101+ in Tregs and Teffs are shown, with corresponding MOF for CD101 in all viable cells (red), CD4+FOXP3+ Tregs (blue) and CD4+FOXP3- Teffs (orange). "Donor" - healthy donors, "AdenoCa" - adenocarcinoma, "SquamCa" - squamous cells carcinoma, "Missing data" patients had confirmed lung cancer, but details of its histological type are unknown.

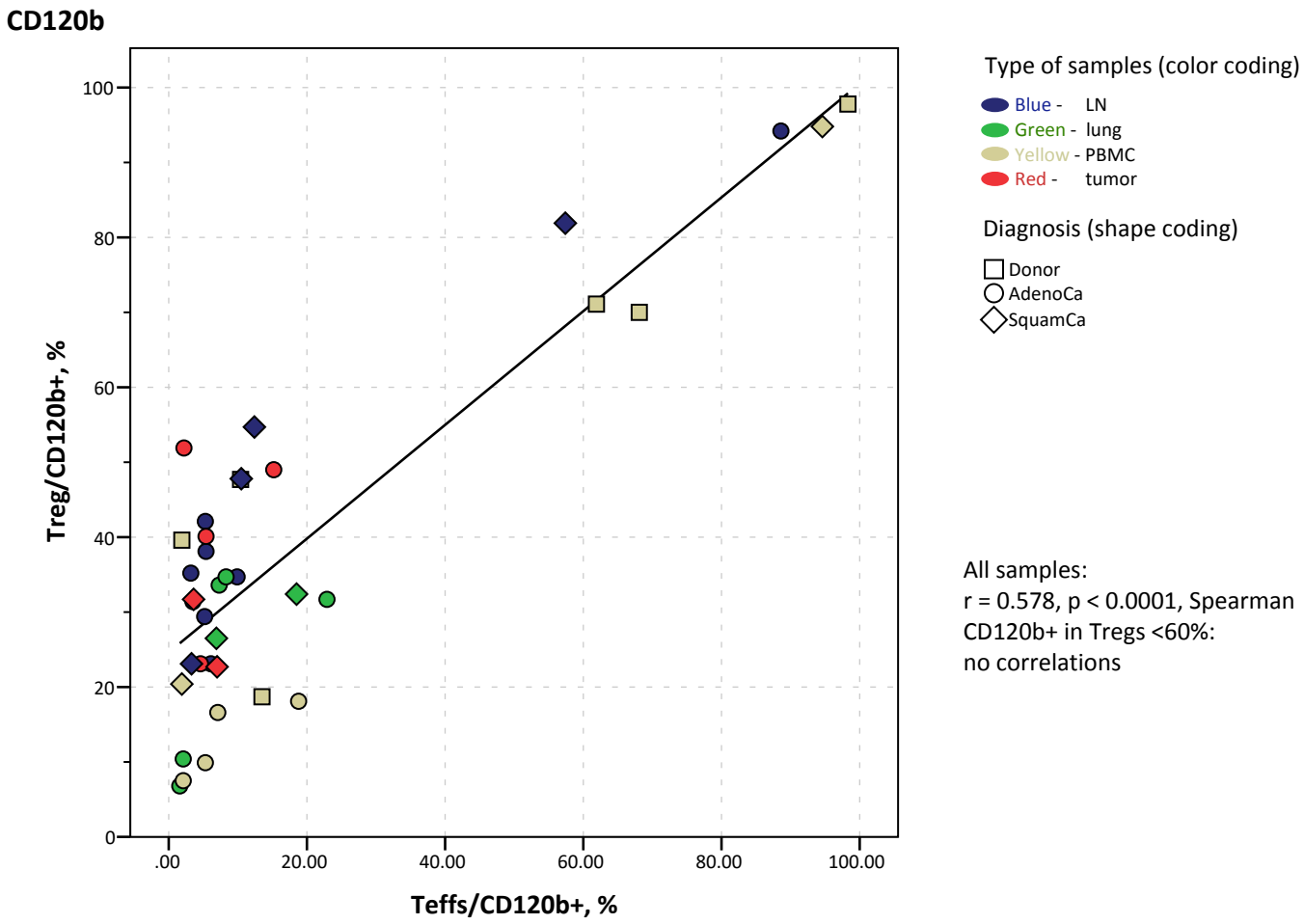

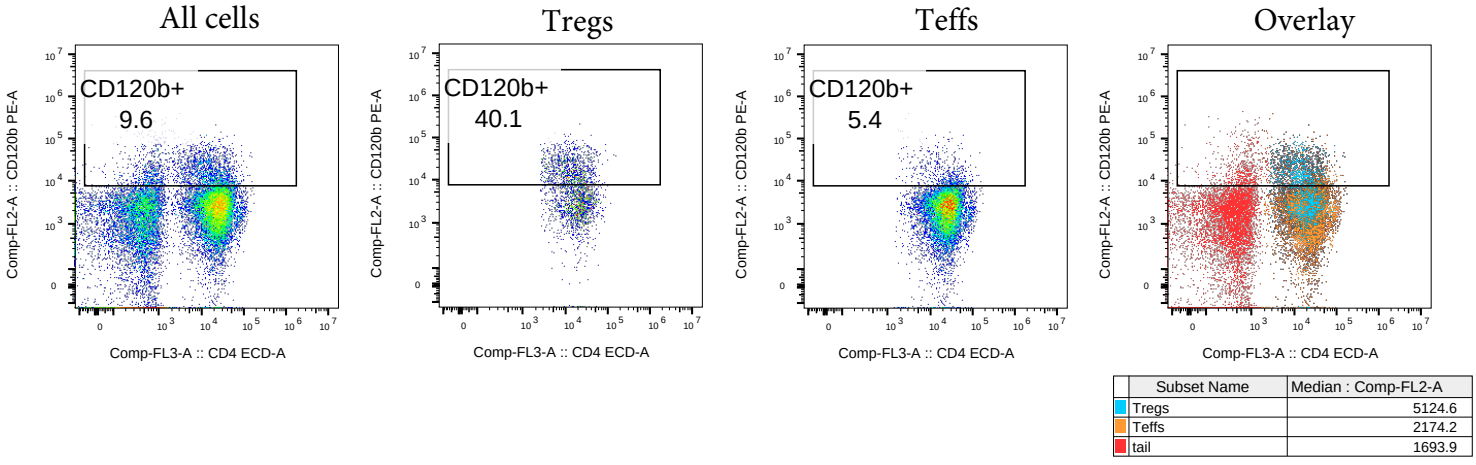

Supplemental Figure 32. CD120b expression in Tregs versus Teffs.
Top: correlation of CD120b+ expression in CD4+FOXP3+ Tregs (y) and in CD4+FOXP3- Teffs (x), Spearman's correlation assay, n = 37. Different types of samples are coded by color, as indicated in legend. Shapes of symbols represent diagnostic categories, as indicated in legend. When Tregs with CD120b expression >60% were excluded, no correlation between CD120b in Tregs vs. Teffs existed. Bottom: gating strategy and the representative expression of CD120b+ in Tregs and Teffs are shown, with corresponding MOF for CD120b in all viable cells (red), CD4+FOXP3+ Tregs (blue) and CD4+FOXP3- Teffs (orange). "Donor", healthy donors; "AdenoCa", adenocarcinoma; "SquamCa", squamous cell carcinoma.

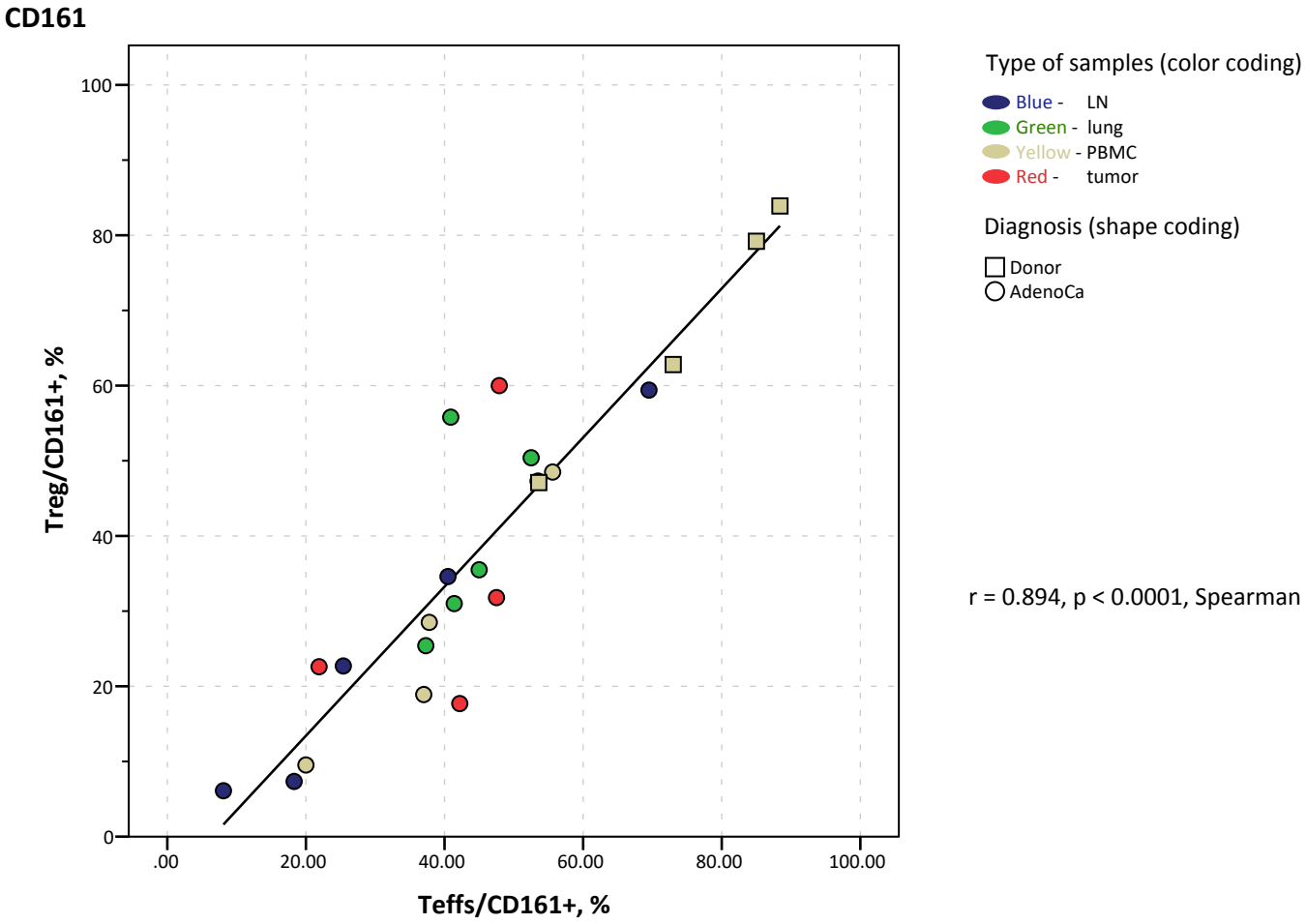

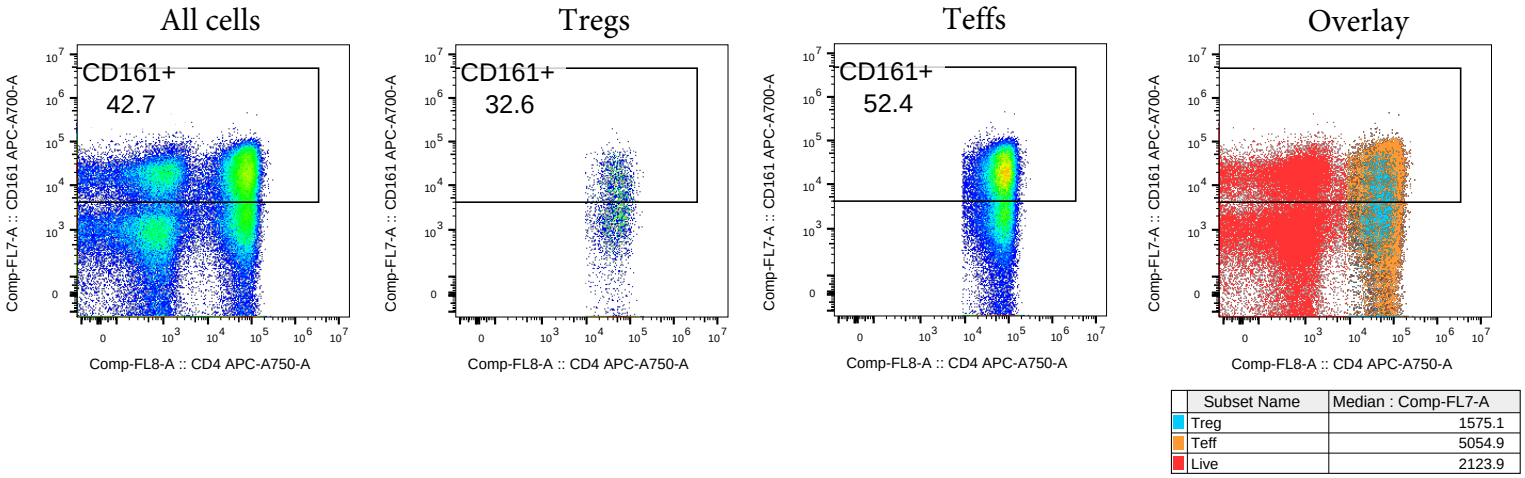

Supplemental Figure 33. CD161 expression in Tregs versus Teffs.
Top: correlation of CD161+ expression in CD4+FOXP3+ Tregs (y) and in CD4+FOXP3- Teffs (x), Spearman's correlation assay, n = 23. Different types of samples are coded by color, as indicated in legend. Shapes of symbols represent diagnostic categories, as indicated in legend. Bottom: gating strategy and the representative expression of CD161+ in Tregs and Teffs are shown, with corresponding MOF for CD161 in all viable cells (red), CD4+FOXP3+ Tregs (blue) and CD4+FOXP3- Teffs (orange). "Donor" - healthy donors, "AdenoCa" - adenocarcinoma.

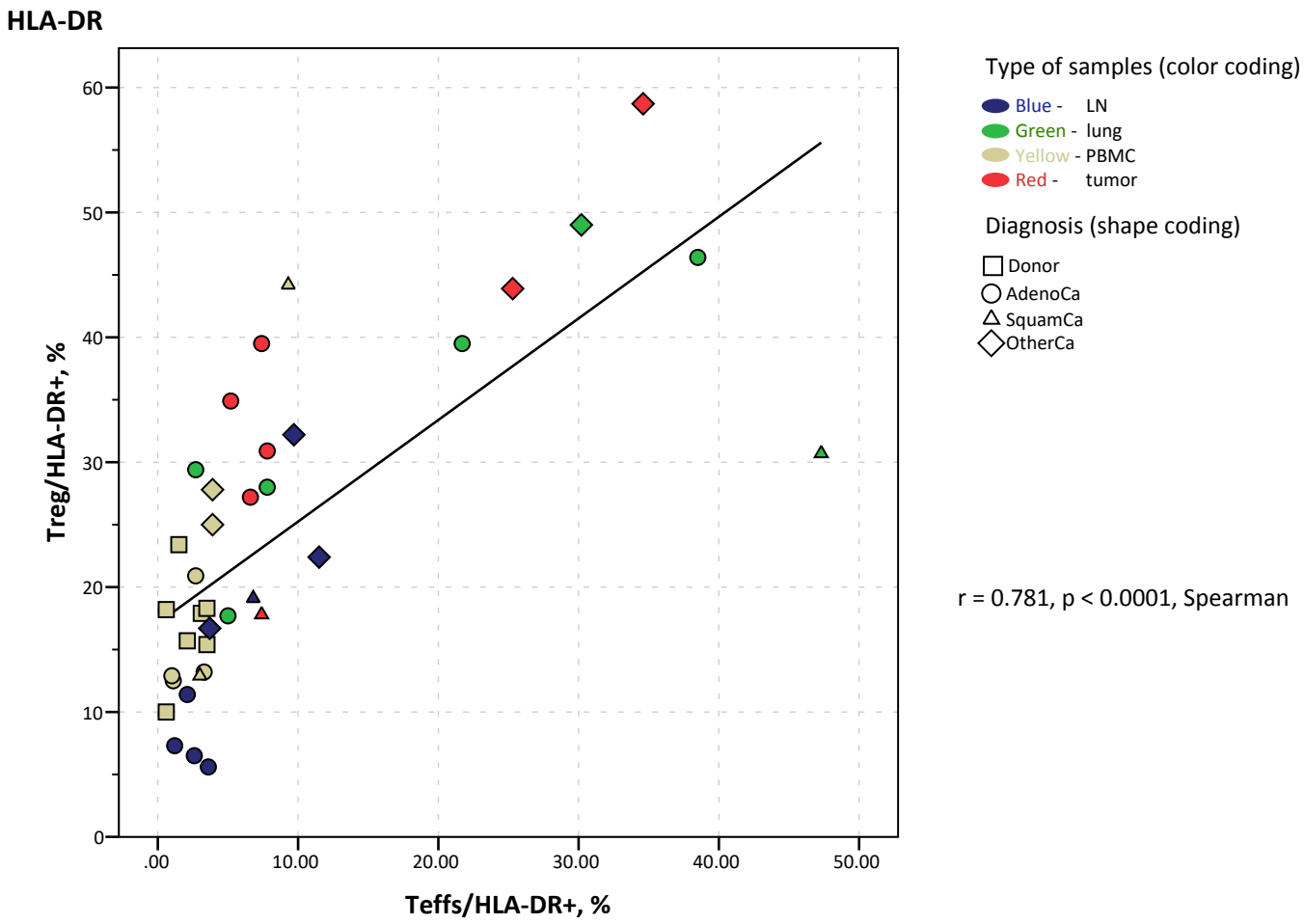

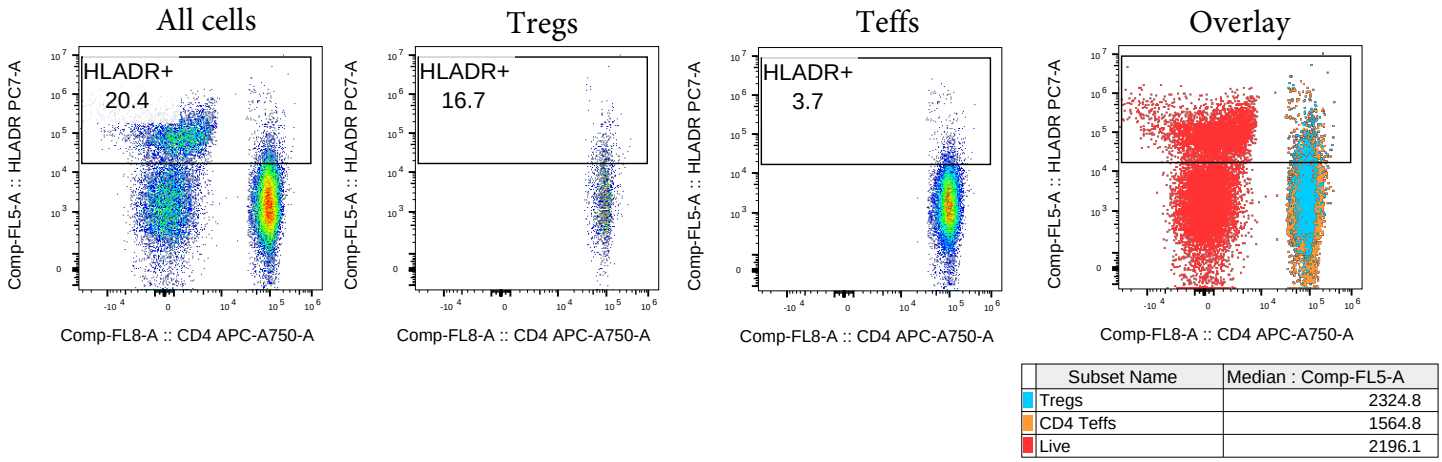

Subset Name	Median : Comp-FL5-A
Tregs	2324.8
CD4 Teffs	1564.8
Live	2196.1

Supplemental Figure 34. HLADR expression in Tregs versus Teffs.
Top: correlation of HLADR+ expression in CD4+FOXP3+ Tregs (y) and in CD4+FOXP3- Teffs (x), Spearman's correlation assay, n = 37. Different types of samples are coded by color, as indicated in legend. Shapes of symbols represent diagnostic categories, as indicated in legend. Bottom: gating strategy and the representative expression of HLADR+ in Tregs and Teffs are shown, with corresponding MOF for HLADR in all viable cells (red), CD4+FOXP3+ Tregs (blue) and CD4+FOXP3- Teffs (orange). "Donor" - healthy donors, "AdenoCa" - adenocarcinoma, "SquamCa" - squamous cell carcinoma, "OtherCa" - other types of cancers: large cell neuroendocrine carcinoma, lung metastasis of colon adenocarcinoma, high grade carcinoma or melanoma.

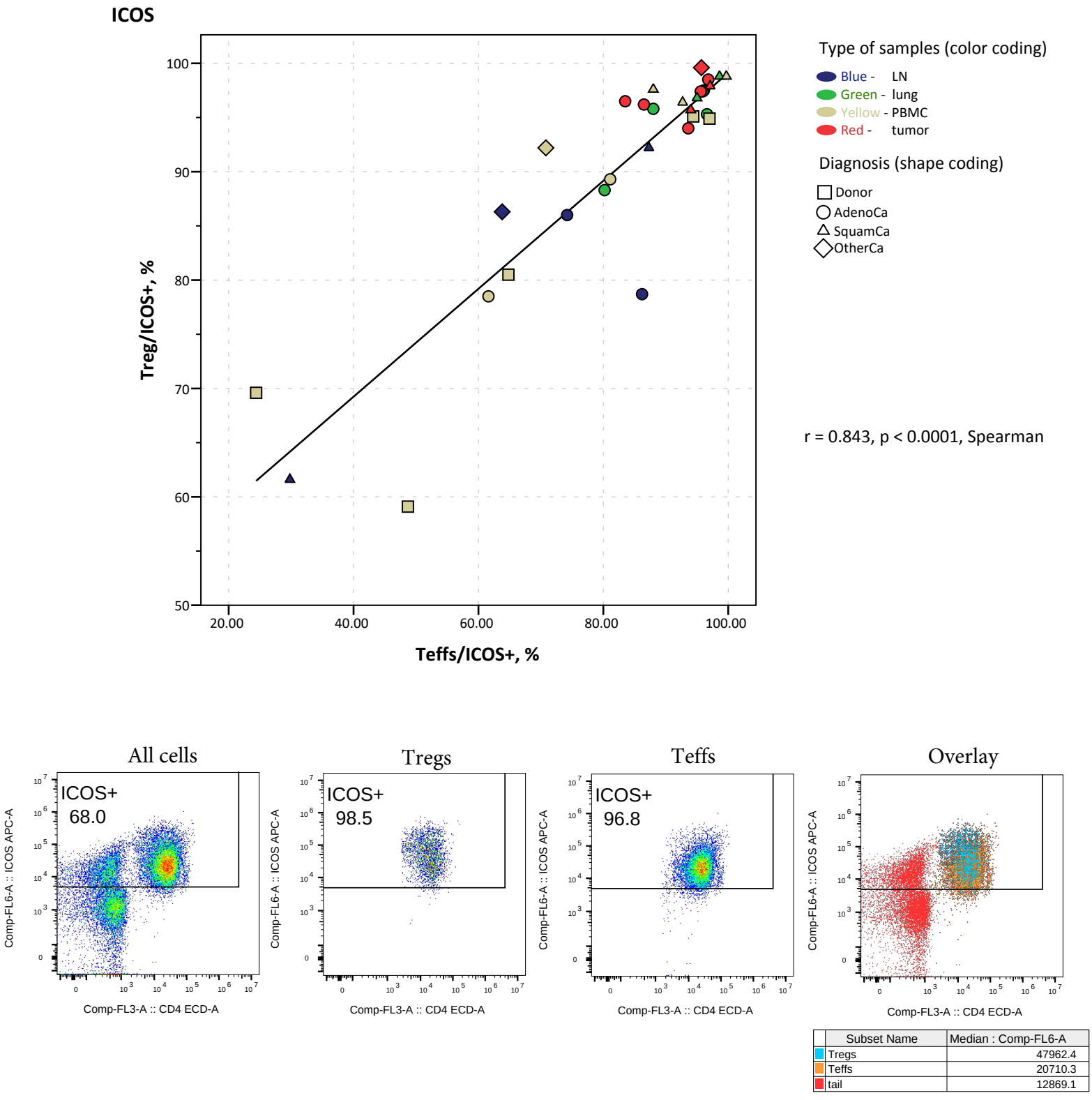

Supplemental Figure 35. ICOS expression in Tregs versus Teffs.
Top: correlation of ICOS+ expression in CD4+FOXP3+ Tregs (y) and in CD4+FOXP3- Teffs (x), Spearman's correlation assay, n = 31. Different types of samples are coded by color, as indicated in legend. Shapes of symbols represent diagnostic categories, as indicated in legend. Bottom: gating strategy and the representative expression of ICOS+ in Tregs and Teffs are shown, with corresponding MOF for ICOS in all viable cells (red), CD4+FOXP3+ Tregs (blue) and CD4+FOXP3- Teffs (orange). "Donor" - healthy donors, "AdenoCa" - adenocarcinoma, "SquamCa" - squamous cell carcinoma, "OtherCa" - other types of cancers: large cell neuroendocrine carcinoma, lung metastasis of colon adenocarcinoma, high grade carcinoma or melanoma.

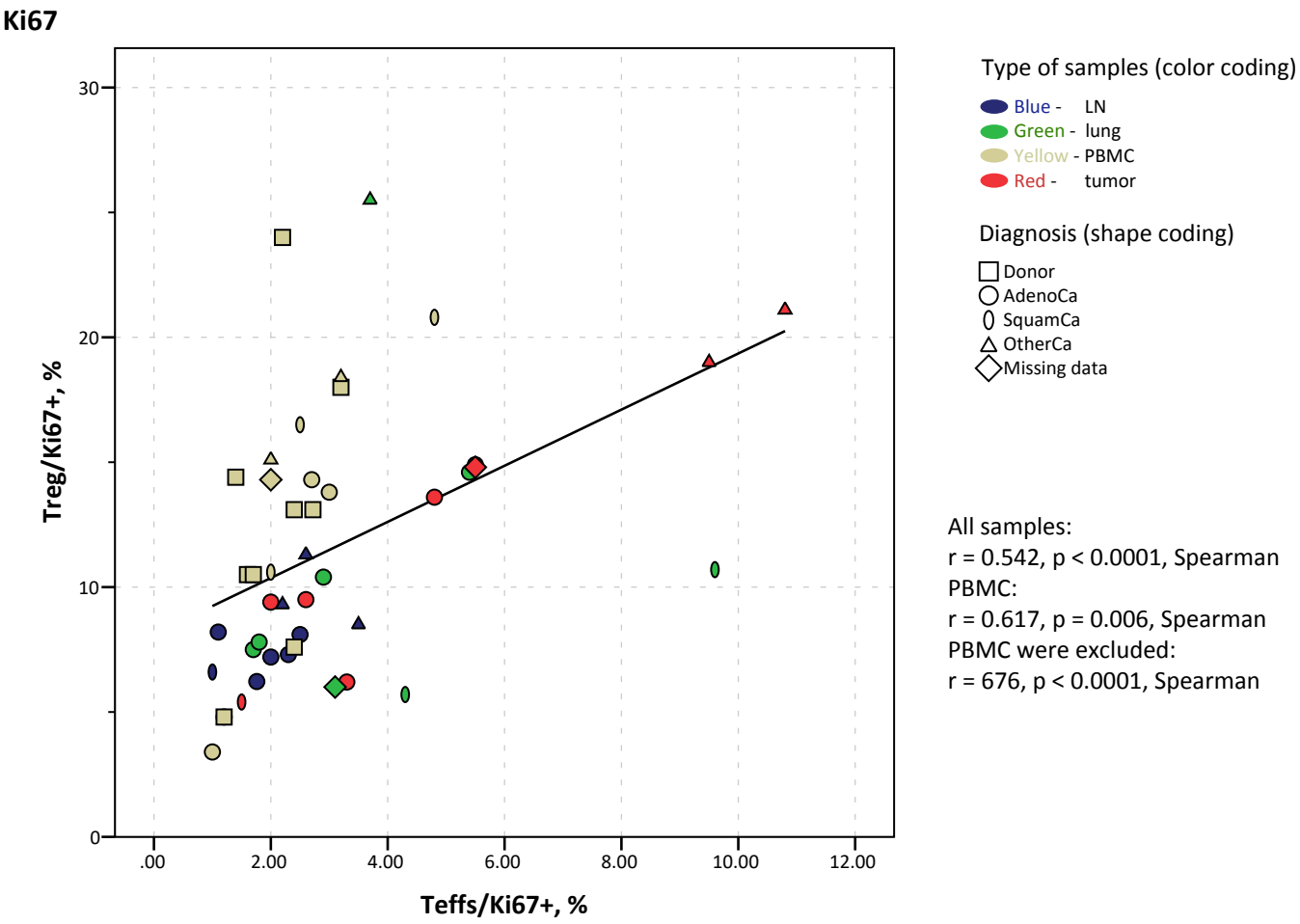

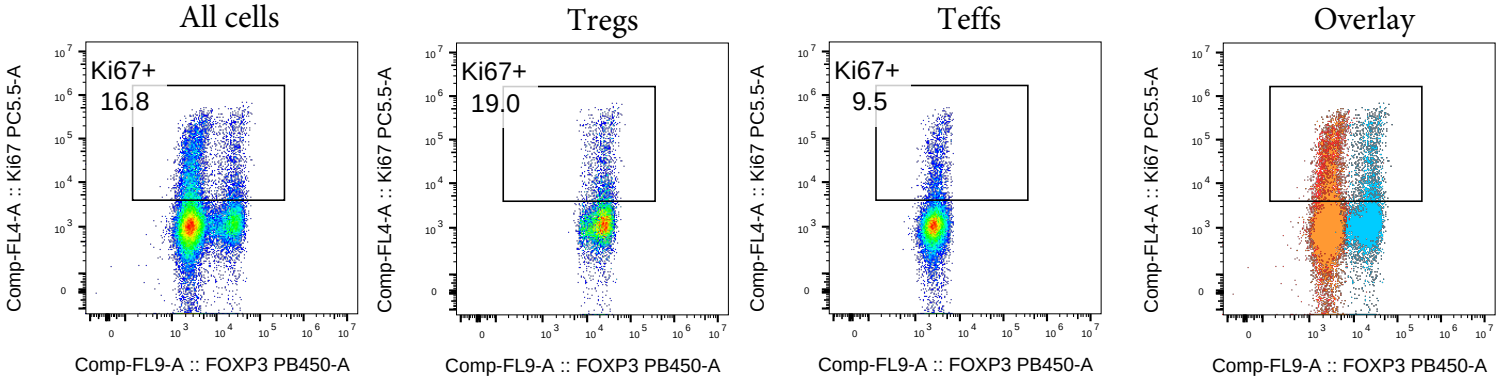

Subset Name	Median : Comp-FL4-A
Tregs	1362.9
CD4 Teffs	1092.1
Live	1188.3

Supplemental Figure 36. Ki67 expression in Tregs versus Teffs.
Top: correlation of Ki67+ expression in CD4+FOXP3+ Tregs (y) and in CD4+FOXP3- Teffs (x), Spearman's correlation assay, n = 27. Different types of samples are coded by color, as indicated in legend. Shapes of symbols represent diagnostic categories, as indicated in legend. Bottom: gating strategy and the representative expression of Ki67+ in Tregs and Teffs are shown, with corresponding MOF for Ki67 in all viable cells (red), CD4+FOXP3+ Tregs (blue) and CD4+FOXP3- Teffs (orange). "Donor" - healthy donors, "AdenoCa" - adenocarcinoma, "SquamCa" - squamous cell carcinoma, "OtherCa" - other types of cancers: large cell neuroendocrine carcinoma, lung metastasis of colon adenocarcinoma, high grade carcinoma or melanoma, "Missing data" patients had confirmed lung cancer, but details of its histological type are unknown.

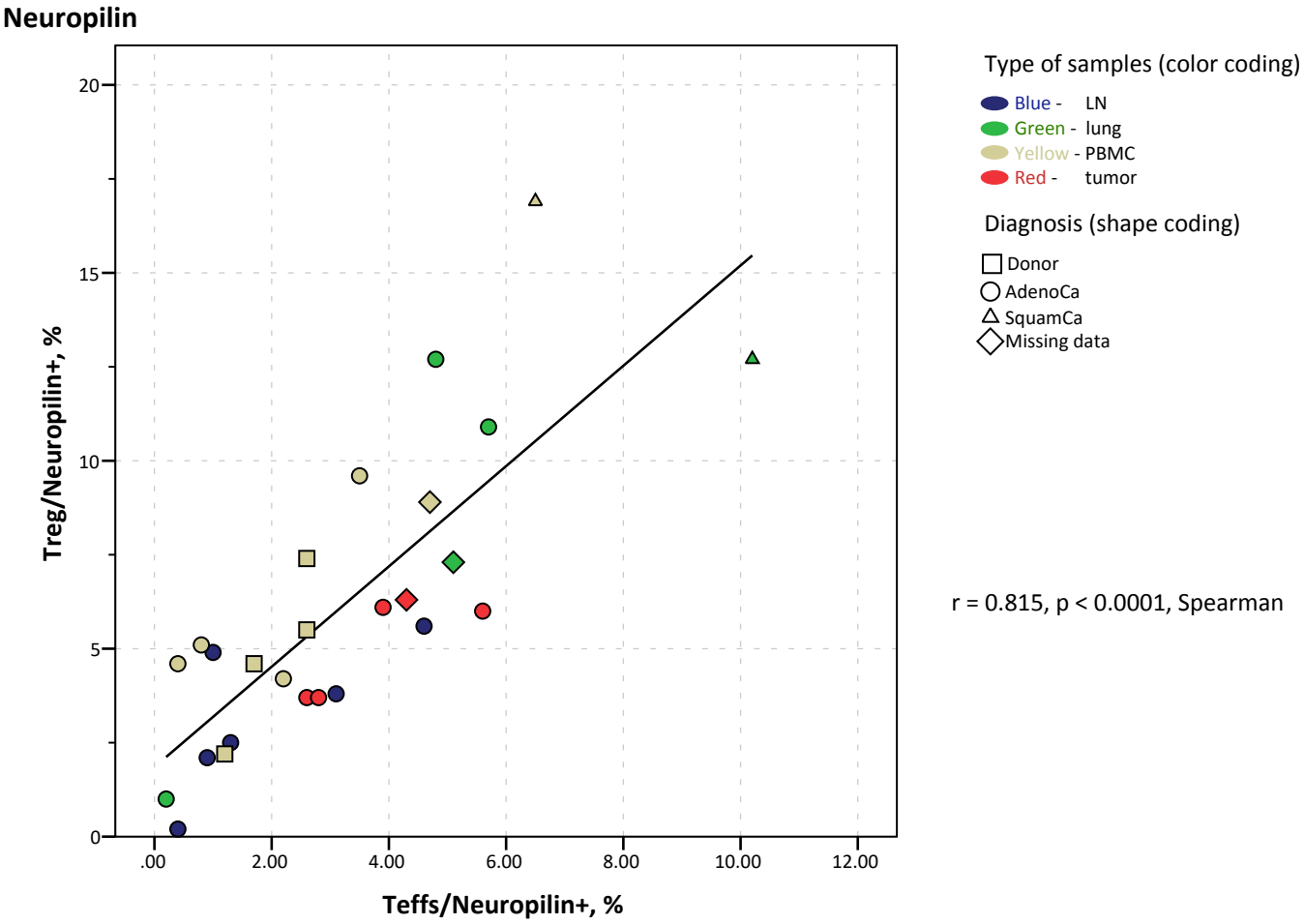

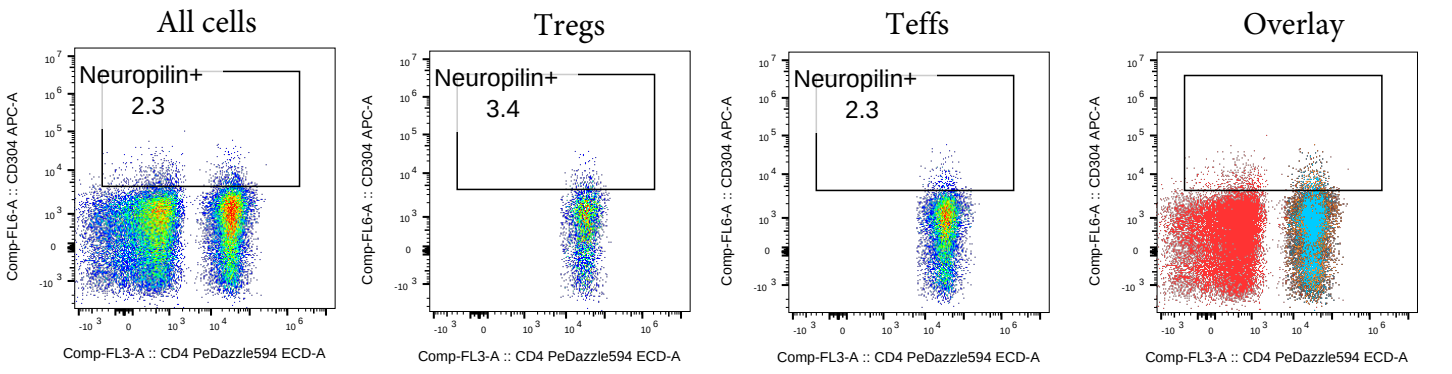

Subset Name	Median : Comp-FL6-A
Tregs	693.8
Teffs	678.0
live	554.4

Supplemental Figure 37. Neuropilin expression in Tregs versus Teffs.
Top: correlation of Neuropilin+ expression in CD4+FOXP3+ Tregs (y) and in CD4+FOXP3- Teffs (x), Spearman's correlation assay, n = 26. Different types of samples are coded by color, as indicated in legend. Shapes of symbols represent diagnostic categories, as indicated in legend. Bottom: gating strategy and the representative expression of Neuropilin+ in Tregs and Teffs are shown, with corresponding MOF for Neuropilin in all viable cells (red), CD4+FOXP3 + Tregs (blue) and CD4+FOXP3- Teffs (orange). "Donor", healthy donors; "AdenoCa", adenocarcinoma; "SquamCa", squamous cell carcinoma; "Missing data" patients had confirmed lung cancer, but of unknown histological type.

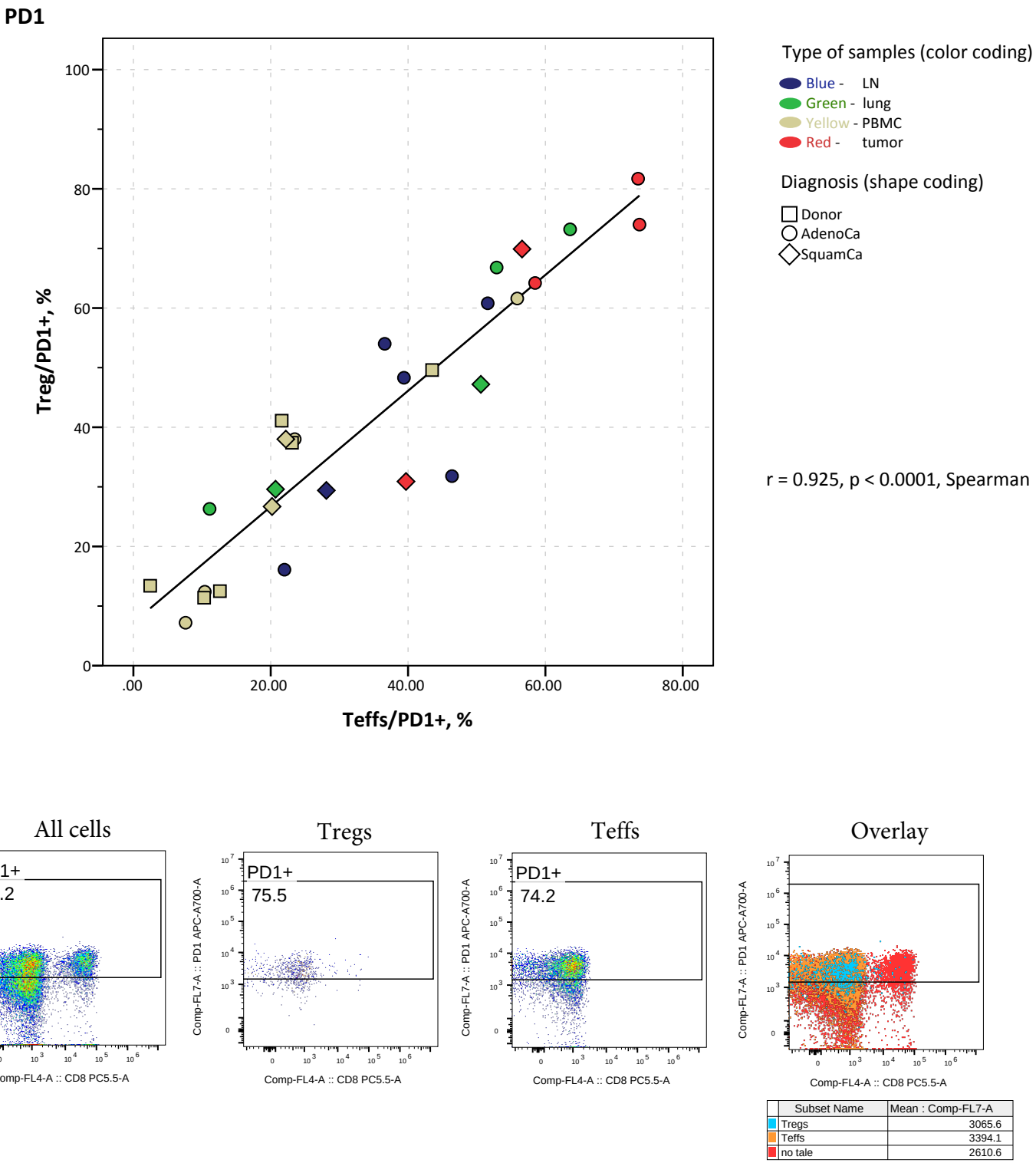

Supplemental Figure 38. PD1 expression in Tregs versus Teffs.
Top: correlation of PD1+ expression in CD4+FOXP3+ Tregs (y) and in CD4+FOXP3- Teffs (x), Spearman's correlation assay, n = 28. Different types of samples are coded by color, as indicated in legend. Shapes of symbols represent diagnostic categories, as indicated in legend. Bottom: gating strategy and the representative expression of PD1+ in Tregs and Teffs are shown, with corresponding MOF for PD1 in all viable cells (red), CD4+FOXP3+ Tregs (blue) and CD4+FOXP3- Teffs (orange). PD1 was evaluated after overnight stimulation with CD3/28 beads at 1/1 ratio in T cell media. "Donor" - healthy donors, "AdenoCa" - adenocarcinoma, "SquamCa" - squamous cells carcinoma.

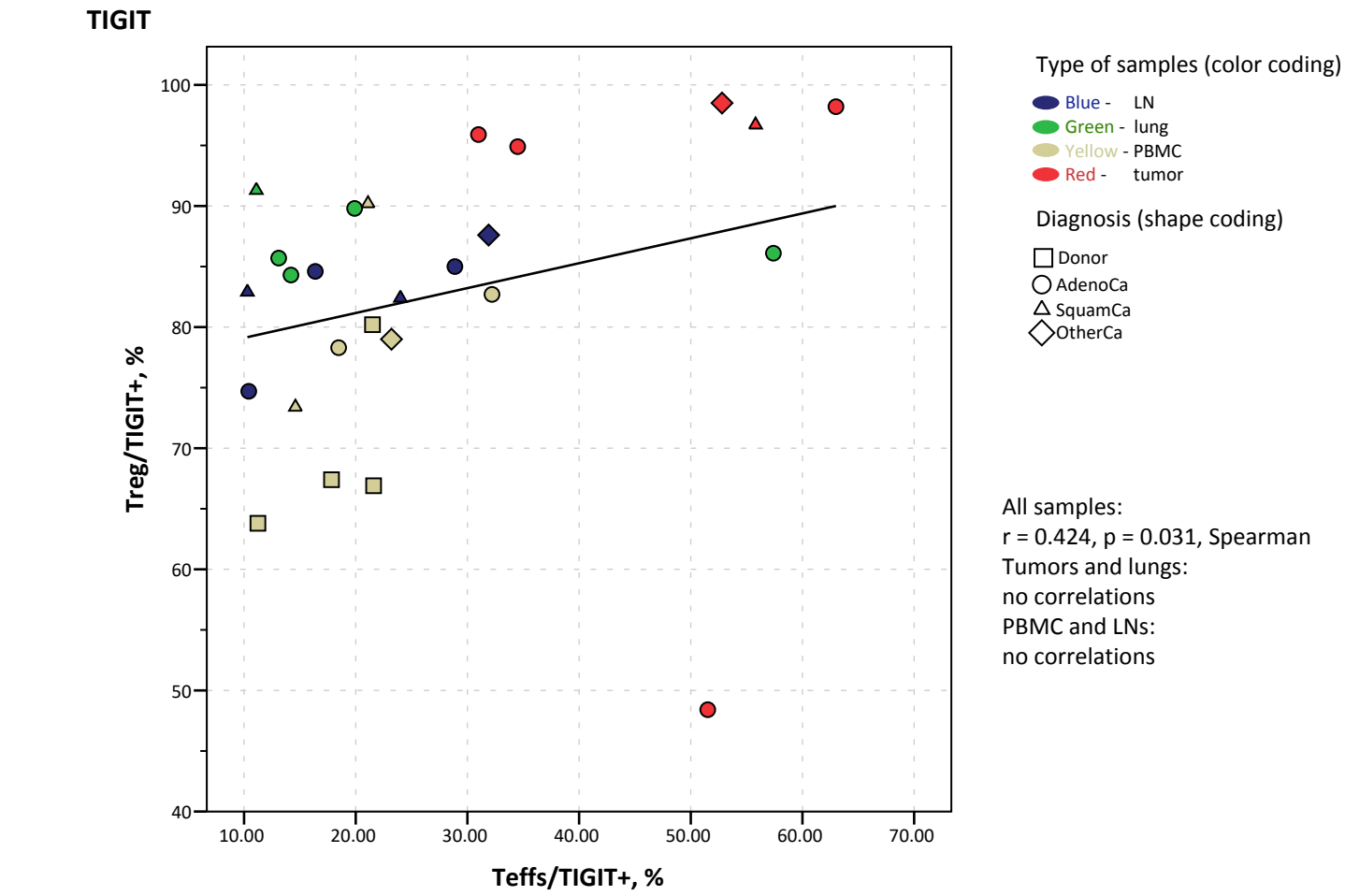

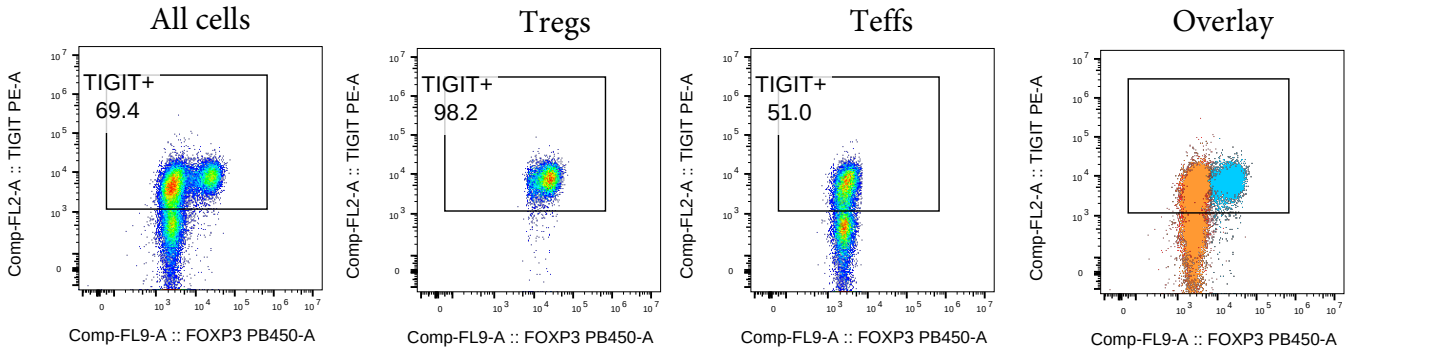

Subset Name	Median : Comp-FL2-A
Tregs	7376.1
CD4 Teffs	1310.4
Live	3369.3

Supplemental Figure 39. TIGIT expression in Tregs versus Teffs.
Top: correlation of TIGIT+ expression in CD4+FOXP3+ Tregs (y) and in CD4+FOXP3- Teffs (x), Spearman's correlation assay, n = 26. Different types of samples are coded by color, as indicated in legend. Shapes of symbols represent diagnostic categories, as indicated in legend. When tumor and lung samples were analyzed separately, TIGIT expression in Tregs and Teffs had no correlation. Similarly, when PBMC and LNs samples were analyzed separately, TIGIT expression in Tregs and Teffs did not correlate. Bottom: gating strategy and the representative expression of TIGIT+ in Tregs and Teffs are shown, with corresponding MOF for TIGIT in all viable cells (red), CD4+FOXP3+ Tregs (blue) and CD4+FOXP3- Teffs (orange). "Donor" - healthy donors, "AdenoCa" - adenocarcinoma, "SquamCa" - squamous cells carcinoma, "OtherCa" - other types of cancers: large cell neuroendocrine carcinoma, lung metastasis of colon adenocarcinoma, high grade carcinoma or melanoma.

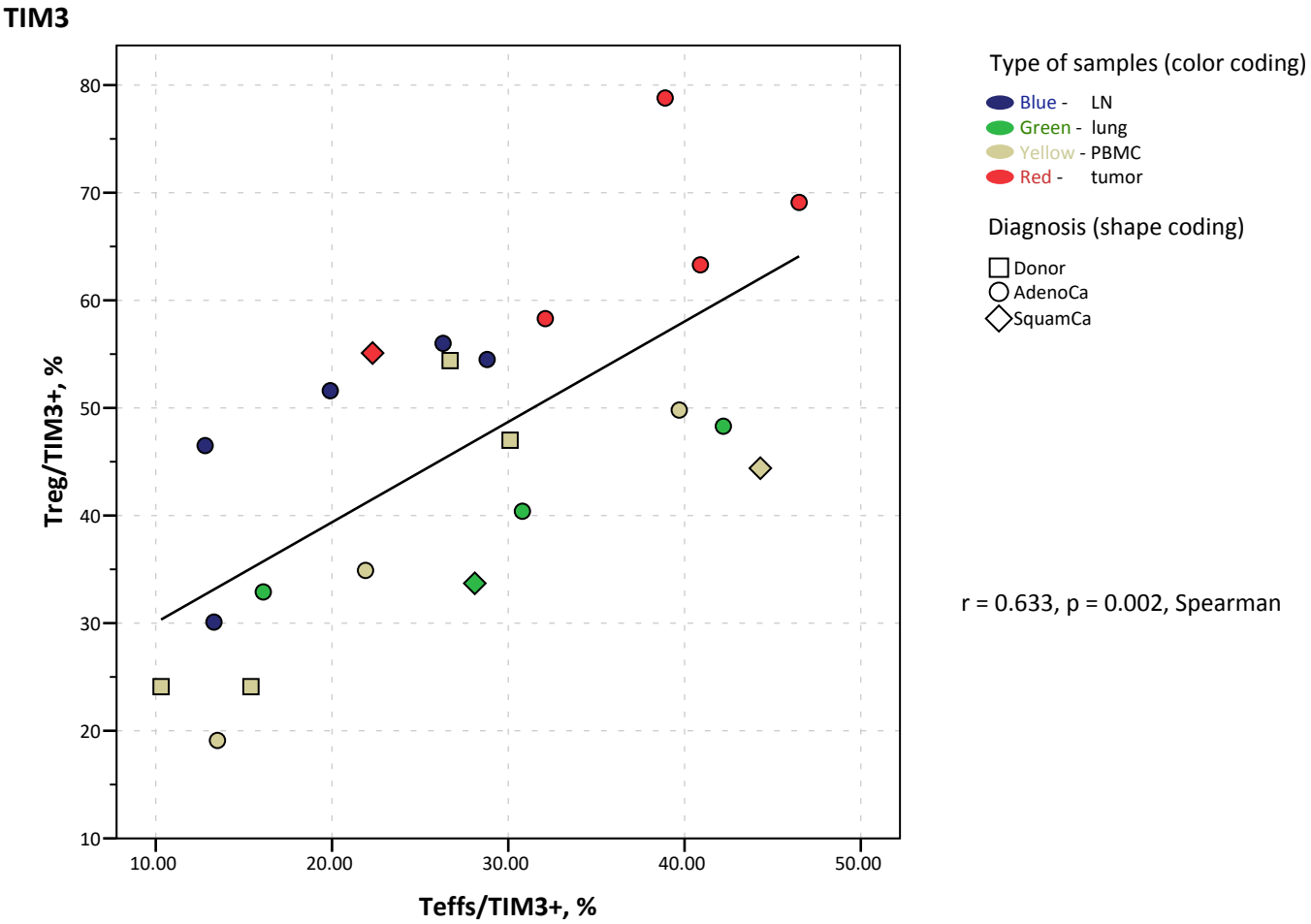

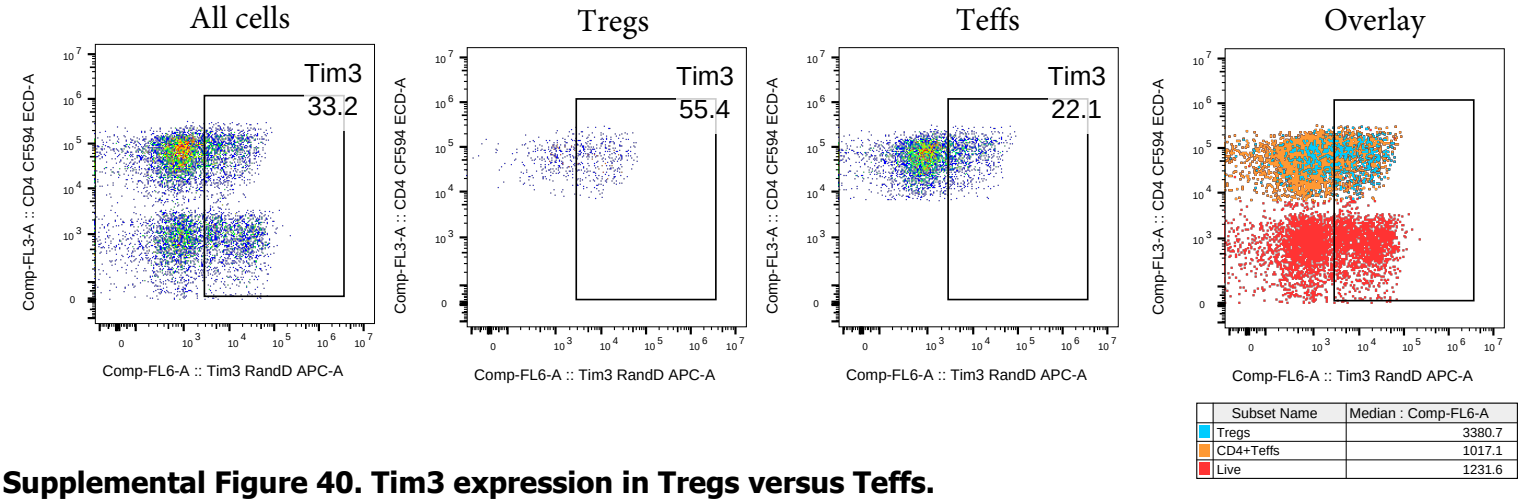

Supplemental Figure 40. Tim3 expression in Tregs versus Teffs.
Top: correlation of Tim3+ expression in CD4+FOXP3+ Tregs (y) and in CD4+FOXP3- Teffs (x), Spearman's correlation assay, n = 22. Different types of samples are coded by color, as indicated in legend. Shapes of symbols represent diagnostic categories, as indicated in legend. When tumor and lung samples were analyzed separately, Tim3 expression in Tregs and Teffs had no correlation. Similarly, when PBMC and LNs samples were analyzed separately, Tim3 expression in Tregs and Teffs did not correlate. Bottom: gating strategy and the representative expression of Tim3+ in Tregs and Teffs are shown, with corresponding MOF for Tim3 in all viable cells (red), CD4+FOXP3+ Tregs (blue) and CD4+FOXP3- Teffs (orange). Tim3 was evaluated after stimulation for 2 days with CD3/28 beads at 1/1 ratio in T cell media. "Donor" - healthy donors, "AdenoCa" - adenocarcinoma, "SquamCa" - squamous cells carcinoma.

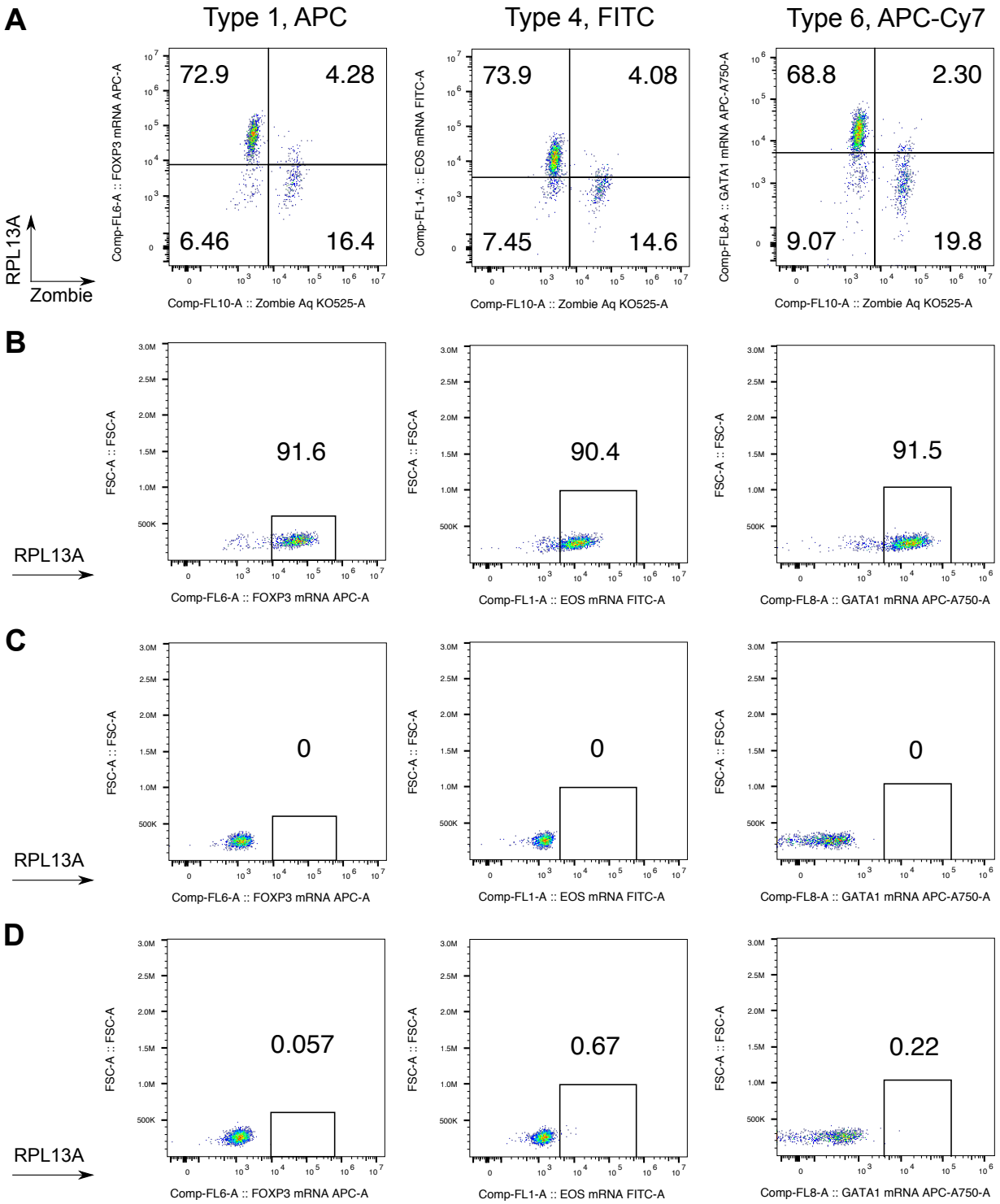

Supplemental Figure 41. PrimeFlow RNA controls.
(A) dot plots with housekeeping genes expression (y) vs. live/dead co-staining (x), showing that only viable cells have mRNA expression of housekeeping gene RPL13A (left, top corners), while cells with impaired membranes that stained positively with fixable live/dead reagent "Zombie", do not express RPL13A mRNA. Three columns correspond with results for three different RPL13A primers with type 1, type 4 and type 6 fluorescent labels, as indicated. (B) Positive control: the viable cells have high (more than 90%) and uniform expression of housekeeping gene RPL13A, in all three types of primers. (C) Negative controls: cells were proceeded for all steps in the method, including pre-amplification and amplification of mRNA signals, but no primers were used at hybridization step. There are no non-specific background signals in all three channels. (D) FMO controls. Cells were stained with all reagents, including live/dead, superficial and intranuclear antibodies, had primers for one or two other channels, but had no primers in the tested channel. There are small shifts in staining of negative populations, but still no non-specific signals exist. Notably that cells were co-stained with PE in Type 4, FITC control and with APC or APC-Cy7 in Type 6 APC-Cy7 or Type 1 APC controls, to ensure an absence of non-specific signals due to flow cytometry compensation issues.

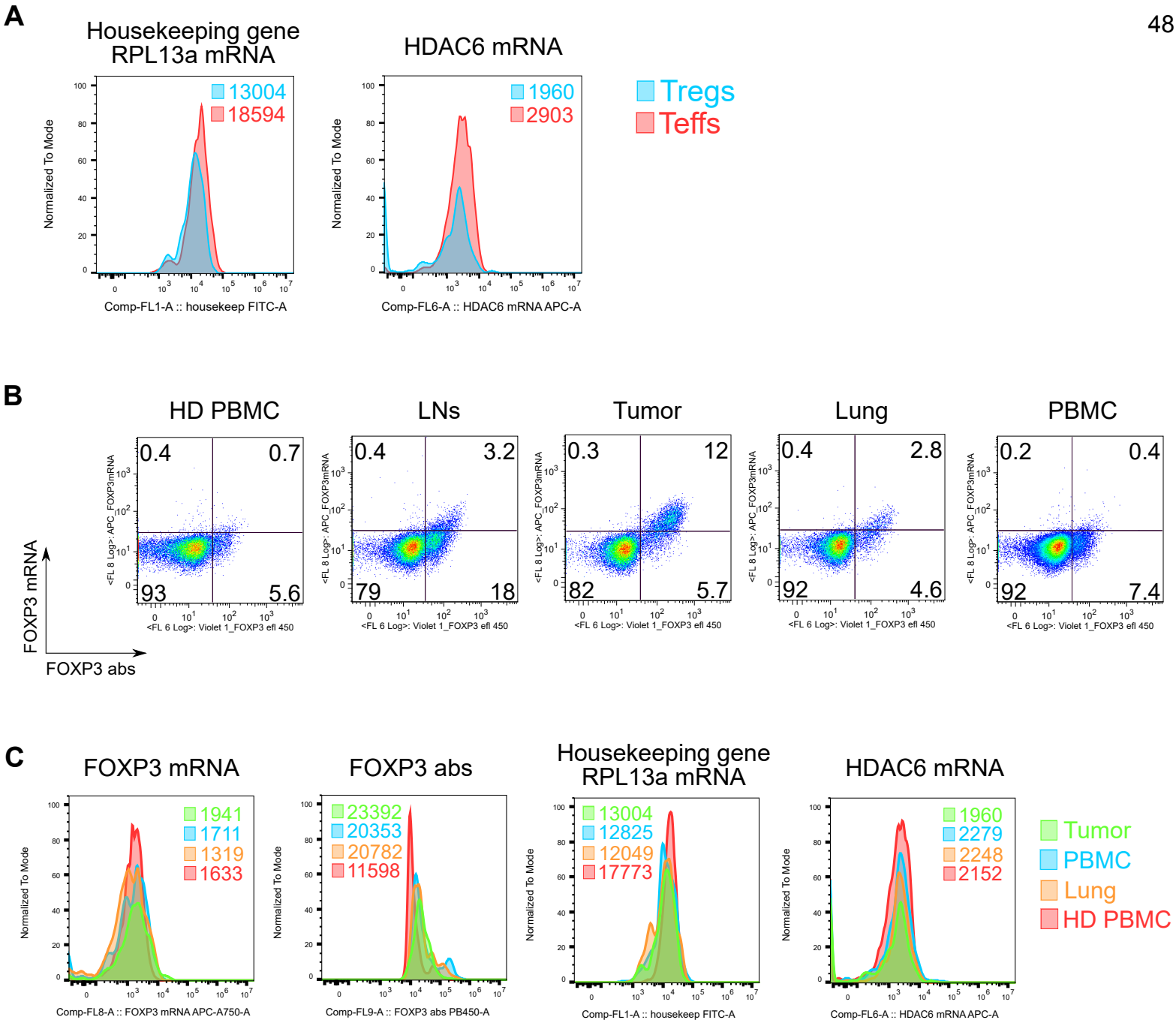

Supplemental Figure 42. PrimeFlow RNA controls of specificity.
(A) histograms showing that tumor Tregs do not upregulate expression of (left) housekeeping gene mRNA or (right) non related gene HDAC6 mRNA, in comparison with Teffs. Histograms show the representative expressions MOFs in Tregs (blue) and Teffs (red). (B) Pseudocolor dot plots of CD4+ gated cells from different samples, showing the representative examples of FOXP3 mRNA (y) versus FOXP3 protein (x) expressions. (C) histograms from the same experiment, showing that while tumor Tregs do have more FOXP3 mRNA and FOXP3 protein in comparison with other Tregs, they do not have more housekeeping gene RPL13A mRNA or non-related gene HDAC6 mRNA expressions. Histograms show the representative expression with MOFs in Tregs from healthy donor PBMC (red), distant lung (orange), PBMC (blue) and tumor (green).

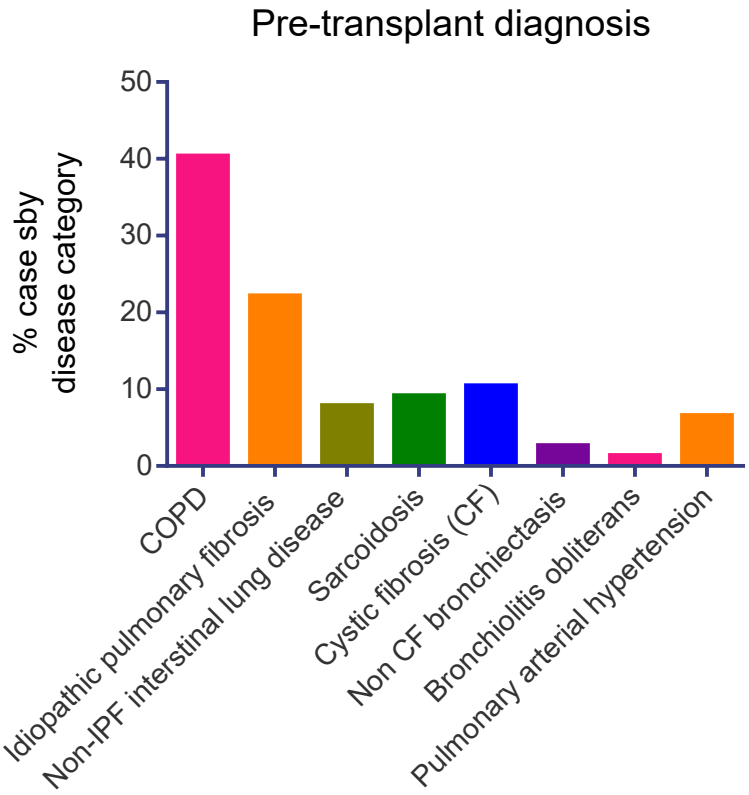

Supplemental Figure 43.
Pre-transplant diagnoses in patients listed for lung transplant (LT). Percent of patients with corresponding diagnosis is shown for each category.

SUPPLEMENTAL TABLES

Supplemental Table 1

Raw data for division of CD4+ and CD8+ responders, followed by calculation of standardized suppression for the same samples and suppression in AUC units(15), for non-diluted Tregs (100%) and Tregs diluted with CD4+CD25-FOXP3-autologous T cells (60%)

Raw Data:	Divisions rate of CD4+, %		Divisions rate of CD8+, %	
	% of Tregs in suppression assay at 1/1		% of Tregs in suppression assay at 1/1	
Ratios Treg/Teffs	100	60	100	60
1/1	46.7	70.3	42.7	57.4
1/2	71.8	73.9	62.8	67.5
1/4	75.9	80.8	70.4	75
1/8	80.3	82	73.7	73.3
1/16	79.9	82.8	73.2	75
No Tregs	81.4	84	74.7	75.4
Standardized suppressions:	Standardized suppression for CD4+, %		Standardized suppression for CD8+, %	
	% of Tregs in suppression assay at 1/1		% of Tregs in suppression assay at 1/1	
Powers of 2 used for AUCs	100	60	100	60
0	42.6	16.3	42.8	23.9
1	11.8	12.0	15.9	10.5
2	6.8	3.8	5.8	0
3	0	0	0	0
4	0	0	0	0
Calculated AUCs	AUC, for CD4+ responders, units		AUC, for CD8+ responders, units	
	% of Tregs in suppression assay at 1/1		% of Tregs in suppression assay at 1/1	
	100	60	100	60
AUCs, Total Peak Area	39.9	24.0	43.1	22.4

Supplemental Table 2

Equations for suppressive capabilities of Tregs to suppress division of CD4+ and CD8+ responders, as a function of Treg FOXP3+ purity after isolation

	Total samples			Linear regression analysis					
	# of X values	Max. # of Y replicates	# of values	Slope	Intercept	F	DFn, DFd	P Value	R^2
CD4+ responders	7	4	12	0.01793 ± 0.001754	-0.1856 ± 0.08991	104.6	1.000, 10.00	< 0.0001	0.9127
CD8+ responders	7	4	12	0.01840 ± 0.002505	-0.2253 ± 0.1285	53.95	1.000, 10.00	< 0.0001	0.8436

Supplemental Table 3

Predicted and observed suppressive function of one healthy donor Tregs sample

	CD4+ responders		CD8+ responders	
	Before dilution	After dilution	Before dilution	After dilution
Tregs purity (% of FOXP3+)	79.40	47.64	79.40	47.64
Observed suppression, AUC units	39.86	23.99	43.11	22.41
Observed AUCs ratios	1.00	0.60	1.00	0.52
Predicted AUCs ratios*	1.24	0.67	1.24	0.65
Predicted AUCs ratios**	1.00	0.54	1.00	0.53
Predicted suppression, AUC units		21.53		22.72
Prediction error (%)		10		1

* 66% of FOXP3+ purity is set up as 1.

** The highest observed $FOXP3^{+}$ purity was re-calculated as 1.

Supplemental Table 4

Treg-associated markers, evaluated in lung cancer patients

#	The reasons to choose	Markers, references
1	Were shown to be important for Treg function	CD15s (24), CD25 (25, 26), CD39 (27, 28), CD45RA/RO (29), CD69 (30), CD101 (31), CD120b (32), CD161 (33), CCR4 (34), CTLA4 (25, 26, 35), GARP (36, 37), GITR (26, 38), Helios (39, 40), HLA-DR (41), ICOS (42), and Tim3 (43)
2	Were upregulated in tumor Tregs, were shown to be related with tumor Tregs or Teffs biology	CD26 (44), CD27 (45, 46), CD39 (47), CD40L (48), CD45RA/RO (49), CD120b (32), CD161 (50), CTLA4 (51, 52) GITR (53), Helios (54), HLA-DR (55), ICOS (56, 57), neuropilin (58, 59), PD-1 (60), TIGIT (61), and Tim3 (62, 63)
3	Were suggested to serve as selective Treg-positive or Treg-negative markers	CD26 (44, 64), CD127 (65), GARP (36, 66), and LAP (67)
4	Were suggested to be important for tumor Treg or Teff cell trafficking	CCR4 (34, 68), CCR5, CCR7 and CXCR3, CXCR4 (68), CCR8 (69, 70), CXCR5(71) and CD62L (72)

Supplemental Table 5

Expression of CD39, CTLA4, GARP and Tim3 in Tregs and Teffs, results of two-way ANOVAs with multiple comparisons tests.

Types of comparison:	Marker, p values			
	CD39	**CTLA4**	**GARP**	**Tim3**
Number of Treg-Teff pairs	65	28	19	22
Two-way ANOVA:				
- Interaction	0.592	0.0203	0.0083	0.1374
- Row factor (type of samples)	< 0.0001	< 0.0001	0.0006	0.0016
- Column factor (Tregs vs. Teffs)	< 0.0001	< 0.0001	< 0.0001	< 0.0001
Tukey's test (type of samples) in Tregs: HD PBMC vs. PBMC	ns	ns	ns	ns
HD PBMC vs. LNs	ns	ns	***	ns
HD PBMC vs. tumors	***	****	**	**
HD PBMC vs. lungs	ns	****	ns	ns
PBMC vs. LNs	ns	ns	ns	ns
PBMC vs. tumors	****	****	ns	**
PBMC vs. lungs	ns	***	ns	ns
LNs vs. tumors	**	****	ns	ns
LNs vs. lungs	ns	**	***	ns
Tumors vs. lungs	ns	ns	**	**
Tukey's test (type of samples) in Teffs: HD PBMC vs. PBMC	ns	ns	ns	ns
HD PBMC vs. LNs	ns	ns	ns	ns
HD PBMC vs. tumors	ns	**	ns	ns
HD PBMC vs. lungs	ns	ns	ns	ns
PBMC vs. LNs	ns	ns	ns	ns
PBMC vs. tumors	ns	**	ns	ns
PBMC vs. lungs	ns	ns	ns	ns
LNs vs. tumors	ns	*	ns	ns
LNs vs. lungs	ns	ns	ns	ns
Tumors vs. lungs	ns	ns	ns	ns
Sidak's test (Tregs vs. Teffs)				
in HD PBMC	< 0.0001	0.001	0.0589	ns
in PBMC	< 0.0001	< 0.0001	0.0008	ns
in LNs	< 0.0001	< 0.0001	< 0.0001	**
in tumors	< 0.0001	< 0.0001	< 0.0001	***
in lungs	< 0.0001	< 0.0001	0.3002	ns

"Number of Treg-Teff pairs" is equal of number of unique samples tested for corresponding marker
"HD PBMC" – healthy donors PBMC
"ns" – not significant, p value >0.05; *p <0.05; ** p<0.01; *** p<0.001; **** p<0.0001

Supplemental Table 6

Correlations between TFs and FOXP protein expression in Tregs, analyzed on single cell levels

Type of Tregs:	TFs:	STAB1		GATA1		EOS		IRF4		LEF1	
	Correlations / Sample IDs	Pearson r	Controlled for FOXP3 mRNA, r	Pearson r	Controlled for FOXP3 mRNA, r	Pearson r	Controlled for FOXP3 mRNA, r	Pearson r	Controlled for FOXP3 mRNA, r	Pearson r	Controlled for FOXP3 mRNA, r
Tumors	LC205	no	-.088	.391	.085	n/d	n/d	n/d	n/d	n/d	n/d
	LC211(4)	n/d	n/d	no	no	.335	no	no	no	.143	no
	LC214	.180	.069	.098	no	.276	.139	.134	no	no	no
	LC228	n/d	n/d	.155	.077	.314	.196	no	.069	.078	no
	LC233	.193	no	.074	no	n/d	n/d	n/d	n/d	n/d	n/d
	LC241	n/d	n/d	.091	no	.248	.086	n/d	n/d	n/d	n/d
	LC268	.103	no	no	no	.194	no	no	no	n/d	n/d
Lungs	LC211(4)	n/d	n/d	no	no	.250	no	-.068	-.123	-.149	-.334
	LC214	.157	.105	.167	.085	.343	.231	.119	no	no	no
	LC228	n/d	n/d	no	no	.211	.208	no	no	.077	.077
	LC233	.279	no	no	no	n/d	n/d	n/d	n/d	n/d	n/d
	LC241	n/d	n/d	.206	.071	.302	.186	n/d	n/d	n/d	n/d
	LC268	.120	no	no	no	-.149	-.136	no	no	n/d	n/d
PBMC	LC211(4)	n/d	n/d	no	no	.104	no	no	no	.125	no
	LC214	.069	no	.149	.094	.306	.230	.141	.089	no	no
	LC228	n/d	n/d	no	no	.100	.062	.073	.091	-.091	-.156
	LC233	no	no	no	no	n/d	n/d	n/d	n/d	n/d	n/d
	LC237	n/d	n/d	no	no	no	no	n/d	n/d	n/d	n/d
LNs	LC81	n/d	n/d	no	no	.216	no	no	no	.170	no
	LC268	-.089	-.089	no	no	-.118	-.103	no	no	n/d	n/d
HD PBMC	ND052	-.260	-.288	.113	no	n/d	n/d	n/d	n/d	n/d	n/d
	ND307	-.309	-.332	.063	no	n/d	n/d	n/d	n/d	n/d	n/d
	ND390	n/d	n/d	no	no	.085	no	no	no	no	no
	ND436	n/d	n/d	no	-.081	no	-.089	n/d	n/d	n/d	n/d
	ND481	n/d	n/d	no	no	.099	.106	n/d	n/d	n/d	n/d
	ND488	no	no	no	no	-.092	-.065	no	no	no	no

“TF” – transcription factors
“HD PBMC” - PBMC of healthy donor
"no" - p value for correlation coefficient was > 0.05;
"n/d" - no data for this sample;
"Controlled for FOXP3 mRNA" -partial correlation coefficient r.
For all presented correlation coefficients, p values were <0.05

Supplemental Table 7

Clinical data of LC patients (n=92)

Characteristics		Number of patients	% within known
Gender:	Males	57	63
	Females	33	37
	No data	2	-
Race:	White	53	73
	Black	16	22
	Other	4	5
	No data	19	-
Tumor Stage:	IA	31	35
	IB	21	24
	IIA	12	14
	IIB	12	14
	IIIA	12	14
	No data	4	-
Tumor Grade:	T1a	20	28
	T1b	12	17
	T2a	21	29
	T2b	6	8
	T3	13	18
	No data	20	-
Nodal Stage:	N0	66	77
	N1	14	16
	N2	6	7
	No data	6	-
Cancer Type:	Adenocarcinoma	57	63
	Squamous Cell Carcinoma	27	30
	Other Cancers*	7	8
	No data	1	-
Smoking Status	Never Smoked	7	10
	Former Smoker	48	66
	Current Smoker	18	25
	Unknown	19	-

* Other Cancers included: large cell neuroendocrine carcinoma (3); lung metastasis of colon adenocarcinoma (1), high grade carcinoma (1) and melanoma (1)

Supplemental Table 8

Expression of trafficking and maturation T cells markers, the results of two-way ANOVAs with multiple comparisons tests. Part 1.

Types of comparison:	Marker, p values				
	CCR4	**CCR5**	**CCR7**	**CCR8**	**CXCR3**
Number of Treg-Teff pairs	41	23	24	38	31
Two-way ANOVA:					
- Interaction	0.5106	0.9011	0.3388	0.9477	0.179
- Row factor (type of samples)	0.0659	0.0292	< 0.0001	0.02	< 0.0001
- Column factor (Tregs vs. Teffs)	< 0.0001	0.2844	0.0028	0.154	0.1244
Tukey's test (type of samples) in Tregs: HD PBMC vs. PBMC	ns	ns	ns	ns	ns
HD PBMC vs. LNs	ns	ns	ns	ns	ns
HD PBMC vs. tumors	ns	ns	ns	ns	**
HD PBMC vs. lungs	ns	ns	**	ns	ns
PBMC vs. LNs	ns	ns	ns	ns	ns
PBMC vs. tumors	ns	ns	ns	ns	*
PBMC vs. lungs	ns	ns	**	ns	ns
LNs vs. tumors	ns	ns	ns	ns	ns
LNs vs. lungs	ns	ns	*	ns	ns
Tumors vs. lungs	ns	ns	ns	ns	ns
Tukey's test (type of samples) in Teffs: HD PBMC vs. PBMC	ns	ns	ns	ns	ns
HD PBMC vs. LNs	ns	ns	ns	ns	ns
HD PBMC vs. tumors	ns	ns	*	ns	****
HD PBMC vs. lungs	ns	ns	****	ns	****
PBMC vs. LNs	ns	ns	ns	ns	ns
PBMC vs. tumors	ns	ns	ns	ns	*
PBMC vs. lungs	ns	*	***	ns	ns
LNs vs. tumors	ns	ns	*	ns	***
LNs vs. lungs	ns	ns	****	ns	**
Tumors vs. lungs	ns	ns	ns	ns	ns
Sidak's test (Tregs vs. Teffs)					
in HD PBMC	0.0081	0.917	0.0987	0.9997	0.9988
in PBMC	< 0.0001	0.8885	0.8286	0.6033	0.4844
in LNs	0.0471	0.9964	0.03	0.9985	0.8794
in tumors	0.0138	0.9934	0.7879	0.9552	0.8017
in lungs	0.0007	0.9991	> 0.9999	0.9838	0.2319

"Number of Treg-Teff pairs" is equal of number of unique samples tested for corresponding marker
"HD PBMC" – healthy donors PBMC
"ns" – not significant, p value >0.05; *p <0.05; ** p<0.01; *** p<0.001; **** p<0.0001

Supplemental Table 9

Expression of trafficking and maturation T cells markers, the results of two-way ANOVAs with multiple comparisons tests. Part 2.

Types of comparison:	Marker, p values				
	CXCR4	**CXCR5**	**CD62L**	**CD45RA**	**CD45RO**
Number of Treg-Teff pairs	29	30	87	44	55
Two-way ANOVA:					
- Interaction	0.9051	P = 0.0059	0.0124	0.0043	0.005
- Row factor (type of samples)	0.0002	P < 0.0001	< 0.0001	< 0.0001	< 0.0001
- Column factor (Tregs vs. Teffs)	0.1576	P = 0.3173	< 0.0001	< 0.0001	< 0.0001
Tukey's test (type of samples) in Tregs: HD PBMC vs. PBMC	ns	ns	ns	*	**
HD PBMC vs. LNs	ns	****	ns	ns	ns
HD PBMC vs. tumors	**	ns	*	****	****
HD PBMC vs. lungs	**	ns	*	***	****
PBMC vs. LNs	ns	****	ns	ns	ns
PBMC vs. tumors	ns	ns	**	ns	ns
PBMC vs. lungs	ns	ns	*	ns	ns
LNs vs. tumors	ns	****	ns	**	***
LNs vs. lungs	ns	****	ns	ns	*
Tumors vs. lungs	ns	ns	ns	ns	ns
Tukey's test (type of samples) in Teffs: HD PBMC vs. PBMC	ns	ns	ns	ns	ns
HD PBMC vs. LNs	ns	****	*	*	*
HD PBMC vs. tumors	ns	ns	****	****	****
HD PBMC vs. lungs	ns	ns	****	****	****
PBMC vs. LNs	ns	****	ns	ns	ns
PBMC vs. tumors	ns	ns	****	****	****
PBMC vs. lungs	ns	ns	****	****	****
LNs vs. tumors	ns	****	***	****	****
LNs vs. lungs	ns	****	**	***	***
Tumors vs. lungs	ns	ns	ns	ns	ns
Sidak's test (Tregs vs. Teffs)					
in HD PBMC	0.6522	0.9996	0.9928	< 0.0001	< 0.0001
in PBMC	0.9306	0.9914	0.314	< 0.0001	< 0.0001
in LNs	0.9503	< 0.0001	0.1663	0.0073	0.0087
in tumors	> 0.9999	0.9955	< 0.0001	0.898	0.8076
in lungs	> 0.9999	> 0.9999	< 0.0001	0.9083	0.6211

"Number of Treg-Teff pairs" is equal of number of unique samples tested for corresponding marker
"HD PBMC" – healthy donors PBMC
"ns" – not significant, p value >0.05; *p <0.05; ** p<0.01; *** p<0.001; **** p<0.0001

Supplemental Table 10

Smoking versus Gender, Crosstabulation

			Gender		Total
			Males	Females	
Smoking status	Never smoked	Count	1	6	7
		% within all	14.3%	85.7%	100.0%
	Former smoker	Count	31	17	48
		% within all	64.6%	35.4%	100.0%
	Current smoker	Count	16	2	18
		% within all	88.9%	11.1%	100.0%
Total		Count	48	25	73
		% within all	65.8%	34.2%	100.0%

Pearson Chi-Square p value is 0.0019

Supplemental Table 11

Antibodies and reagents used for flow cytometry and cell stimulation

Flow cytometry				
#	**Name**	**Clone/catalog #**	**Color/Type**	**Manufacturer**
1	CFSE	cat# C1157	492/517 nm	Life Technologies
2	Live/dead fixable	cat# L34957	405/525 nm	Life Technologies
3	Zombie Yellow fixable	cat# 423103	405/572 nm	Biolegend
4	Zombie Aqua fixable	cat#423102	405/516	Biolegend
5	Ghost Dye, violet 510	cat#13-0870-T100	405/510	Tonbo Bioscience
5	CD3	HIT3a	AF488	Biolegend
6	CD3	OKT3	eVolve 605	eBioscience
7	CD4	SK3	APC, Pacific Blue, APC-Cy7, PE, FITC, PerCP/Cy5.5, AF647, AF700	Biolegend
8	CD4	RPA-T4*	APC-Cy7, PerCP/Cy5.5, violetFluor™ 450	Biolegend, Tonbo Bioscience
9	CD4	RPA-T4*	PE-CF594	BD Biosciences
10	CD4	OKT4	APC, PE	Biolegend
11	CD8	HIT8a	PerCP/Cy5.5, FITC, APC-Cy7	Biolegend
12	CD8a	RPA-T8	FITC, PE-CF594	BD Biosciences
13	CD15s	cat#563526	AF647	BD Biosciences
14	CD16	368	PerCP	Biolegend
15	CD25	M-A251	PerCP-Cy5.5, APC, FITC	Biolegend
16	CD26	cat#555437	PE	BD Biosciences
17	CD27	cat#302815	APC-Cy7	Biolegend
18	CD39	eBioA1 (A1)	Pe-Cy7	eBioscience
19	CD45	HI30	FITC, AF700, redFluor™ 710, Pe-Cy7	Biolegend, Tonbo Biosciences
20	CD45RA	HI100	Pacific Blue, Pe-Cy7, Brilliant Violet 785	Biolegend
21	CD45RA	L48	Pe-Cy7	BD Biosciences
22	CD45RO	UCHL1	PE	BD Biosciences, Biolegend
23	CD62L	DREG-56	Pe-Cy5, APC-Cy7	BD Biosciences, Biolegend
24	CD64	10.1	FITC	Biolegend
25	CD69	cat#310906	PE	Biolegend
26	CD84	cat#326008	PE	Biolegend
27	CD89	A59	PE	Biolegend
28	CD95 (Fas)	DX2	Pe-Cy7	Biolegend
29	CD101(BB27)	cat#331010	AF647	Biolegend
30	CD120b	cat#562909	AF647	BD Biosciences
31	CD127	A019D5	Brilliant Violet 785, PE	Biolegend
32	CD127	eBioRDR5	FITC, PE	eBioscience
33	CD152 (CTLA-4)	BNI3	Pe-Cy5, PE	BD Biosciences
34	CD154 (CD40L)	24-31	eFluor450	eBioscience

35	CD161	HP-3G10	PE, AF700	Biolegend
36	CD183 (CXCR3)	557185	PE	BD Biosciences
37	CD185 (CXCR5)	J252D4	PerCP-Cy5.5, AF647	Biolegend
38	CD194 (CCR4)	cat#359403	AF647	Biolegend
39	CD195 (CCR5)	cat#359105	PE	Biolegend
40	CD197 (CCR7)	cat#353215	FITC, Pe-Cy7	Biolegend
41	CD198 (CCR8)	cat#FAB1429P-025	PE	R&D systems
42	CD278 (ICOS)	cat#313510	APC	Biolegend
43	CD279 (PD-1)	cat#329952	AF700	Biolegend
44	CD304 (Neuropilin-1)	cat354506	APC	Biolegend
45	CD357 (GITR)	cat#311610	APC	Biolegend
46	CXCR4	cat#FAB173P-100	PE	R&D systems
47	FOXP3	PCH101	APC, AF647, FITC, PE, PerCP-Cy5.5, eFluor 450	eBioscience
48	FOXP3	259D/C7	AF647, PE	BD Biosciences
49	FOXP3	150D	PE	Biolegend
50	GARP (LRRC32)	352504	PE	Biolegend
51	Helios	22F6	PE, FITC, APC	Biolegend
52	HLA-DR	307616	Pe-Cy7	Biolegend
53	Ki-67	cat#561284	PerCP-Cy5.5	BD Biosciences
54	Ki-67	cat#46-5699-42	PerCP-eFluor® 710	eBioscience
55	LAP (TGF-β1)	cat#349607	APC	Biolegend
56	TIGIT	cat#12-9500-42	PE	eBioscience
57	TIM-3	cat#FAB2365A	APC	R&D systems
Stimulation/conversion				
1	CD3 mAbs-coated beads	OKT3 and Dynabeads	MACS GMP pure and M-450 Tosylactivated beads	Miltenyi Biotec and Life Technologies
2	CD3/28 beads	Dynabeads	Human T-Activator CD3/CD28	Life Technologies
3	CD3, CD28	OKT3, CD28.2	LEAF™ Purified	Biolegend
5	IL-2, human	11011456001	10,000U (5 µg, 1 ml)	Roche
6	TGF-β1 human	cat#100-21C	10 ug	Peprotech

*Does not work properly in PrimeFlow assay

Supplemental References

1. Provinciali M, Moresi R, Donnini A, and Lisa RM. Reference values for CD4+ and CD8+ T lymphocytes with naive or memory phenotype and their association with mortality in the elderly. *Gerontology.* 2009;55(3):314-21.
2. Hannet I, Erkeller-Yuksel F, Lydyard P, Deneys V, and DeBruyere M. Developmental and maturational changes in human blood lymphocyte subpopulations. *Immunol Today.* 1992;13(6):215, 8.
3. Neuber K, Schmidt S, and Mensch A. Telomere length measurement and determination of immunosenescence-related markers (CD28, CD45RO, CD45RA, interferon-gamma and interleukin-4) in skin-homing T cells expressing the cutaneous lymphocyte antigen: indication of a non-ageing T-cell subset. *Immunology.* 2003;109(1):24-31.
4. Koch S, Larbi A, Derhovanessian E, Ozcelik D, Naumova E, and Pawelec G. Multiparameter flow cytometric analysis of CD4 and CD8 T cell subsets in young and old people. *Immun Ageing.* 2008;5(6.
5. Yan J, Greer JM, Hull R, O'Sullivan JD, Henderson RD, Read SJ, and McCombe PA. The effect of ageing on human lymphocyte subsets: comparison of males and females. *Immun Ageing.* 2010;7(4.
6. Lages CS, Suffia I, Velilla PA, Huang B, Warshaw G, Hildeman DA, Belkaid Y, and Chougnet C. Functional regulatory T cells accumulate in aged hosts and promote chronic infectious disease reactivation. *J Immunol.* 2008;181(3):1835-48.
7. Jagger A, Shimojima Y, Goronzy JJ, and Weyand CM. Regulatory T cells and the immune aging process: a mini-review. *Gerontology.* 2014;60(2):130-7.
8. Fessler J, Ficjan A, Duftner C, and Dejaco C. The impact of aging on regulatory T-cells. *Front Immunol.* 2013;4(231.
9. Santner-Nanan B, Seddiki N, Zhu E, Quent V, Kelleher A, Fazekas de St Groth B, and Nanan R. Accelerated age-dependent transition of human regulatory T cells to effector memory phenotype. *Int Immunol.* 2008;20(3):375-83.
10. Chatila WM, Criner GJ, Hancock WW, Akimova T, Moldover B, Chang JK, Cornwell W, Santerre M, and Rogers TJ. Blunted expression of miR-199a-5p in regulatory T cells of patients with chronic obstructive pulmonary disease compared to unaffected smokers. *Clin Exp Immunol.* 2014;177(1):341-52.
11. Bhat TA, Panzica L, Kalathil SG, and Thanavala Y. Immune Dysfunction in Patients with Chronic Obstructive Pulmonary Disease. *Ann Am Thorac Soc.* 2015;12 Suppl 2(S169-75.
12. Blanco JA, Toste IS, Alvarez RF, Cuadrado GR, Gonzalvez AM, and Martin IJ. Age, comorbidity, treatment decision and prognosis in lung cancer. *Age Ageing.* 2008;37(6):715-8.
13. Young RP, Hopkins RJ, Christmas T, Black PN, Metcalf P, and Gamble GD. COPD prevalence is increased in lung cancer, independent of age, sex and smoking history. *Eur Respir J.* 2009;34(2):380-6.
14. Janssen-Heijnen ML, Smulders S, Lemmens VE, Smeenk FW, van Geffen HJ, and Coebergh JW. Effect of comorbidity on the treatment and prognosis of elderly patients with non-small cell lung cancer. *Thorax.* 2004;59(7):602-7.
15. Akimova T, Levine MH, Beier UH, and Hancock WW. Standardization, Evaluation, and Area-Under-Curve Analysis of Human and Murine Treg Suppressive Function. *Methods Mol Biol.* 2016;1371(43-78.
16. Faint JM, Tuncer C, Garg A, Adams DH, and Lalor PF. Functional consequences of human lymphocyte cryopreservation: implications for subsequent interactions of cells with endothelium. *J Immunother.* 2011;34(8):588-96.
17. Weinberg A, Song LY, Wilkening C, Sevin A, Blais B, Louzao R, Stein D, Defechereux P, Durand D, Riedel E, et al. Optimization and limitations of use of cryopreserved peripheral blood mononuclear cells for functional and phenotypic T-cell characterization. *Clin Vaccine Immunol.* 2009;16(8):1176-86.

18. Porichis F, Hart MG, Griesbeck M, Everett HL, Hassan M, Baxter AE, Lindqvist M, Miller SM, Soghoian DZ, Kavanagh DG, et al. High-throughput detection of miRNAs and gene-specific mRNA at the single-cell level by flow cytometry. *Nat Commun.* 2014;5(5641.
19. Gaublomme JT, Yosef N, Lee Y, Gertner RS, Yang LV, Wu C, Pandolfi PP, Mak T, Satija R, Shalek AK, et al. Single-Cell Genomics Unveils Critical Regulators of Th17 Cell Pathogenicity. *Cell.* 2015;163(6):1400-12.
20. Soh KT, Tario JD, Jr., Colligan S, Maguire O, Pan D, Minderman H, and Wallace PK. Simultaneous, Single-Cell Measurement of Messenger RNA, Cell Surface Proteins, and Intracellular Proteins. *Curr Protoc Cytom.* 2016;75(7 45 1-7 33.
21. Eruslanov EB, Bhojnagarwala PS, Quatromoni JG, Stephen TL, Ranganathan A, Deshpande C, Akimova T, Vachani A, Litzky L, Hancock WW, et al. Tumor-associated neutrophils stimulate T cell responses in early-stage human lung cancer. *J Clin Invest.* 2014;124(12):5466-80.
22. Tang Q, Bluestone JA, and Kang SM. CD4(+)Foxp3(+) regulatory T cell therapy in transplantation. *J Mol Cell Biol.* 2012;4(1):11-21.
23. Akimova T, Kamath BM, Goebel JW, Meyers KE, Rand EB, Hawkins A, Levine MH, Bucuvalas JC, and Hancock WW. Differing effects of rapamycin or calcineurin inhibitor on T-regulatory cells in pediatric liver and kidney transplant recipients. *Am J Transplant.* 2012;12(12):3449-61.
24. Miyara M, Chader D, Sage E, Sugiyama D, Nishikawa H, Bouvry D, Claer L, Hingorani R, Balderas R, Rohrer J, et al. Sialyl Lewis x (CD15s) identifies highly differentiated and most suppressive FOXP3high regulatory T cells in humans. *Proc Natl Acad Sci U S A.* 2015;112(23):7225-30.
25. Sakaguchi S, Wing K, Onishi Y, Prieto-Martin P, and Yamaguchi T. Regulatory T cells: how do they suppress immune responses? *Int Immunol.* 2009;21(10):1105-11.
26. Levings MK, Sangregorio R, Sartirana C, Moschin AL, Battaglia M, Orban PC, and Roncarolo MG. Human CD25+CD4+ T suppressor cell clones produce transforming growth factor beta, but not interleukin 10, and are distinct from type 1 T regulatory cells. *J Exp Med.* 2002;196(10):1335-46.
27. Deaglio S, Dwyer KM, Gao W, Friedman D, Usheva A, Erat A, Chen JF, Enjyoji K, Linden J, Oukka M, et al. Adenosine generation catalyzed by CD39 and CD73 expressed on regulatory T cells mediates immune suppression. *J Exp Med.* 2007;204(6):1257-65.
28. Borsellino G, Kleinewietfeld M, Di Mitri D, Sternjak A, Diamantini A, Giometto R, Hopner S, Centonze D, Bernardi G, Dell'Acqua ML, et al. Expression of ectonucleotidase CD39 by Foxp3+ Treg cells: hydrolysis of extracellular ATP and immune suppression. *Blood.* 2007;110(4):1225-32.
29. Miyara M, Yoshioka Y, Kitoh A, Shima T, Wing K, Niwa A, Parizot C, Taflin C, Heike T, Valeyre D, et al. Functional delineation and differentiation dynamics of human CD4+ T cells expressing the FoxP3 transcription factor. *Immunity.* 2009;30(6):899-911.
30. Cortes JR, Sanchez-Diaz R, Bovolenta ER, Barreiro O, Lasarte S, Matesanz-Marin A, Toribio ML, Sanchez-Madrid F, and Martin P. Maintenance of immune tolerance by Foxp3+ regulatory T cells requires CD69 expression. *J Autoimmun.* 2014;55(51-62.
31. Fernandez I, Zeiser R, Karsunky H, Kambham N, Beilhack A, Soderstrom K, Negrin RS, and Engleman E. CD101 surface expression discriminates potency among murine FoxP3+ regulatory T cells. *J Immunol.* 2007;179(5):2808-14.
32. Chen X, Subleski JJ, Kopf H, Howard OM, Mannel DN, and Oppenheim JJ. Cutting edge: expression of TNFR2 defines a maximally suppressive subset of mouse CD4+CD25+FoxP3+ T regulatory cells: applicability to tumor-infiltrating T regulatory cells. *J Immunol.* 2008;180(10):6467-71.
33. Pesenacker AM, Bending D, Ursu S, Wu Q, Nistala K, and Wedderburn LR. CD161 defines the subset of FoxP3+ T cells capable of producing proinflammatory cytokines. *Blood.* 2013;121(14):2647-58.
34. Chang DK, Sui J, Geng S, Muvaffak A, Bai M, Fuhlbrigge RC, Lo A, Yammanuru A, Hubbard L, Sheehan J, et al. Humanization of an anti-CCR4 antibody that kills cutaneous T-cell lymphoma cells and abrogates suppression by T-regulatory cells. *Mol Cancer Ther.* 2012;11(11):2451-61.
35. Erfani N, Mehrabadi SM, Ghayumi MA, Haghshenas MR, Mojtahedi Z, Ghaderi A, and Amani D. Increase of regulatory T cells in metastatic stage and CTLA-4 over expression in lymphocytes of patients with non-small cell lung cancer (NSCLC). *Lung Cancer.* 2012;77(2):306-11.

36. Wang R, Wan Q, Kozhaya L, Fujii H, and Unutmaz D. Identification of a regulatory T cell specific cell surface molecule that mediates suppressive signals and induces Foxp3 expression. *PLoS One.* 2008;3(7):e2705.
37. Stockis J, Colau D, Coulie PG, and Lucas S. Membrane protein GARP is a receptor for latent TGF-beta on the surface of activated human Treg. *Eur J Immunol.* 2009;39(12):3315-22.
38. McHugh RS, Whitters MJ, Piccirillo CA, Young DA, Shevach EM, Collins M, and Byrne MC. CD4(+)CD25(+) immunoregulatory T cells: gene expression analysis reveals a functional role for the glucocorticoid-induced TNF receptor. *Immunity.* 2002;16(2):311-23.
39. Baine I, Basu S, Ames R, Sellers RS, and Macian F. Helios induces epigenetic silencing of IL2 gene expression in regulatory T cells. *J Immunol.* 2013;190(3):1008-16.
40. Golding A, Hasni S, Illei G, and Shevach EM. The percentage of FoxP3+Helios+ Treg cells correlates positively with disease activity in systemic lupus erythematosus. *Arthritis Rheum.* 2013;65(11):2898-906.
41. Baecher-Allan C, Wolf E, and Hafler DA. MHC class II expression identifies functionally distinct human regulatory T cells. *J Immunol.* 2006;176(8):4622-31.
42. Zheng J, Chan PL, Liu Y, Qin G, Xiang Z, Lam KT, Lewis DB, Lau YL, and Tu W. ICOS regulates the generation and function of human CD4+ Treg in a CTLA-4 dependent manner. *PLoS One.* 2013;8(12):e82203.
43. Bu M, Shen Y, Seeger WL, An S, Qi R, Sanderson JA, and Cai Y. Ovarian carcinoma-infiltrating regulatory T cells were more potent suppressors of CD8(+) T cell inflammation than their peripheral counterparts, a function dependent on TIM3 expression. *Tumour Biol.* 2016;37(3):3949-56.
44. Mandapathil M, Szczepanski M, Harasymczuk M, Ren J, Cheng D, Jackson EK, Gorelik E, Johnson J, Lang S, and Whiteside TL. CD26 expression and adenosine deaminase activity in regulatory T cells (Treg) and CD4(+) T effector cells in patients with head and neck squamous cell carcinoma. *Oncoimmunology.* 2012;1(5):659-69.
45. Marc MM, Korosec P, Kern I, Sok M, Ihan A, and Kosnik M. Lung tissue and tumour-infiltrating T lymphocytes in patients with non-small cell lung carcinoma and chronic obstructive pulmonary disease (COPD): moderate/severe versus mild stage of COPD. *Scand J Immunol.* 2007;66(6):694-702.
46. Riether C, Schurch C, and Ochsenbein AF. Modulating CD27 signaling to treat cancer. *Oncoimmunology.* 2012;1(9):1604-6.
47. Schuler PJ, Schilling B, Harasymczuk M, Hoffmann TK, Johnson J, Lang S, and Whiteside TL. Phenotypic and functional characteristics of CD4+ CD39+ FOXP3+ and CD4+ CD39+ FOXP3neg T-cell subsets in cancer patients. *Eur J Immunol.* 2012;42(7):1876-85.
48. Khong A, Nelson DJ, Nowak AK, Lake RA, and Robinson BW. The use of agonistic anti-CD40 therapy in treatments for cancer. *Int Rev Immunol.* 2012;31(4):246-66.
49. Phillips JD, Knab LM, Blatner NR, Haghi L, DeCamp MM, Meyerson SL, Heiferman MJ, Heiferman JR, Gounari F, Bentrem DJ, et al. Preferential expansion of pro-inflammatory Tregs in human non-small cell lung cancer. *Cancer Immunol Immunother.* 2015;64(9):1185-91.
50. Iliopoulou EG, Karamouzis MV, Missitzis I, Ardavanis A, Sotiriadou NN, Baxevanis CN, Rigatos G, Papamichail M, and Perez SA. Increased frequency of CD4+ cells expressing CD161 in cancer patients. *Clin Cancer Res.* 2006;12(23):6901-9.
51. Hodi FS, O'Day SJ, McDermott DF, Weber RW, Sosman JA, Haanen JB, Gonzalez R, Robert C, Schadendorf D, Hassel JC, et al. Improved survival with ipilimumab in patients with metastatic melanoma. *N Engl J Med.* 2010;363(8):711-23.
52. Woo EY, Yeh H, Chu CS, Schlienger K, Carroll RG, Riley JL, Kaiser LR, and June CH. Cutting edge: Regulatory T cells from lung cancer patients directly inhibit autologous T cell proliferation. *J Immunol.* 2002;168(9):4272-6.
53. Cohen AD, Schaer DA, Liu C, Li Y, Hirschhorn-Cymmerman D, Kim SC, Diab A, Rizzuto G, Duan F, Perales MA, et al. Agonist anti-GITR monoclonal antibody induces melanoma tumor immunity in

mice by altering regulatory T cell stability and intra-tumor accumulation. *PLoS One.* 2010;5(5):e10436.
54. Fialova A, Partlova S, Sojka L, Hromadkova H, Brtnicky T, Fucikova J, Kocian P, Rob L, Bartunkova J, and Spisek R. Dynamics of T-cell infiltration during the course of ovarian cancer: the gradual shift from a Th17 effector cell response to a predominant infiltration by regulatory T-cells. *Int J Cancer.* 2013;132(5):1070-9.
55. Kovacsovics-Bankowski M, Chisholm L, Vercellini J, Tucker CG, Montler R, Haley D, Newell P, Ma J, Tseng P, Wolf R, et al. Detailed characterization of tumor infiltrating lymphocytes in two distinct human solid malignancies show phenotypic similarities. *J Immunother Cancer.* 2014;2(1):38.
56. Strauss L, Bergmann C, Szczepanski MJ, Lang S, Kirkwood JM, and Whiteside TL. Expression of ICOS on human melanoma-infiltrating CD4+CD25highFoxp3+ T regulatory cells: implications and impact on tumor-mediated immune suppression. *J Immunol.* 2008;180(5):2967-80.
57. Tu JF, Ding YH, Ying XH, Wu FZ, Zhou XM, Zhang DK, Zou H, and Ji JS. Regulatory T cells, especially ICOS+ FOXP3+ regulatory T cells, are increased in the hepatocellular carcinoma microenvironment and predict reduced survival. *Sci Rep.* 2016;6(35056.
58. Weiss JM, Bilate AM, Gobert M, Ding Y, Curotto de Lafaille MA, Parkhurst CN, Xiong H, Dolpady J, Frey AB, Ruocco MG, et al. Neuropilin 1 is expressed on thymus-derived natural regulatory T cells, but not mucosa-generated induced Foxp3+ T reg cells. *J Exp Med.* 2012;209(10):1723-42, S1.
59. Battaglia A, Buzzonetti A, Monego G, Peri L, Ferrandina G, Fanfani F, Scambia G, and Fattorossi A. Neuropilin-1 expression identifies a subset of regulatory T cells in human lymph nodes that is modulated by preoperative chemoradiation therapy in cervical cancer. *Immunology.* 2008;123(1):129-38.
60. Topalian SL, Hodi FS, Brahmer JR, Gettinger SN, Smith DC, McDermott DF, Powderly JD, Carvajal RD, Sosman JA, Atkins MB, et al. Safety, activity, and immune correlates of anti-PD-1 antibody in cancer. *N Engl J Med.* 2012;366(26):2443-54.
61. Kurtulus S, Sakuishi K, Ngiow SF, Joller N, Tan DJ, Teng MW, Smyth MJ, Kuchroo VK, and Anderson AC. TIGIT predominantly regulates the immune response via regulatory T cells. *J Clin Invest.* 2015;125(11):4053-62.
62. Anderson AC. Tim-3: an emerging target in the cancer immunotherapy landscape. *Cancer Immunol Res.* 2014;2(5):393-8.
63. Gao X, Zhu Y, Li G, Huang H, Zhang G, Wang F, Sun J, Yang Q, Zhang X, and Lu B. TIM-3 expression characterizes regulatory T cells in tumor tissues and is associated with lung cancer progression. *PLoS One.* 2012;7(2):e30676.
64. Salgado FJ, Perez-Diaz A, Villanueva NM, Lamas O, Arias P, and Nogueira M. CD26: a negative selection marker for human Treg cells. *Cytometry A.* 2012;81(10):843-55.
65. Seddiki N, Santner-Nanan B, Martinson J, Zaunders J, Sasson S, Landay A, Solomon M, Selby W, Alexander SI, Nanan R, et al. Expression of interleukin (IL)-2 and IL-7 receptors discriminates between human regulatory and activated T cells. *J Exp Med.* 2006;203(7):1693-700.
66. Wang R, Kozhaya L, Mercer F, Khaitan A, Fujii H, and Unutmaz D. Expression of GARP selectively identifies activated human FOXP3+ regulatory T cells. *Proc Natl Acad Sci U S A.* 2009;106(32):13439-44.
67. Tran DQ, Andersson J, Hardwick D, Bebris L, Illei GG, and Shevach EM. Selective expression of latency-associated peptide (LAP) and IL-1 receptor type I/II (CD121a/CD121b) on activated human FOXP3+ regulatory T cells allows for their purification from expansion cultures. *Blood.* 2009;113(21):5125-33.
68. Ondondo B, Jones E, Godkin A, and Gallimore A. Home sweet home: the tumor microenvironment as a haven for regulatory T cells. *Front Immunol.* 2013;4(197.
69. Shipman L. Tumour immunology: Interrogating intratumoral Treg cells. *Nat Rev Immunol.* 2017;17(1):4-5.

70. Plitas G, Konopacki C, Wu K, Bos PD, Morrow M, Putintseva EV, Chudakov DM, and Rudensky AY. Regulatory T Cells Exhibit Distinct Features in Human Breast Cancer. *Immunity.* 2016;45(5):1122-34.
71. Pimenta EM, De S, Weiss R, Feng D, Hall K, Kilic S, Bhanot G, Ganesan S, Ran S, and Barnes BJ. IRF5 is a novel regulator of CXCL13 expression in breast cancer that regulates CXCR5(+) B- and T-cell trafficking to tumor-conditioned media. *Immunol Cell Biol.* 2015;93(5):486-99.
72. Wang C, Lee JH, and Kim CH. Optimal population of FoxP3+ T cells in tumors requires an antigen priming-dependent trafficking receptor switch. *PLoS One.* 2012;7(1):e30793.